This is to certify that the

thesis entitled

Active Flow Control for Maximizing Performance of
Spark-Ignited Stratified Charge Engines

presented by

Alvin Chun Hun Goh

has been accepted towards fulfillment
of the requirements for

Master degree in Mechanical Engineering

M. M. Koochesfahani
Major professor

Date 7/18/2001

ACTIVE FLOW CONTROL FOR MAXIMIZING PERFORMANCE OF SPARK-IGNITED STRATIFIED CHARGE ENGINES

By

Alvin Chun Hun Goh

A THESIS

Submitted to
Michigan State University
in partial fulfillment of the requirements
for the degree of

MASTER OF SCIENCE

Department of Mechanical Engineering

2001

ABSTRACT

ACTIVE FLOW CONTROL FOR MAXIMIZING PERFORMANCE OF SPARK-IGNITED STRATIFIED CHARGE ENGINES

By

Alvin Chun Hun Goh

Cycle-to-cycle variation in stratified charge engines is a serious problem in the automotive industry. Due to cycle-to-cycle variation in engines, fuel injectors need to inject more fuel than necessary in order to have complete combustion in the engines. By reducing cycle-to-cycle variation, a better fuel economy could be achieved.

The present study investigates the possibility of acoustically perturbing the intake flow at different frequencies and amplitudes to control the in-cylinder flow field. This research work concentrates mainly on an engine speed of 600 rpm and 270 crank angle degree (CAD), with the interest of changing the flow field in compression before ignition. Molecular Tagging Velocimetry (MTV) was used to measure the 2D-velocity field at the mid-plane of the engine cylinder.

The experimental results showed that perturbing the flow acoustically has an effect in reducing the cycle-to-cycle variation. The level of cycle-to-cycle variation is measured based on U rms and V rms values. The free-run perturbation method and fixed-time perturbation method managed to reduce the U rms and V rms by about 30% in certain regions of the flow.

This thesis is dedicated to

My parents and my girlfriend, Sarah Keok

For their love and moral support throughout my studies

ACKNOWLEDGEMENTS

I would like to thank all the people who have helped and assisted me in this research work. It would be impossible to complete this work without the help from all of them. I would like to thank my advisor, Dr. Manoochehr Koochesfahani, for his assistance, support and patient guidance throughout my research and studies. A special thanks to Dr. Harold Schock and Dr. Giles Brereton for being on my committee and for their guidance.

I would like to thank Tom Stuecken, Edward Timm and Hooman Rezaei for all the help in setting up the engine and all the technical assistance. I would also like to thank my fellow friends at MSU TMUAL and MSU ERL, Chee Lum, Doug Bohl, Dr. Hu Hui, Adeel Khalid, Andrew Fedewa, Andrew Sasak, Anthony Christie, Boon-Keat Chui, Mark Novak, Dr. Kyle Judd, Yuan Shen, Mahmood Rahi, Jan Chappell and Bobbie Slider, for all the help and moral support. This work would also not have been possible without the financial supports of the Ford Motor Company and Department of Energy (DOE) under Research Grant # DE-FC02-99EE50574 and also made use of shared facilities of the MRSEC Program of the National Science Foundation.

Finally, I would like to thank my parents again for their love and prayers. Last but not the least, I would like to thank my girlfriend, Sarah Chui San Keok, for her love and patience throughout my Masters Program. This day would not have been possible without your support. Thank you!

TABLE OF CONTENTS

LIST OF TABLES

LIST OF FIGURES

LIST OF SYMBOLS AND ABBREVIATIONS

Symbol	Description
CAD	Crank Angle Degree
MTV	Molecular Tagging Velocimetry
N	Number of Engine Cycles
Re	Reynolds Number
St	Strouhal Number
TDC	Top Dead Center
U	X Component of Velocity
V	Y Component of Velocity
W	Z Component of Velocity
rpm	Revolutions per Minute
u,v,w	X, Y, Z Components of Velocity
x,y,z	Coordinate System Axis

Greek	Description
ω	Vorticity
Γ	Circulation
Ψ	A Variable of Interest

Overscores	Description
~	RMS
–	Mean

Chapter 1

INTRODUCTION

1.1 Motivation

In the area of automotive engines, cycle-to-cycle variation is of main concern of many researchers. In recent years, a significant amount of work has been done to improve engine's performance and fuel efficiency. Recent research supports the concept of a significant interaction between the mean flow and the fluctuating parts of the in-cylinder velocity [1]. Due to cycle-to-cycle variation, the engine fuel injectors are sometimes programmed to inject more fuel than required. In order to design better lean burn engines, one has to have a better understanding of the flow patterns during compression stroke and one also has to find ways to reduce cycle-to-cycle variation. If cycle-to-cycle variation is reduced and the in-cylinder flows are made more predictable, one can design a leaner fuel injector. In return, this would improve fuel economy in engines. The ultimate desire of this study is to find a way of controlling the flow and reducing the cycle-to-cycle variation. As a result, it would provide control of the mixing and burning rates of an internal combustion engine.

1.2 Previous Work

Cycle-to-cycle variation in internal combustion engines has always existed and has become an interest of automotive researchers since the invention of the internal combustion engines. The results of previous works have shown that the flow fields inside the combustion chamber are unsteady with a wide range of spatial and temporal

fluctuations[2]. Zhang et al., 1995[2] stated that the fluctuations of the flow fields are result from cycle-to-cycle variation and the center of swirl changes its location from one cycle to the next. Dai, Trigui et al., 2000[5] found that in nature, cyclic variations are superposition of a non-chaotic deterministic process on a stochastic process. There are deterministic effects from previous cycles on the combustion process in subsequent cycles.

It is true that cycle-to-cycle variation does exist. Throughout this research, numerous data and images have shown that cycle-to-cycle variation is very significant in internal combustion engines. Several examples of cycle-to-cycle variation phenomena velocity field are shown in Figure 1. All the instantaneous velocity fields were taken at successive cycle at 270 CAD with the engine running at 600 rpm.

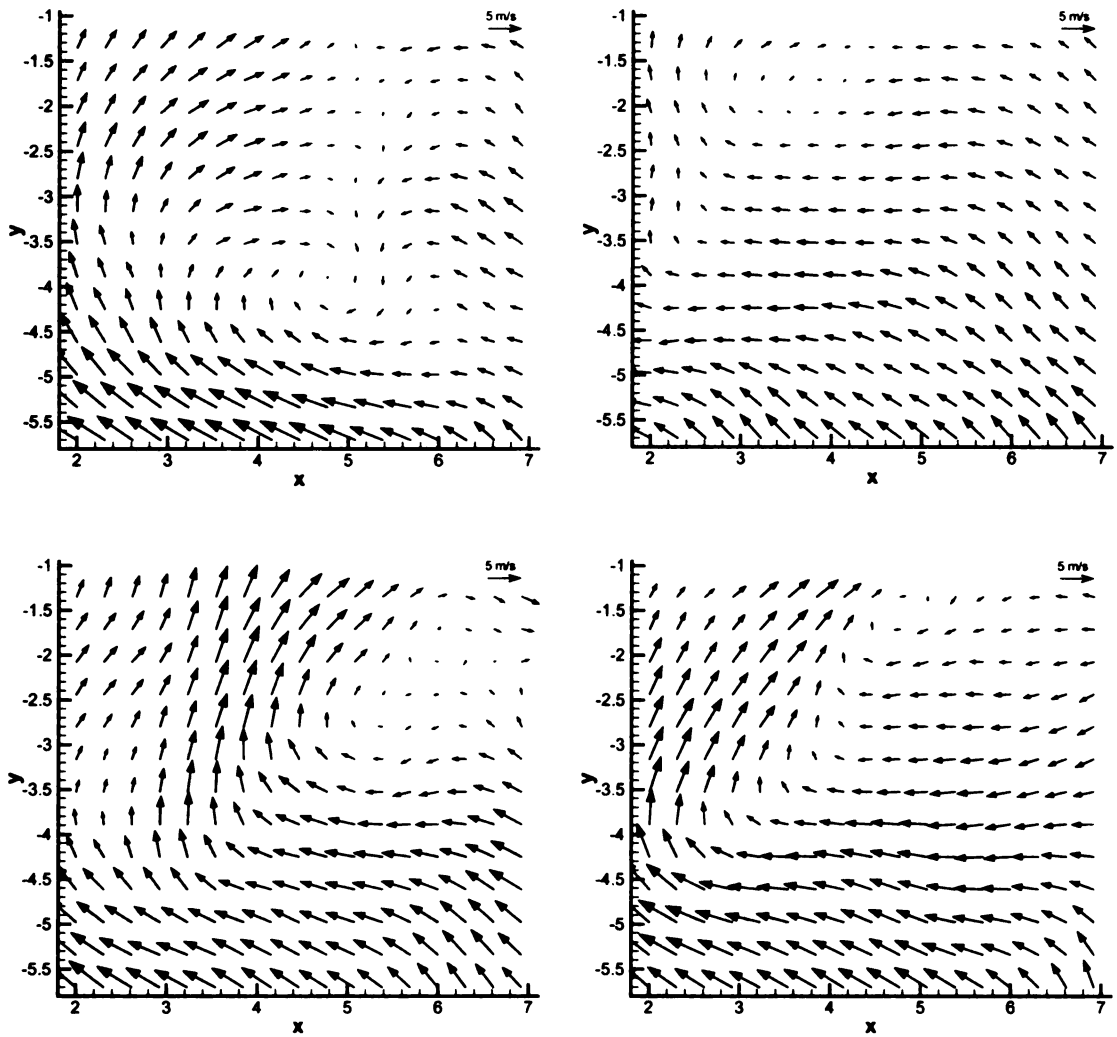

Figure 1. Examples of cycle-to-cycle variation at 270 CAD with engine running at 600 rpm

In addition, excited flows have been studied in other geometries. Several studies have shown that the natural flows' behaviors could be altered or controlled by exciting the natural flows at certain frequency. For example, in round jets, coaxial jets and two-stream mixing layers, it had been shown that perturbing the flow can modify the amount of the mixing downstream of the wake and the turbulence intensities [4, 7, 8, 9]. As for the case of an engine, the enhancement of turbulence in the flow promotes mixing of unburned gas, reacting gas, quenched gas and burned gas in the late compression stroke. An example of the round jet perturbation is Koochesfahani's experiment. Koochesfahani et al., 1997 [6] indicated that in round jet experiment, the forcing increased the growth rate of the shear layer vortices, the roll-up occurred much closer to the jet nozzle and the vortical structures were larger in size. Results of the experiment are shown in Figure 2.

Recent studies by Ambrose [3] had indicated that by exciting the intake flow in an internal combustion engine water analog model, the mean circulation and the mean kinetic energy increased 40% and 30% respectively. Ambrose also found that the amount of amplification of the measured parameters as a function of frequency generally showed the preferred frequency at 40 Hz or a Strouhal Number of 1.19 based upon the maximum velocity of the flow entering through the valve inlet [3]. Since water was used in Ambrose's experiment, the compression stroke was not examined. He only investigated the effects during the intake stroke. Therefore, Ambrose's research motivated this current study to investigate the effect of perturbation in a real internal combustion engine.

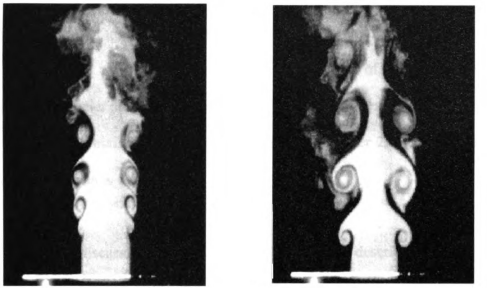

Natural Flow Excited Flow

Figure 2. Flow visualization of a natural and excited (St=0.48) round jet at a Reynolds number of 5,500

1.3 Thesis Arrangement

This thesis is arranged as follow:

Chapter 2 reviews and discusses the experimental measurement techniques and procedures. The first part of Chapter 2 describes the specification of the engine used in the experiment, Molecular Tagging Velocimetry (MTV) measurement method, data acquisition and data processing method. In the last part of Chapter 2, the experimental procedure for a typical run is described briefly.

The results and discussions are in Chapter 3. This chapter describes the results of all the cases studied and discusses the effects of the forcing parameters on the mean flow and the RMS of the flow at 270 CAD and 600 rpm. In Chapter 4, some results from the experiment for 90 CAD and 180 CAD are presented. As for Chapter 5, the results of all the effects of the forcing on the mean flow and the RMS of the flow at 270 CAD and 1200 rpm are presented. Finally, the conclusions of this research can be found in Chapter 6.

Chapter 2

EXPERIMENTAL MEASUREMENT TECHNIQUES AND PROCEDURES

2.1 Optically Accessible Research Engine

The schematic of the experiment and optical arrangement are shown in Figure 3 and 4. Two close-up pictures of the experiment were shown in Figure 5. This study was conducted with a 1999 model year Ford cylinder head with 4 valves and double overhead cams. The engine cylinder head was part of the left bank of a V8 prototype engine with 90.2 mm bore and 90^0 degrees bank angle. The engine specifications are listed in Table 1.

Table 1. Prototype Engine Specifications.

Model and Make	Ford 4-Valve 4.6L
Bore and Stroke	90.2 mm / 90.0 mm
Connecting Rod Length	150.7 mm
Valve Activation	DOHC
Intake Valve Diameter	37.0 mm
Exhaust Valve Diameter	30.0 mm
Maximum Valve Lift	10.02 mm at 120 CAD
Zero CAD	Intake TDC
Intake Valve Opening	6 CAD Before TDC
Intake Valve Closure	250 CAD After TDC
Exhaust Valve Opening	126 CAD After TDC
Exhaust Valve Closure	16 CAD After TDC
Compression Ratio	9.85 : 1
Piston Top	Flat

A flat-head, optically accessible piston was used in the experiment. The bore and stroke were 90.2 mm and 90.0 mm respectively. The length of the connecting rod was 150.7 mm. The cylinder used in the experiment was made from quartz so that it would be optically accessible. The cylinder was mounted on a single-cylinder research engine that served as a reciprocating mechanism. The engine was connected to a 10-HP electrical

motor through a rubber-damped coupling. Two different belt drive setups were connected to the exhaust camshaft that would allow interchanging between the two engine stroke variants. The exhaust camshaft was linked by a roller-chain to the intake camshaft. The intake valve diameter was 37 mm and the exhaust valve diameter was 30 mm. The maximum valve lift was 10.02 mm at 120^0 crank angle. Only the valves of the investigated cylinder were activated. A 4-ohm, 4½ inch mid-woofer speaker was mounted at the modified intake manifold (refer Figure 4 and 5 for the location of the speaker). The speaker had wattage of 40 W and was driven by an amplified sine wave signal through a Hafler P1000 amplifier. The amplifier had a full power bandwidth of 0.1 Hz to 100 kHz. The sine wave was generated originally from a function generator.

Nitrogen was used as the working fluid in the experiment. The reason was that MTV measurement methods in gas-phase applications rely on the phosphorescence of biacetyl and it requires an oxygen-free environment due to the phosphorescence quenching by oxygen (refer section 2.2 for detail description on MTV) [21].

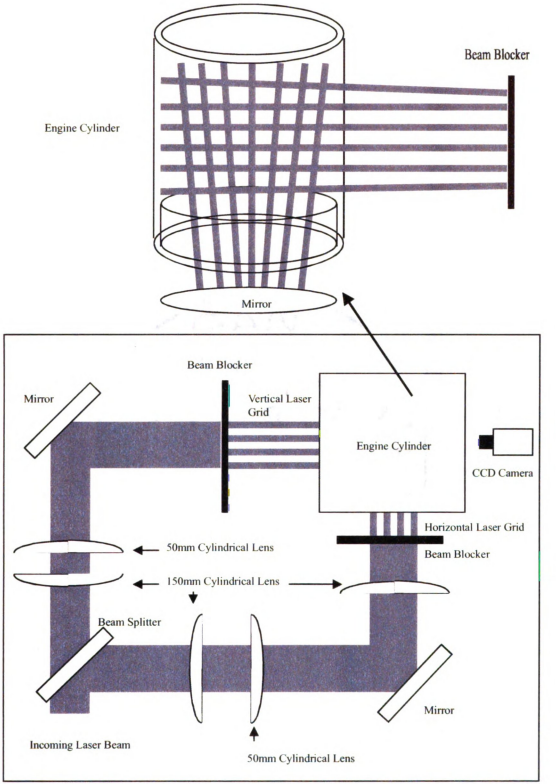

Figure 3. Schematic and optical arrangement of the experiment setup

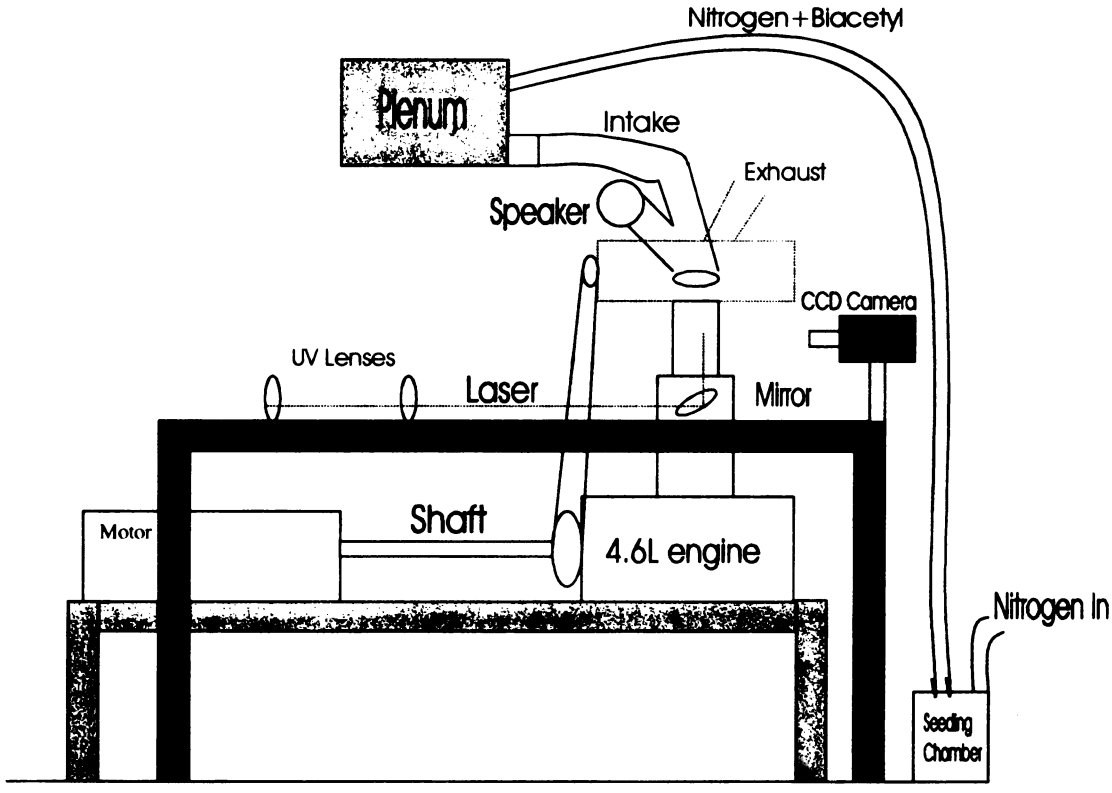

Figure 4. Schematic of the research engine setup

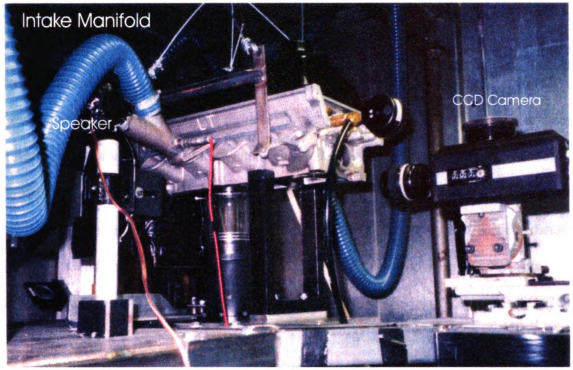

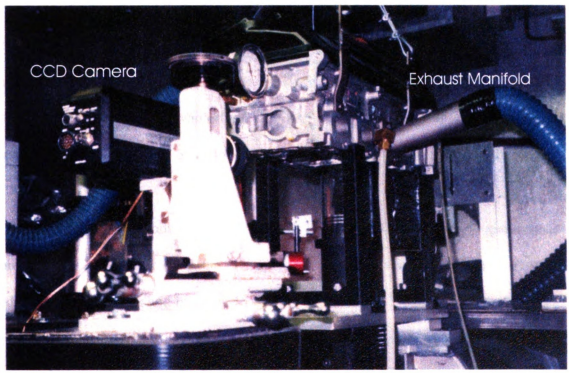

Figure 5. Engine setup viewing from the front and back

*Images in this thesis are presented in color.

2.2 Molecular Tagging Velocimetry (MTV) Set-up

The velocity measurements were done using Molecular Tagging Velocimetry (MTV). MTV is a whole-field optical diagnostic that allows for the non-intrusive measurement of the velocity field in a flowing medium. This technique has been previously used by several authors such as Cohn *et al.* 1995[10], Stier and Koochesfahani 1998[19], Koochesfahani 1999[20], Hill and Klewicki 1996[15], Koochesfahani *et al.* 1996[13], Cohn and Koochesfahani 1997[11], and Gendrich, Bohl, and Koochesfahani 1997[12], Gendrich, Koochesfahani, and Nocera 1997[14] to make measurements in a wide variety of flows. For gas-phase application, Molecular Tagging Velocimetry, MTV, uses nitrogen as a working fluid and biacetyl as a long-lived luminescence. Nitrogen is used due to the phosphorescence quenching by oxygen. A pulsed UV laser is used to tag the regions of interest, and those tagged regions are interrogated at two successive times within the lifetime of the tracer. The measured Lagrangian displacement vector and the time over which the displacement occurred provide the velocity vector [20]. This velocimetry approach yields whole-field, instantaneous maps of velocity vectors over a plane allowing the derivation of various kinematic quantities from the velocity field [21].

For MTV, a Lambda Physik LPX 200 (308nm) laser capable of operating at approximately 290 mJ provided the energy to excite phosphorescence from a working fluid mixture of nitrogen and biacetyl. In order to measure the velocity field throughout a region, a series of vertical and horizontal laser lines were generated. These lines were orthogonal to each other. Each intersection was a "location" where a velocity measurement was made. At this point, images were recorded by the intensified CCD

camera. These images were considered as reference images or zero-delayed images. At certain delay later, normally it was about 200 microseconds for 270 CAD measurement, the tagged region was recorded again using the intensified CCD camera. These images were considered as delayed images. Post-processing by correlation-based techniques allowed the instantaneous planar velocity field to be deducted the reference and delayed images. Examples of reference and delayed images are shown in Figure 6.

A

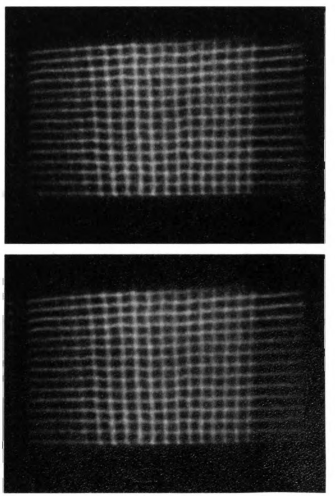

B

Figure 6. Examples of zero-delayed (A) and delayed (B) images

The MTV experiments were done with a field of view of approximately 5 cm x 5 cm. It was located about 1 cm below the intake and exhaust valves and about 2 cm from the cylinder wall (refer Figure 7). The original laser beam was first split into two laser beams (horizontal and vertical beams). Each laser beam was focused using a combination of two cylindrical lenses with focal lengths of 150mm and 50mm. By going through these two lenses, a very thin laser sheet was generated for each beam. Beam blockers with series of thin lines cut through them were used in each beam path to generate a series of 12 lines for the horizontal and 15 lines for the vertical.

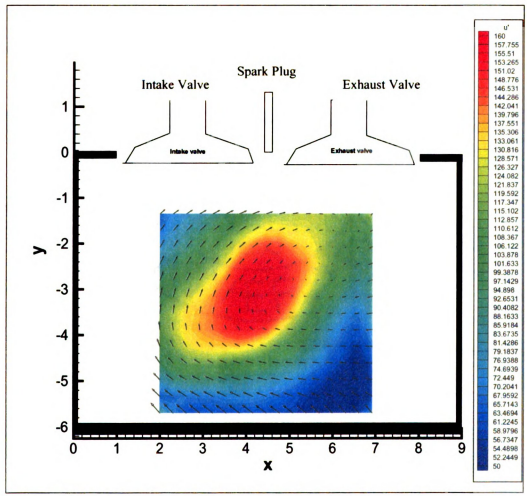

Figure 7. Field of view for the MTV measurement in the engine cylinder

2.3 Data Acquisition

An intensified CCD video camera, Xybion model ISG-350, and together with Nikkor 50mm f1.2 lens were used to record images in the experiment (refer Figure 8). An engine encoder was hooked up at the camshaft to produce a 5-V TTL signal at the desired crank angle. The signal was then used to trigger the laser. At that time, the signal triggered the intensified camera and acquisition board to record zero-delay images. The digital delay generators were then used to delay the original signal from the engine encoder to trigger the intensified camera to record the delayed images. The delayed time of 200 microseconds would provide approximately 5 to 10 pixels of displacement of the phosphorescent lines at 270 CAD.

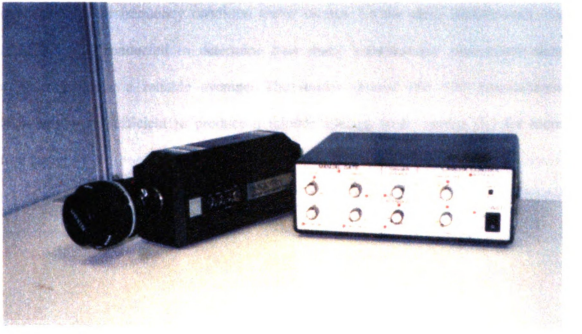

Figure 8. Intensified CCD video camera, Xybion model ISG-350, together with Nikkor 50 mm f1.2 lens

The image acquisition board used in the experiment was the M-Vision 1000 by MuTech Corporation. The M-VISION 1000 (MV-1000) is a single slot video digitizer board for the PCI (Peripheral Component Interconnect) bus. It digitizes standard or non-standard analog camera video into 8 bits per pixel at a rate up to 40 million samples per second. The digitized video is stored in on-board VRAM or transferred in real time to system memory and/or the VGA card for display. The software used together with the acquisition board was the MV-1000 Grab Sequence Application version 1.3 for Windows NT.

A total of 500 instantaneous realization of the velocity field was measured for each measurement condition except for the free-run perturbation method. In the free-run perturbation method, only 200 instantaneous realization of the velocity fields were measured for each frequency condition (refer section 3.4 for more information). An experiment was conducted to determine how many instantaneous realizations were needed to produce a reliable average. The results showed that 500 instantaneous realizations were sufficient to produce a reliable average (refer section 3.2 for more information).

2.4 Data Processing

The data processing process was performed using an in-house code developed over the past few years at MSU Turbulent Mixing and Unsteady Aerodynamics Laboratory (TMUAL). At the earlier stage, a four-processor Silicon Graphics Origin 200 was used as the primary data processing device. Recently, the in-house code has evolved and become available in PC version too.

When processing the data, the main objective was to determine the displacement vector of the tagged regions with the highest possible sub-pixel accuracy in order to increase the dynamic range of the velocity measurements. The displacement of the tagged regions was determined using a direct digital spatial correlation technique. The details of this approach can be found in Gendrich and Koochesfahani 1996[13]. The basic idea of this approach is that a small window called a source window is selected from a tagged region in the reference or zero-delay image. It is then spatially correlated with a larger roam window in the delayed image. A well-defined correlation peak occurs at the location corresponding to the displacement of the tagged region by the 2-component of the velocity flow. The displacement peak is found by using a multi-dimensional polynomial fit.

2.5 Experimental Procedures

Typical procedures for running an experiment are given. First, start the water chiller for the UV laser and then start the UV laser. The UV laser will need about 10 minutes to warm up. While waiting for the laser to warm up, turn on all the necessary devices namely, crank angle encoder, delay generators, function generator, amplifier, and TV monitor. Next, check the nitrogen bank and make sure that there is enough gas pressure to run the experiment. The nitrogen pressure has to be above 400psi for a typical experimental run. Once the laser is warmed up, turn on the oil pump and vacuum pump for the engine. After that, open a little bit of the valve regulator of the nitrogen bank and let a small amount of nitrogen flow into the engine cylinder. Turn off the room lights and start the engine. At the same time, open the valve regulator of the nitrogen bank completely. Let the engine run for while to reach its stability. Before turning on the camera, make sure that the intensifier of the camera is at minimum position. Turn on the camera and run the MV-1000 Grab Sequence Application program. Remove the camera cap and slowly increase the camera intensifier. Key in the appropriate delay time at the delay generators and start taking data and images.

Chapter 3

RESULTS AND DISCUSSION FOR 270 CAD

3.1 Introduction

The results of the experiments will be presented in this section and are organized in chronological order starting with the early stages of the experiment and progressing through the end stage of the experiment.

The experiment was done at an engine speed of 600 rpm, focusing on 270 CAD. The reason 270 CAD was chosen is because 270 CAD is in late compression stroke. Furthermore, the ability to control the flow before ignition would improve fuel economy in engines because one can design a leaner fuel injector if the in-cylinder flows are more predictable. However, in the beginning of this research, 90 CAD and 180 CAD were investigated too. These results will be presented after all the 270 CAD results are presented. The experimental parameters were the number of velocity realizations needed for averaging, the amplitude, the forcing frequencies, and the duration of forcing.

The field of view of the MTV measurement forcing experiment was about 4.5cm x 5.0cm which located at the center of the cylinder, about 2cm from each side of the cylinder wall (refer Figure 9). The intake line was modified and the speaker was put at the intake line with the purpose of perturbing the shear layer of the flow at the intake valves.

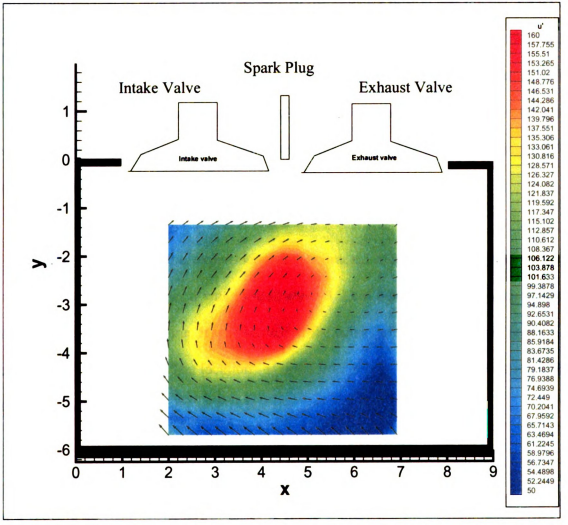

Figure 9. Field of view in the engine cylinder

3.2 Number of realizations needed for averaging

The purpose of this experiment was to determine the number of velocity realizations needed to give a reliable average of the velocity profile and fluctuating level that would represent stability and convergence. The experiment was done for the natural flow (unforced) case with the engine running at 600 rpm without any perturbation. 1200 instantaneous images were taken at 270 CAD. They were then processed and averaged using different numbers of images namely, the average of 200 images, 500 images, 750 images and 1200 images.

The velocities for the experiment were extracted along horizontal and vertical lines. For the horizontal line, it was located about 1.2 cm below the intake and exhaust valves. As for the vertical line, it was located at the center of the cylinder and about 4.5 cm from the cylinder wall. The locations of these lines extracted were arbitrary and with no specific reason.

The results showed that the average of 200 realizations is the minimum number for a reliable average. However, in order to make it more accurate, the 500 realizations were chosen as the number of realizations needed for the all experiment except for the free-run perturbation experiment. In the free-run perturbation experiment, only 200 realizations were used in each average.

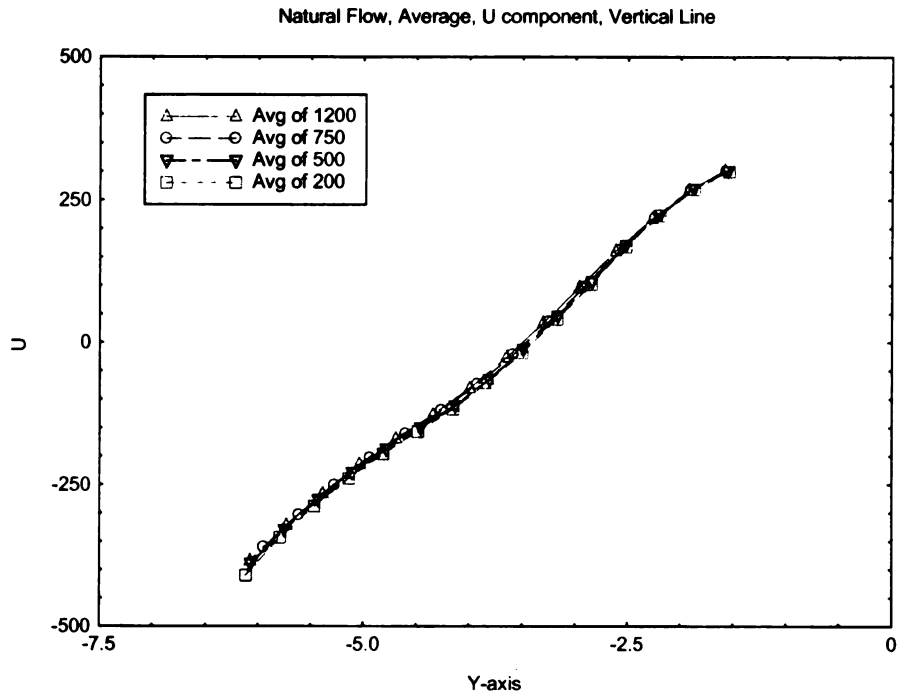

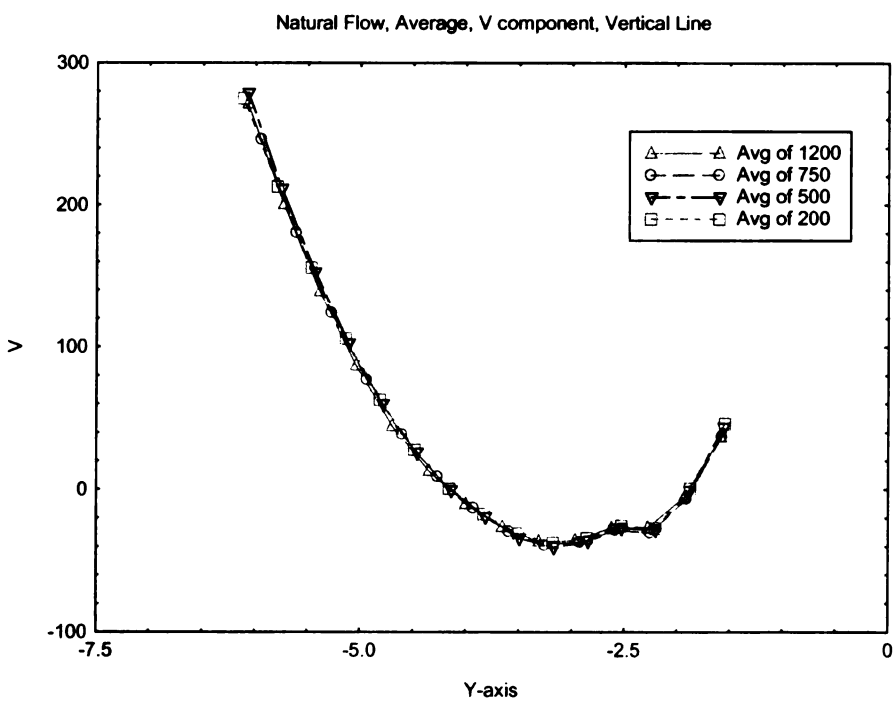

Figure 10. U mean (cm/s) and V mean (cm/s) for vertical line taken at x = 4.5 cm from cylinder wall

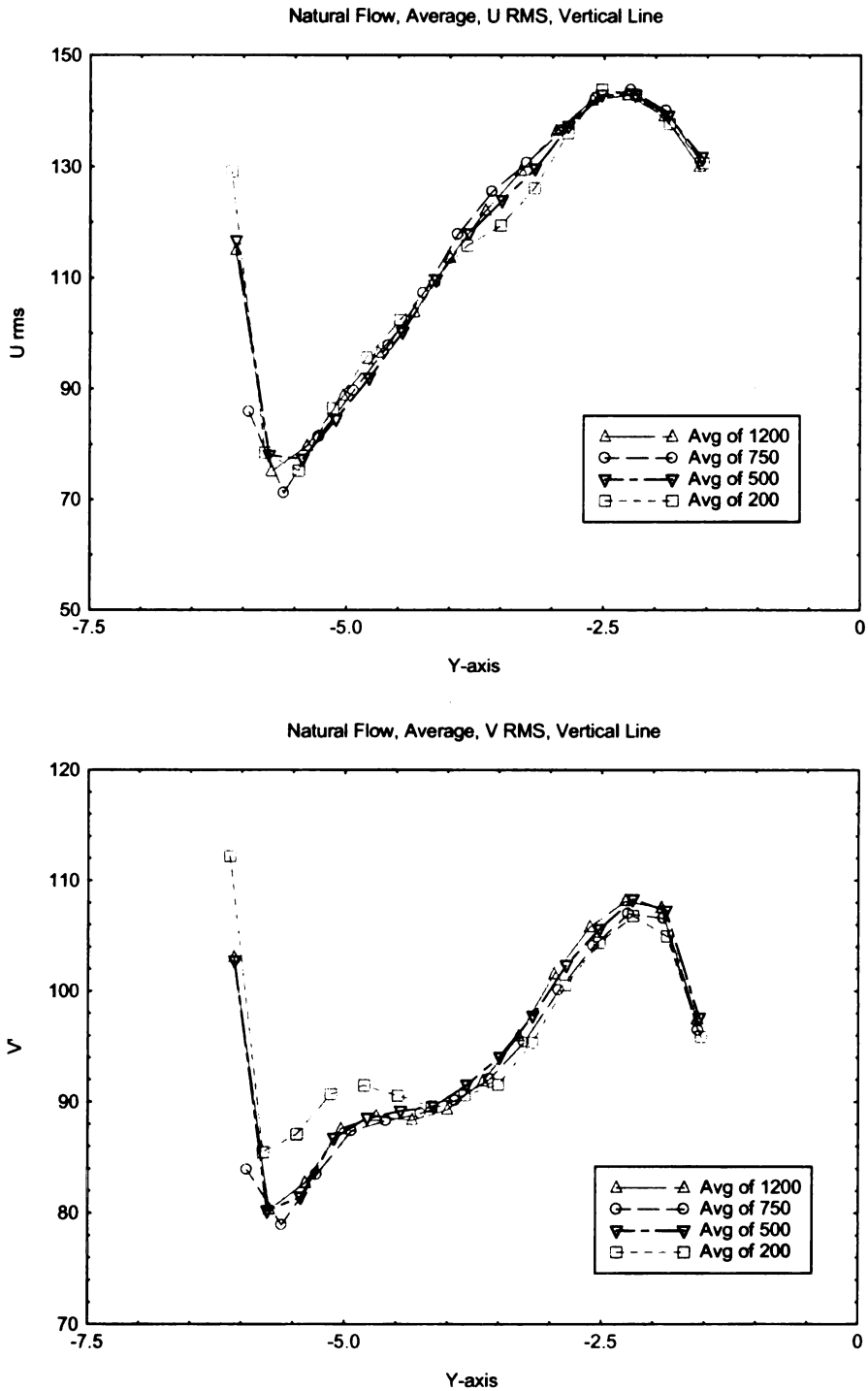

Figure 11. U rms (cm/s) and V rms (cm/s) for vertical line taken at x = 4.5 cm from cylinder wall

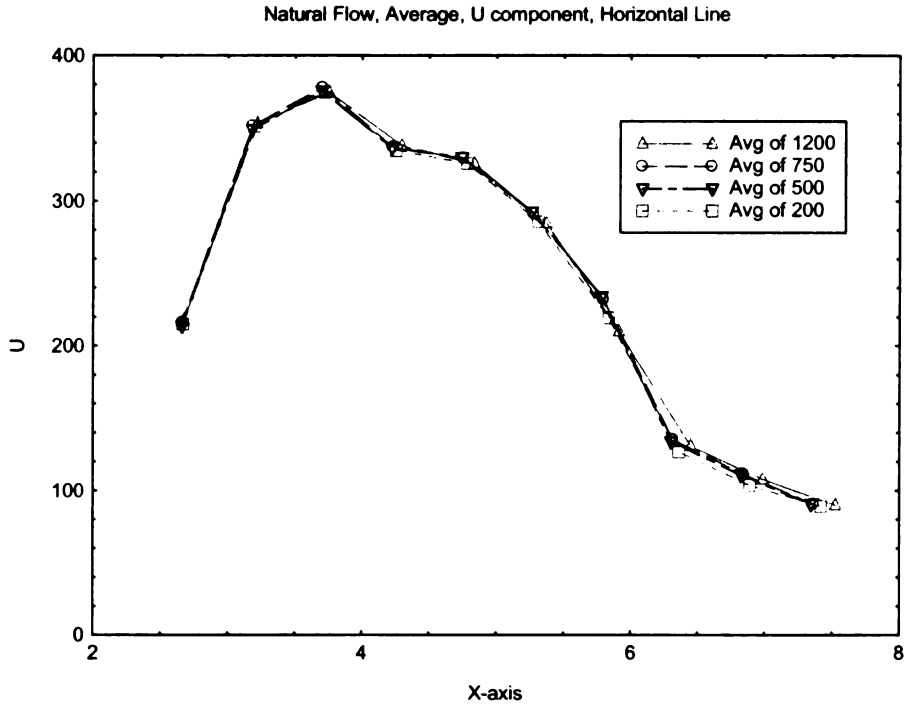

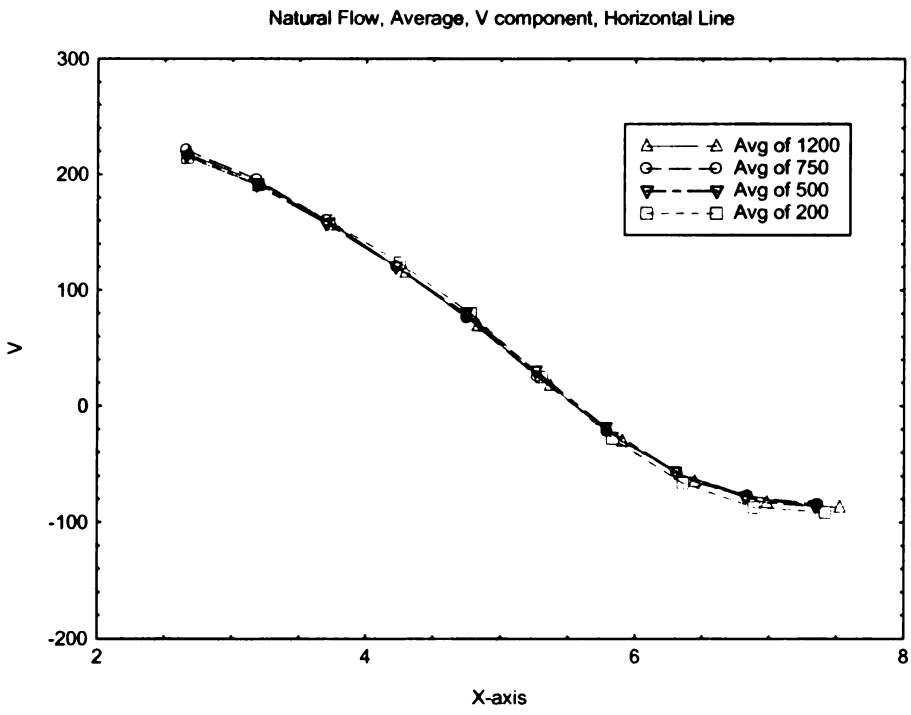

Figure 12. U mean (cm/s) and V mean (cm/s) for horizontal line taken at y = 1.2 cm below the intake and exhaust valves

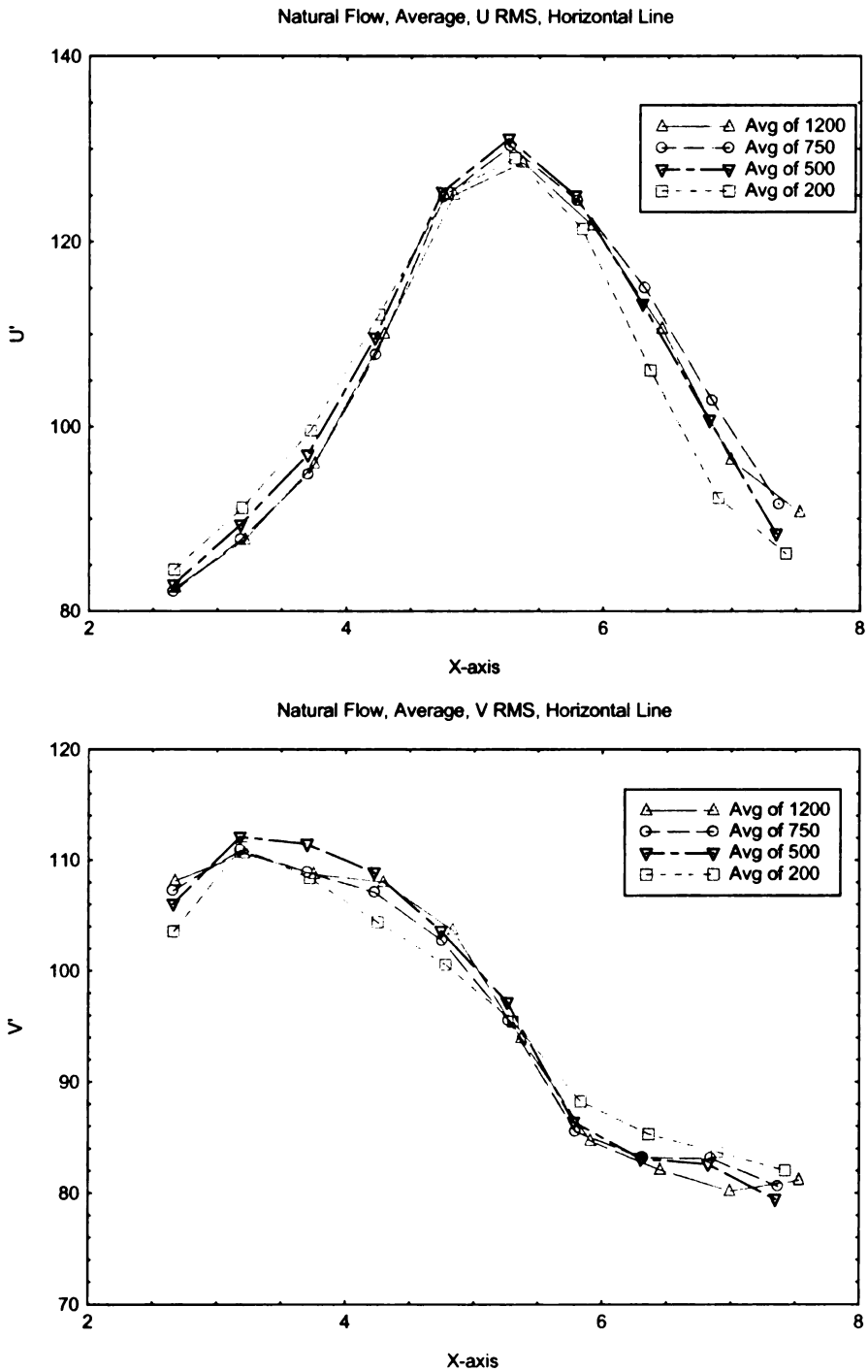

Figure 13. U rms (cm/s) and V rms (cm/s) for horizontal line taken at y = 1.2 cm below the intake and exhaust valves

3.3 Amplitude effects

The next experiment was performed to determine the amplitude effect of the acoustic perturbations. The amplitude here was referred to the amplitude of the sine wave coming out from the amplifier. This experiment was done at three different amplitudes with the engine running at 600 rpm and the crank angle of investigation was at 270 CAD. The three different amplitudes investigated were a small amplitude of 675 mV, a medium amplitude of 10 V and a large amplitude of 28 V (28 V is the maximum amplitude that the amplifier can produce). The perturbation frequency was at 50 Hz. This frequency was arbitrary chosen which later proven that it was not the optimal reduction frequency. However, the trend of the results found in this experiment is expected to the same if it was done with the optimal reduction frequency which was at 400 Hz.

The results of the experiment indicated that as the amplitude of the perturbation increased, the U rms and V rms were reduced. In other words, the trend of the experiment was the higher the amplitude, the lower the cycle-to-cycle variations. For U mean and V mean, the results showed that there were some changes in the mean as the amplitude increased, but they were small. Thus, from the experiment, the highest amplitude (28V) was chosen as the best parameter for the rest of the research and experiments.

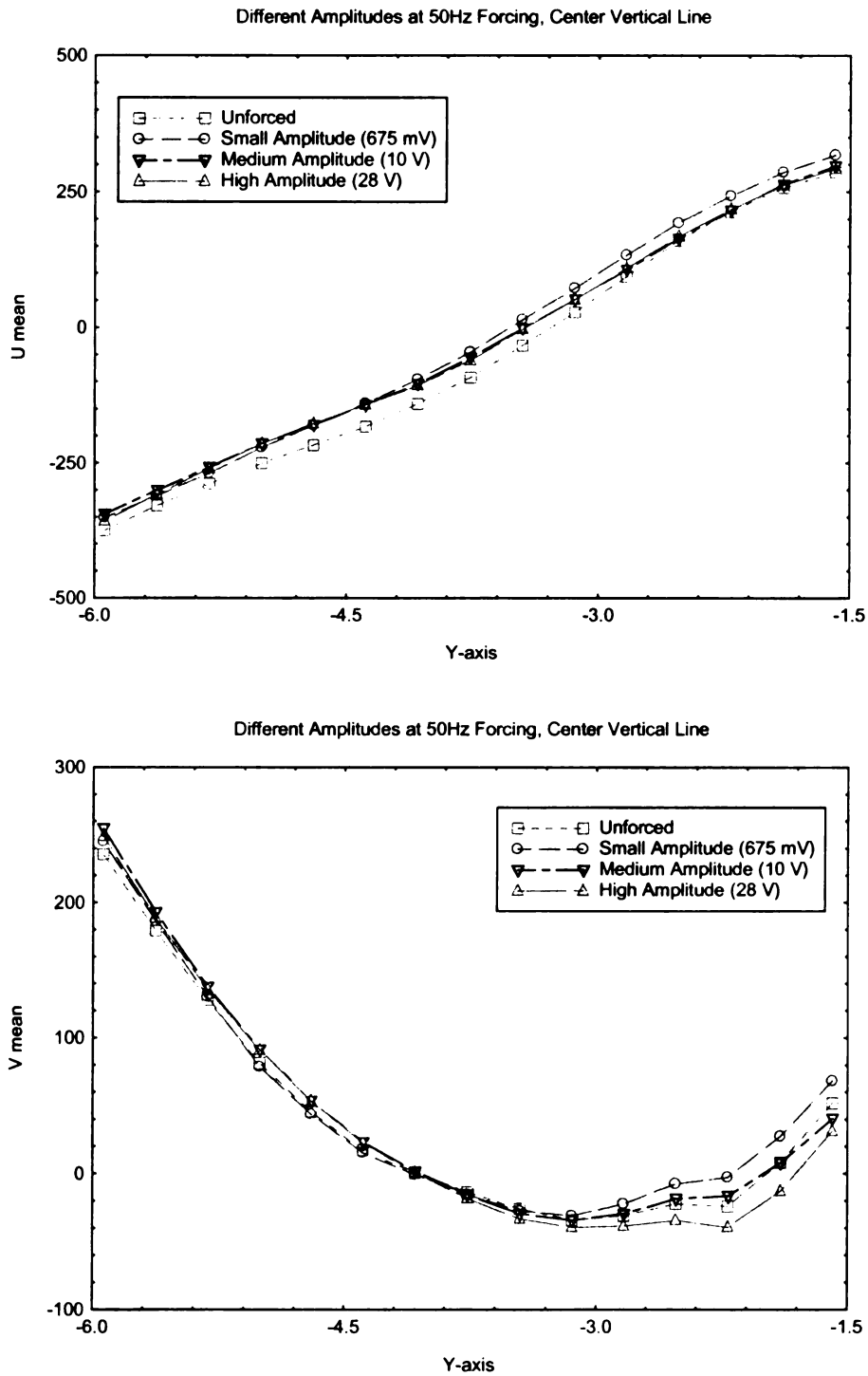

Figure 14. U mean (cm/s) and V mean (cm/s) of different amplitudes for vertical line taken at x = 4.5 cm from cylinder wall

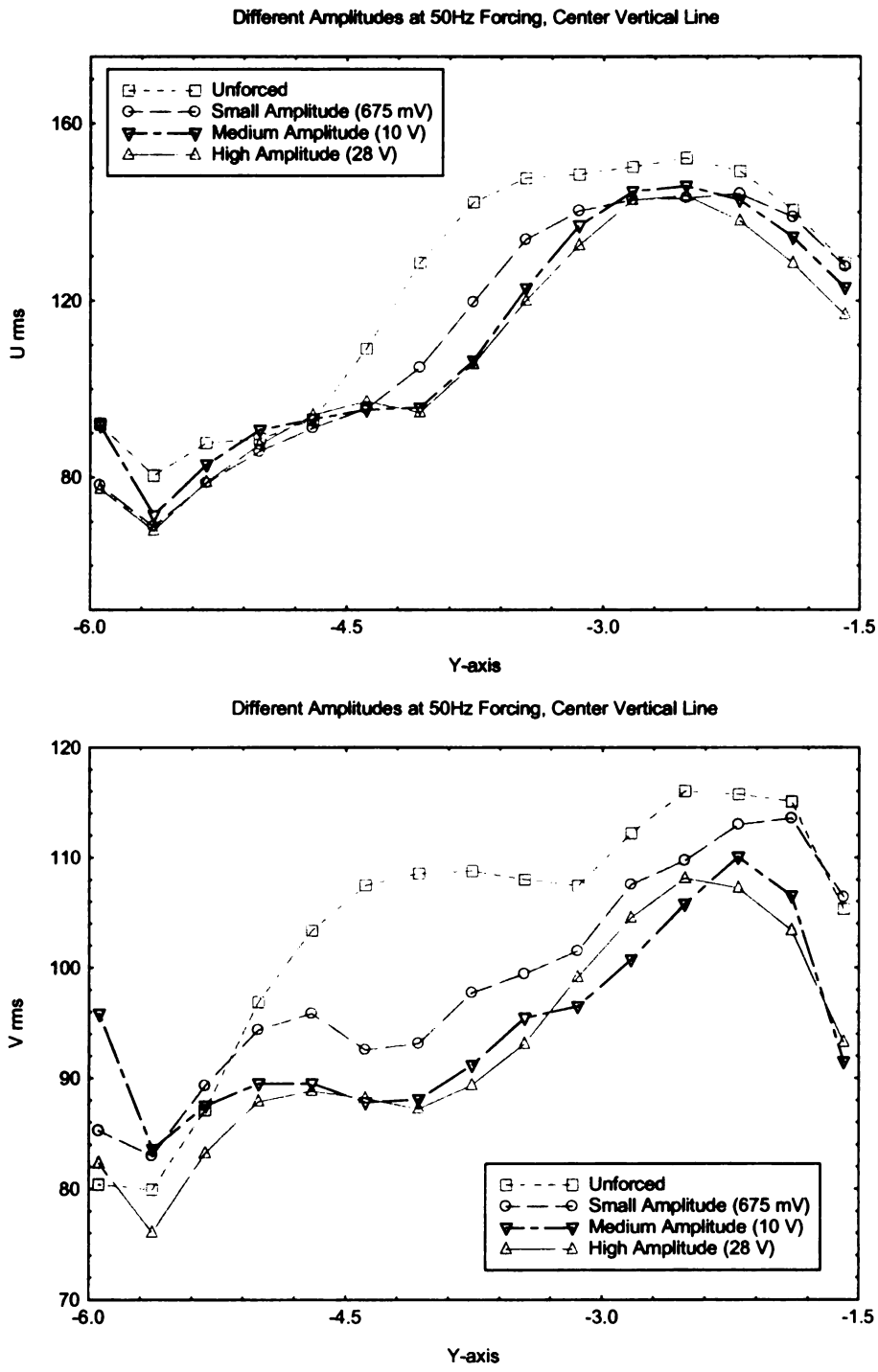

Figure 15. U rms (cm/s) and V rms (cm/s) of different amplitudes for vertical line taken at x = 4.5 cm from cylinder wall

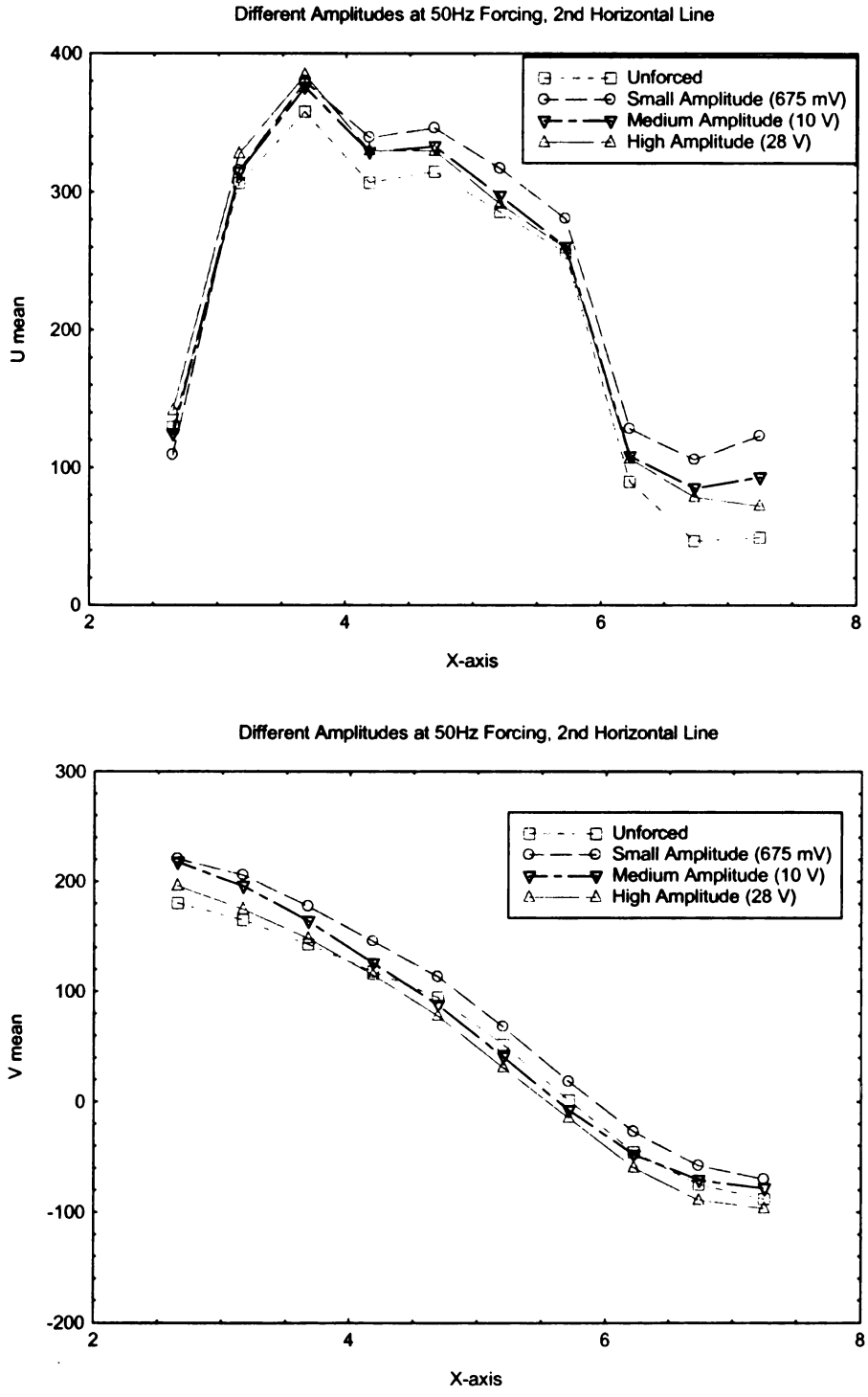

Figure 16. U mean (cm/s) and V mean (cm/s) of different amplitudes for horizontal line taken at y = 1.2 cm below the intake and exhaust valves

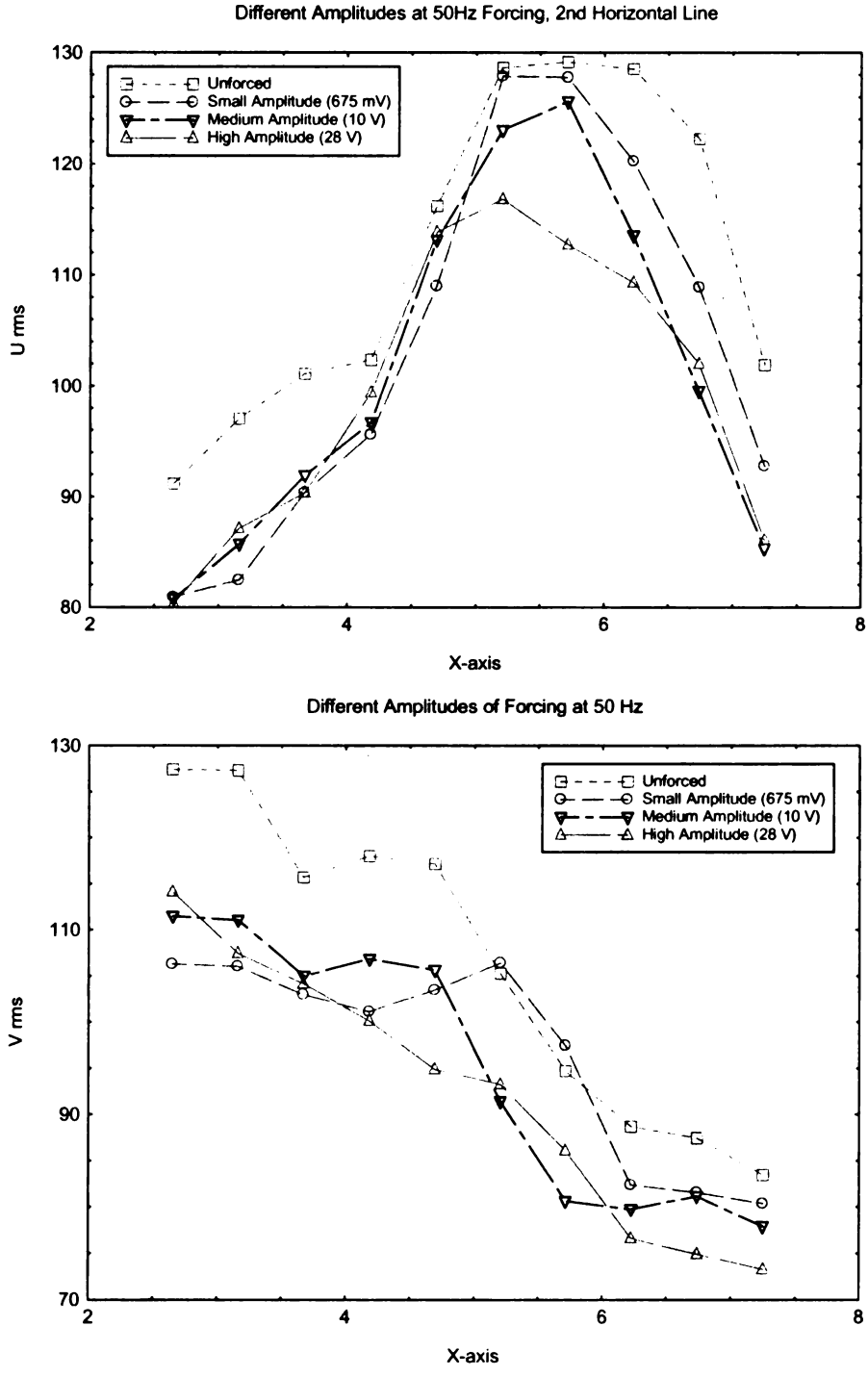

Figure 17. U rms (cm/s) and V rms (cm/s) of different amplitudes for horizontal line taken at y = 1.2 cm below the intake and exhaust valves

3.4 Free-run perturbations

At early stages of this research, the perturbation was done on free run mode. In this mode, the speaker was turned "on" continuously with the engine at respective frequency. The number of realizations averaged was 200 realizations for each frequency case in the experiment. This was the only experiment with 200-realization average. The rests of the experiments in the thesis were with 500-realization average.

In the experiment, the range of frequencies investigated was from 50Hz to 4000Hz. Nevertheless, from this experiment, it was found that the best reduction occurred at low frequency, namely frequency below 400Hz. Beyond 400Hz, there was no significant reduction in velocity rms or cycle-to-cycle variation. This is consistent with what Ambrose had found. Ambrose found that the preferred frequency was at 40 Hz or a Strouhal Number of 1.19 [3]. According to Ambrose, a Strouhal number ($St_D = fD/U$) for the piston-cylinder configuration could be based on the maximum mean velocity of the flow through the intake valve opening, the diameter of the valve and the forcing frequency [3]. In this research, with the valve diameter of 37 mm and the maximum mean velocity of 10 m/s, the preferred frequency would be at 321.62 Hz.

The results are organized in the following manner; starting with U mean and U rms, then followed by V mean and V rms. Figure 18 showed the results for U mean and U rms taken from running the engine at 600 rpm and 270 CAD. The color contour showed the U rms. In other words, the cycle-to-cycle variation is reduced if the rms value is reduced. The trend of the results was as the frequency of the perturbation increased, the U rms decreased.

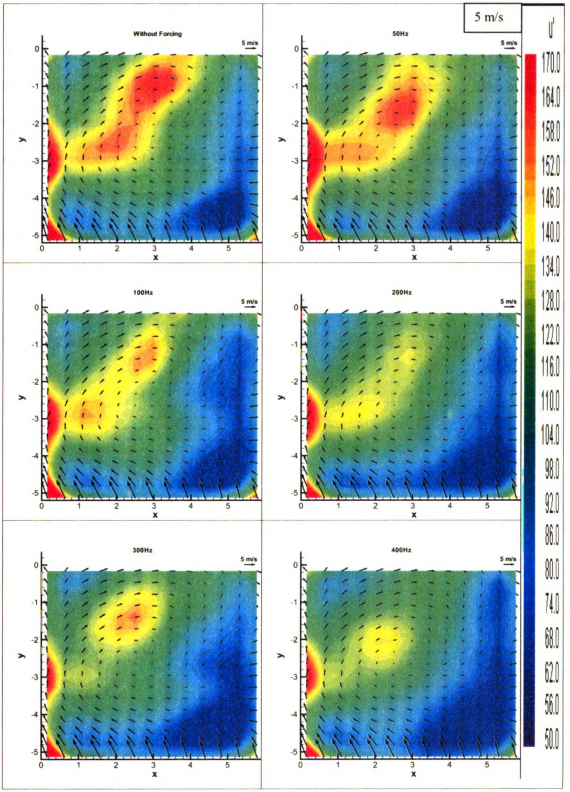

Figure 18. Ensemble averaged results showing rms velocity (cm/s),U mean, without perturbation and with perturbation of 50Hz, 100Hz, 200Hz, 300Hz and 400Hz at 270 CAD

Figure 19 and 20 show lines plots of U mean and U rms. From Figure 19 and 20, it is obvious that the perturbation did not have effect on the U mean flow. The U mean stayed about the same values throughout the whole frequencies. However, the perturbation had huge effect on the U rms that represents the cycle-to-cycle variation and fluctuating velocity field. As the frequency increased, the U rms decreased. The largest reduction among all was the 400Hz case. It showed about 25% to 30% reduction at certain region of the flow field.

The results for V mean and V rms are shown in Figure 21 with the same way of organizing the results; starting with color contour plots and then line plots.

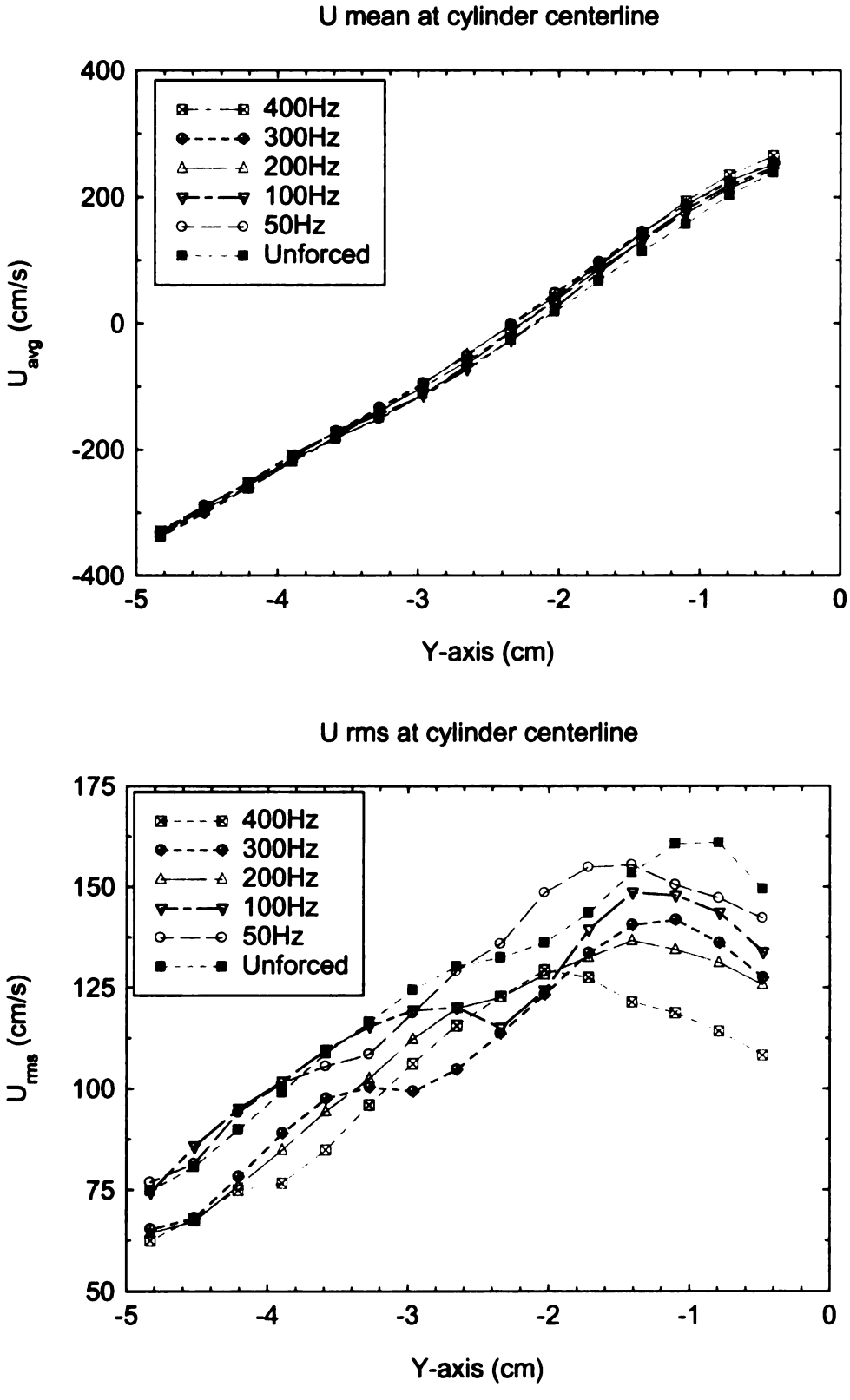

Figure 19. Effect of perturbations on the U mean and U rms at cylinder centerline, about 4.5 cm from cylinder wall

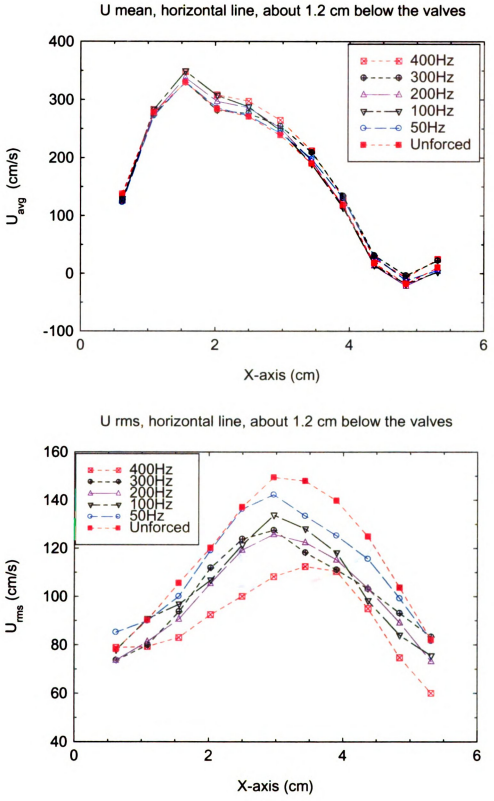

Figure 20. Effect of perturbations on the U mean and U rms at horizontal line about 1.2 cm below the intake and exhaust valves

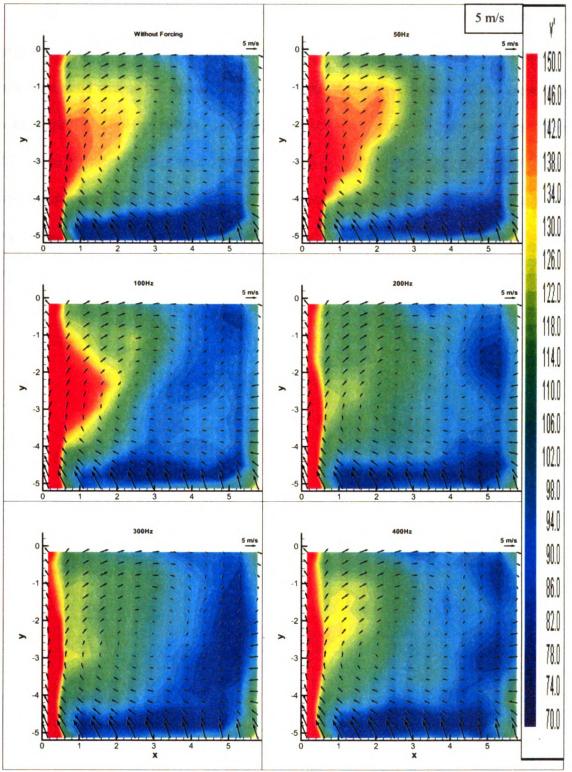

Figure 21. Ensemble averaged results showing rms velocity (cm/s),V mean, without perturbation and with perturbation of 50Hz, 100Hz, 200Hz, 300Hz and 400Hz at 270 CAD

Figure 21 showed the results for V mean and V rms taken from running the same engine condition which was at 600 rpm and 270 CAD. The color contour showed the V rms. The trend was as the frequency increased, the V rms was reduced. There were huge reductions for 200Hz, 300Hz and 400Hz cases. One could notice huge reduction difference between 100Hz and 200Hz. The red-and-yellow-color region in the 100Hz case disappeared when the frequency was increased to 200Hz. In order words, the V rms was reduced to smaller value by increasing frequency from 100Hz to 200Hz. The line plots for V mean and V rms are shown in Figure 22 and 23.

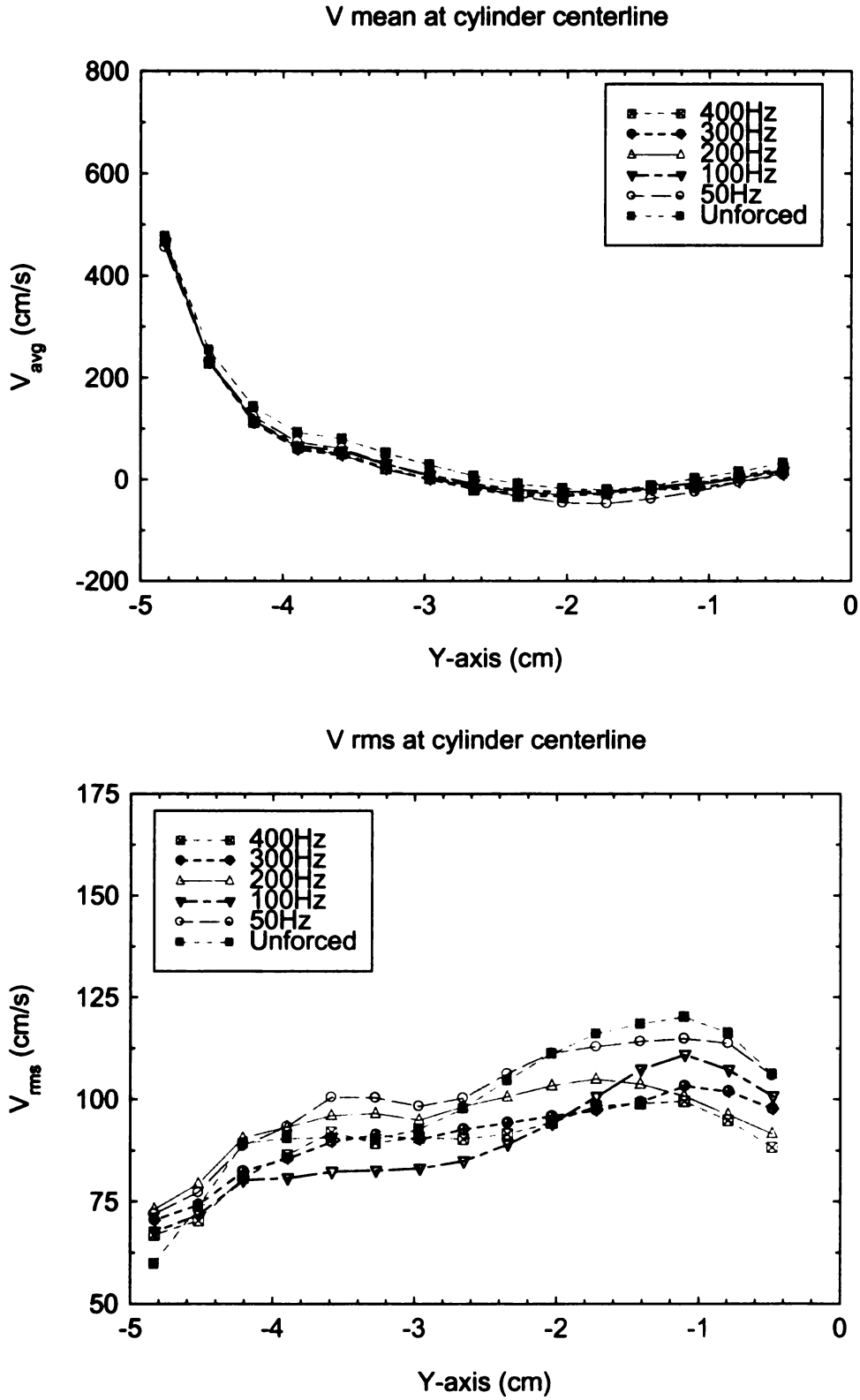

Figure 22. Effect of perturbations on the V mean and V rms at cylinder centerline, about 4.5 cm from cylinder wall

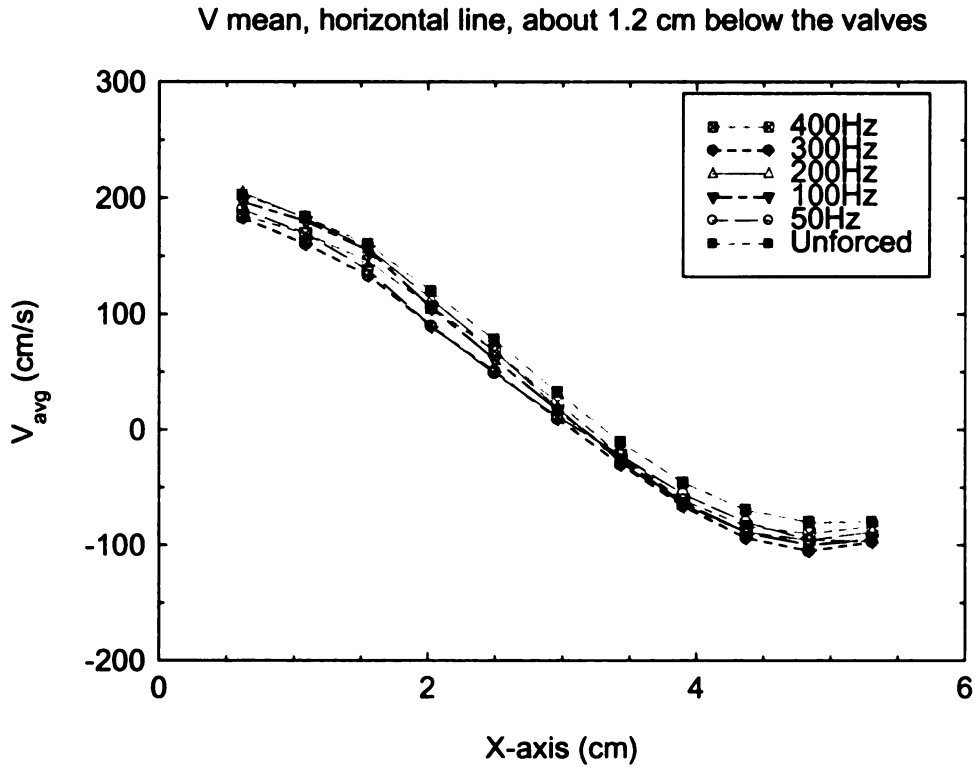

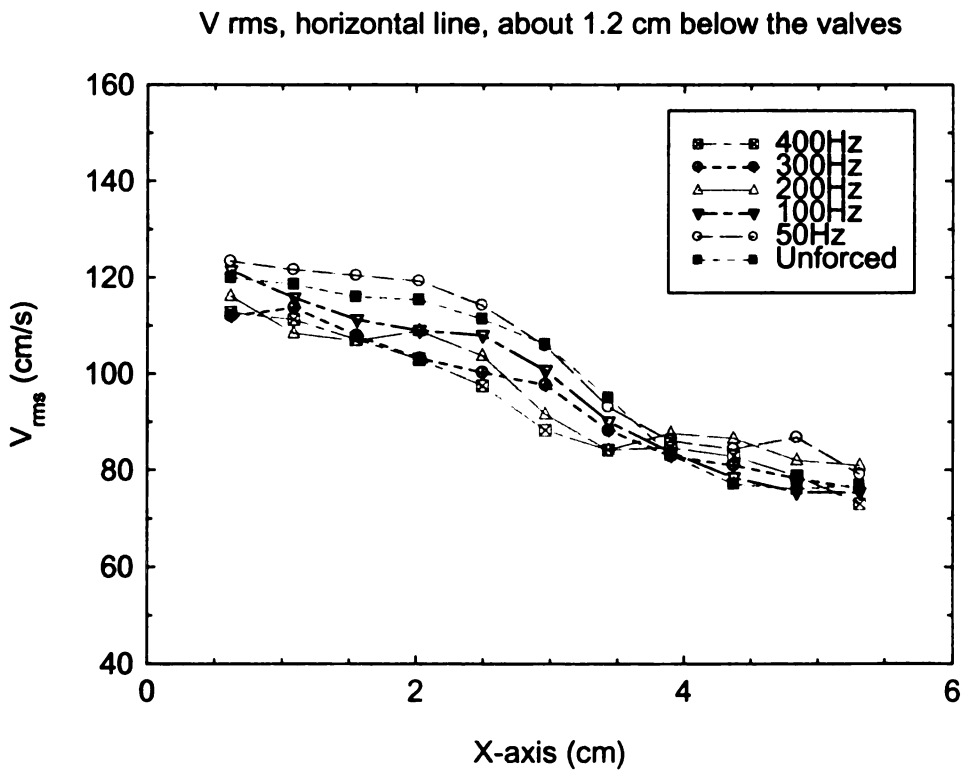

Figure 23. Effect of perturbations on the V mean and V rms at horizontal line about 1.2 cm below the intake and exhaust valves

3.5 Fixed-time perturbations : Perturbation from 0 CAD to 180 CAD

In all these experiments, the starting and ending points of the perturbation were timed. The timing of the perturbation was done by using the burst mode of a function generator. The speaker would only start perturbing when the piston reached Top Dead Center (TDC). It would continue to perturb from 0 CAD to 180 CAD. The duration of perturbation was 0.05 seconds.

3.5.1 Perturbation from 0 CAD to 180 CAD with no phase shift

The engine condition was the same as in the previous experiments. The experiment was done at 600 rpm and 270 CAD. The range of frequencies investigated was from 50 Hz to 4000 Hz. Each frequency case was averaged from 500 continuous, instantaneous realizations. The reason for choosing this frequency range was based on the previous experiment (free-run experiment). From the free-run experiment, it was found that the perturbation had no noticeable effect beyond 4000 Hz and below 50 Hz. Perturbation with no phase shift here is referring to the sine wave coming out from the amplifier. The starting point of the sine wave was at 0 degree.

The results had the same trend as the free run results. There was a noticeable reduction in U rms and V rms at 300 Hz and 400 Hz. The reduction was about 20%-30%. As the frequency increased, the U rms and V rms decreased until 400 Hz and it increased beyond 400 Hz.

The best results of the experiment, namely from 30Hz to 1000Hz are shown in Figure 24, 25, 28 and 29. The results are organized in following manner; starting with U mean and U rms, then followed by V mean, V rms.

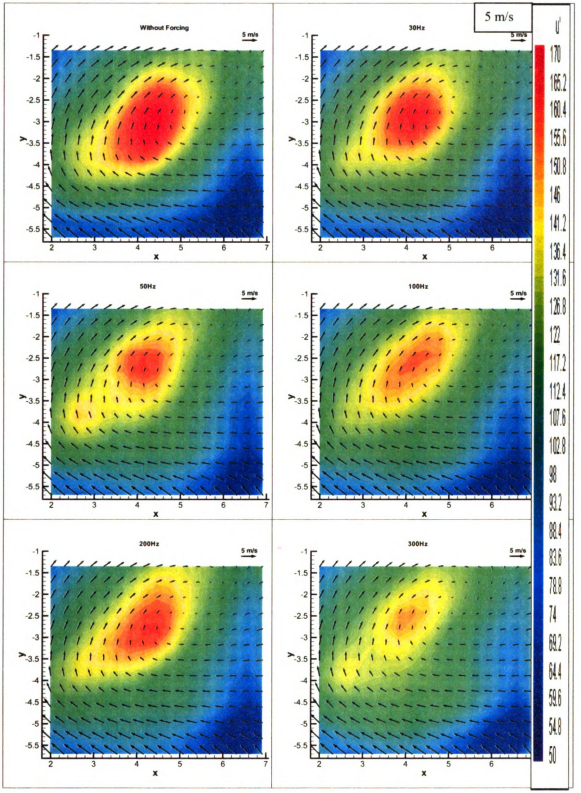

Figure 24. Ensemble averaged results showing rms velocity (cm/s),U mean, without perturbation and with perturbation of 30Hz, 50Hz, 100Hz, 200Hz and 300Hz at 270 CAD

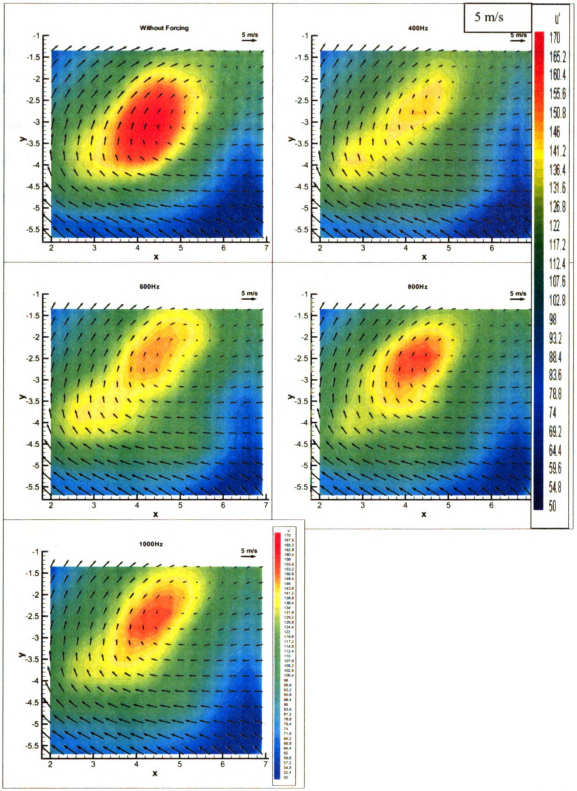

Figure 25. Ensemble averaged results showing rms velocity (cm/s),U mean, without perturbation and with perturbation of 400Hz, 600Hz, 800Hz and 1000Hz at 270 CAD

The trend of the results was as the frequency of the perturbation increased, the U rms decreased until 400Hz and then it started to increase beyond 400Hz. In the previous free-run perturbation experiment, the U mean and V mean of the flow did not change for cases with or without perturbation. However, for this fixed-time perturbation, the U mean and V mean of the flow decreased in velocity. They appeared to be slowing down with the perturbation.

The next few line plots of the same conditions, U mean and U rms, are shown in Figure 26 and 27.

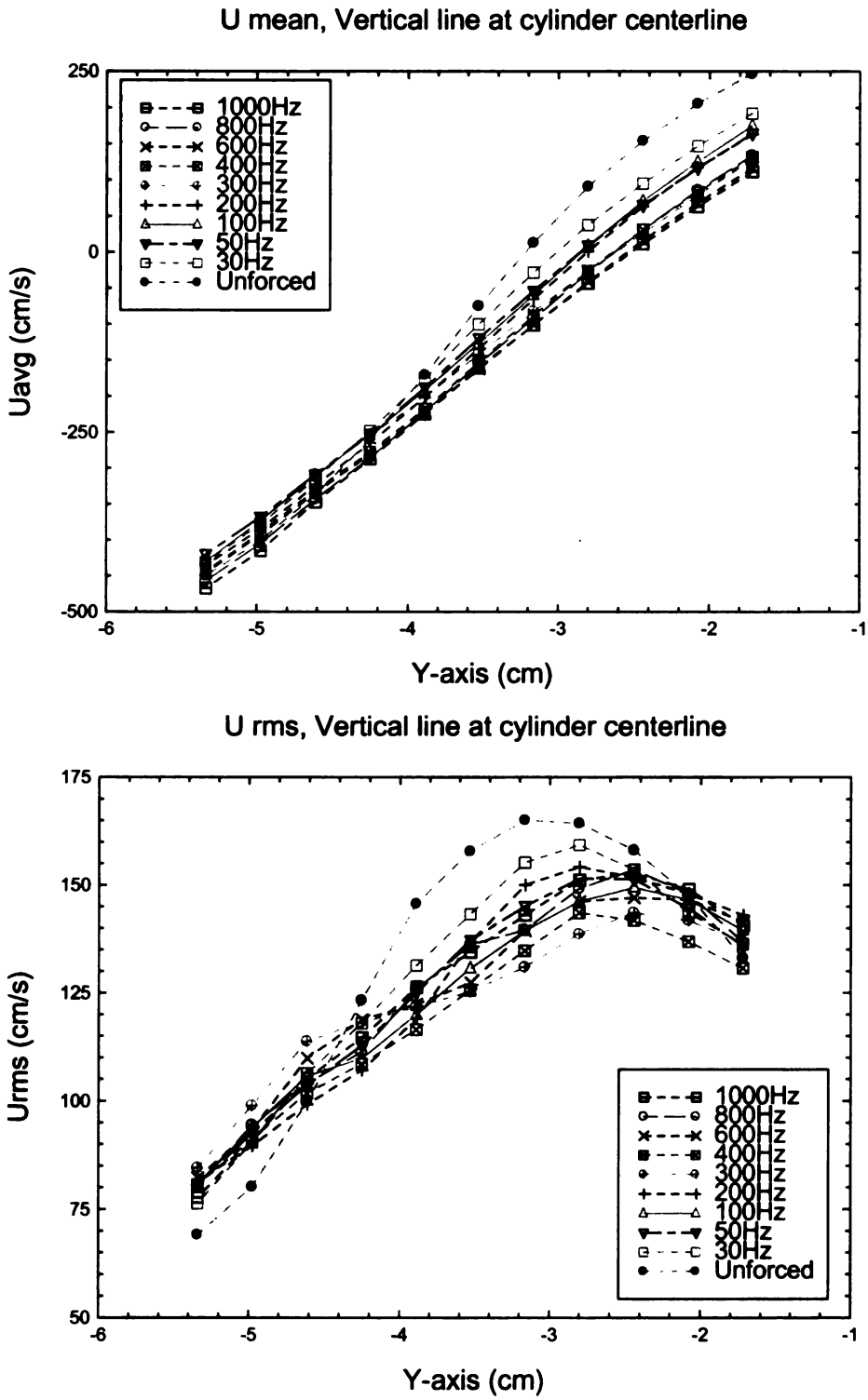

Figure 26. Effect of perturbations on the U mean and U rms at cylinder centerline, about 4.5 cm from cylinder wall

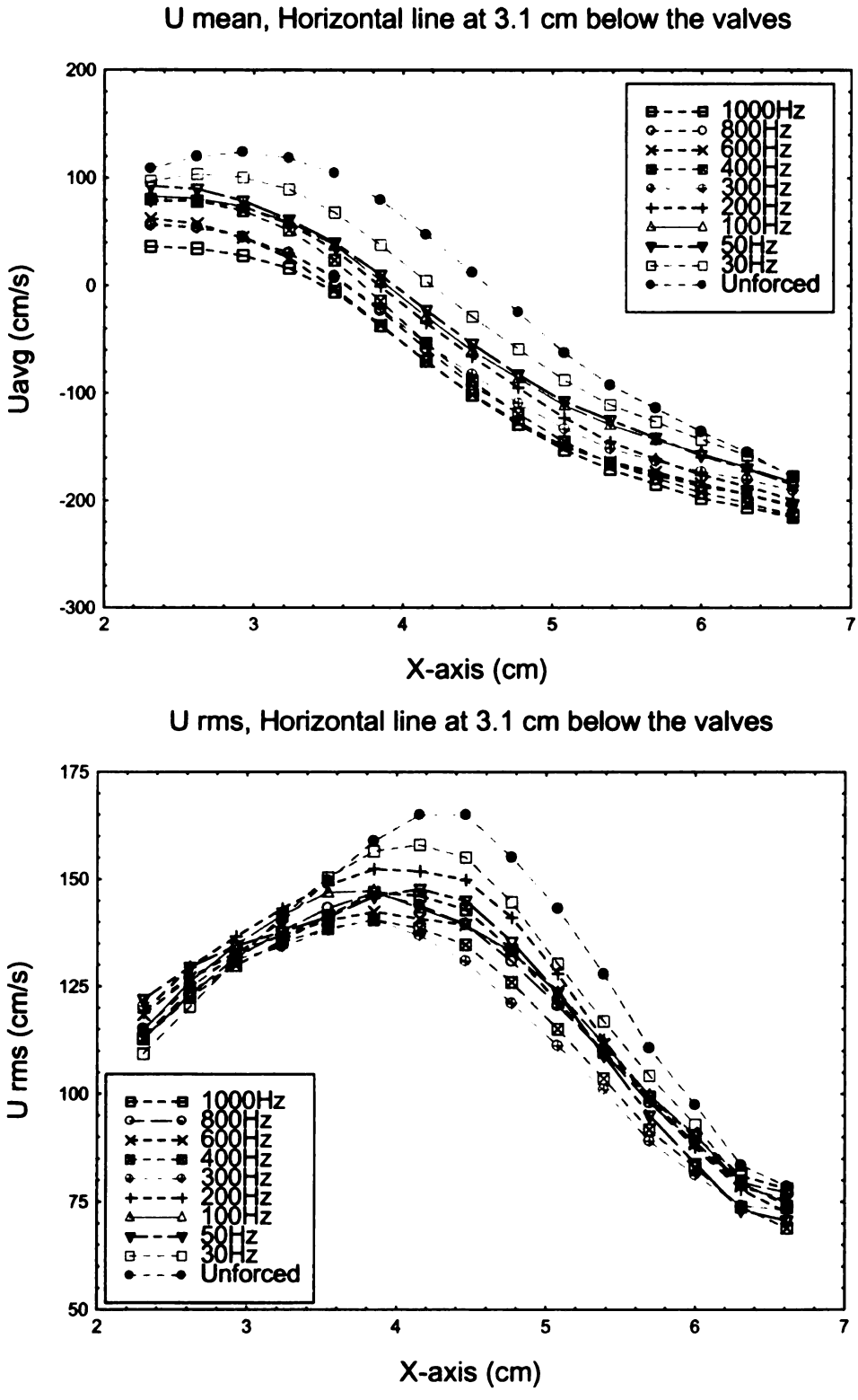

Figure 27. Effect of perturbations on the U mean and U rms at horizontal line about 3.1 cm below the intake and exhaust valves

From Figure 26 and 27, it is obvious that the perturbation had some effects on the U mean flow. The U mean decreased as the frequency increased. In some places of the flow, the U mean decreased as much as 70% to 80% of the unperturbed flow. The flow direction had changed too in some places of the flow. As for the U rms, the perturbation had huge effect on the U rms that represents the cycle-to-cycle variation and fluctuating velocity field. As the frequency increased, the U rms decreased until 400Hz and then it increased beyond 400Hz. The largest reduction among all were at 300Hz and 400Hz. In 300Hz case, it showed about 20% to 30% reduction at certain region of the flow field.

The results for V mean and V rms are shown in Figure 28 and 29 with the same way of organizing the result; starting from color contour plots and then line plots version of the results.

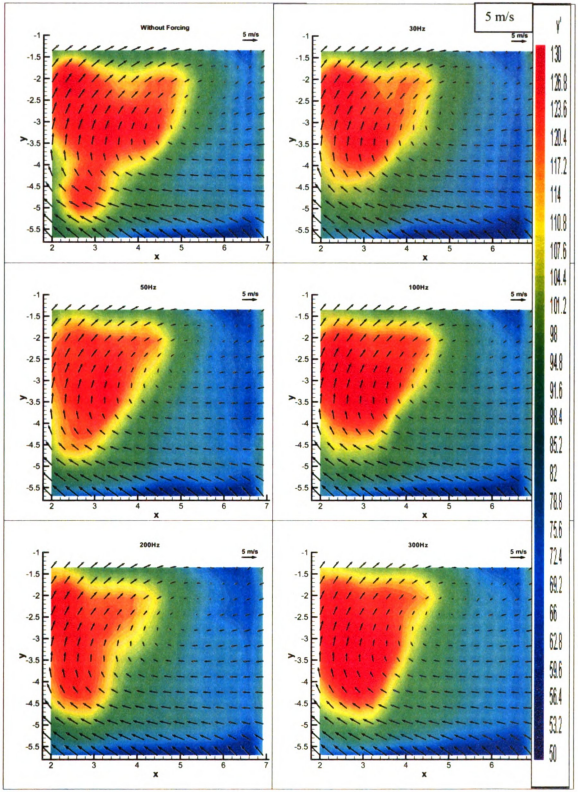

Figure 28. Ensemble averaged results showing rms velocity (cm/s),V mean, without perturbation and with perturbation of 30Hz, 50Hz, 100Hz, 200Hz and 300Hz at 270 CAD

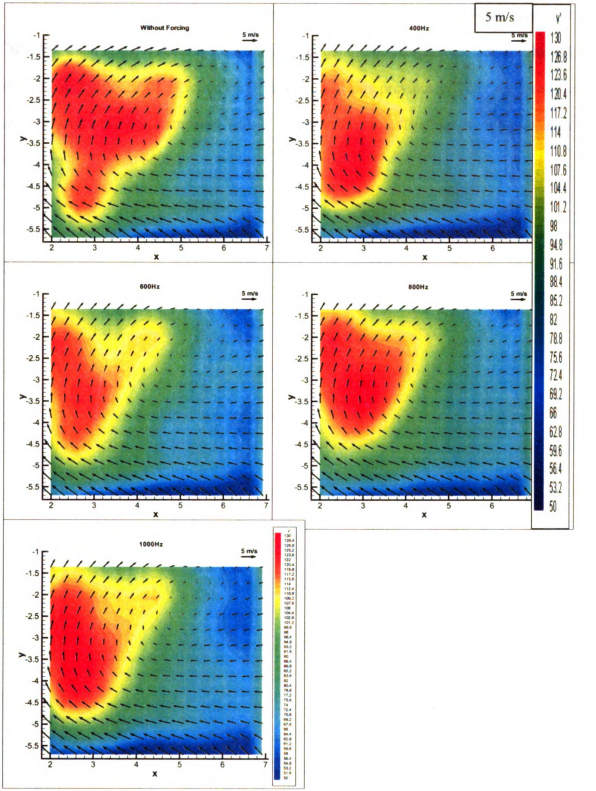

Figure 29. Ensemble averaged results showing rms velocity (cm/s),V mean, without perturbation and with perturbation of 400Hz, 600Hz, 800Hz and 1000Hz at 270 CAD

Figure 28 and 29 showed the results for V mean and V rms taken at 600 rpm and 270 CAD. Each of the frequency case had an average of 500 realizations. The results did not show any clear trend as found in U mean and U rms previously. They appeared to have less rms reduction compared with U mean and U rms. The best V rms reduction cases were 400Hz and 600Hz.

The next few line plots of the same conditions, V mean and V rms, are shown in Figure 30 and 31.

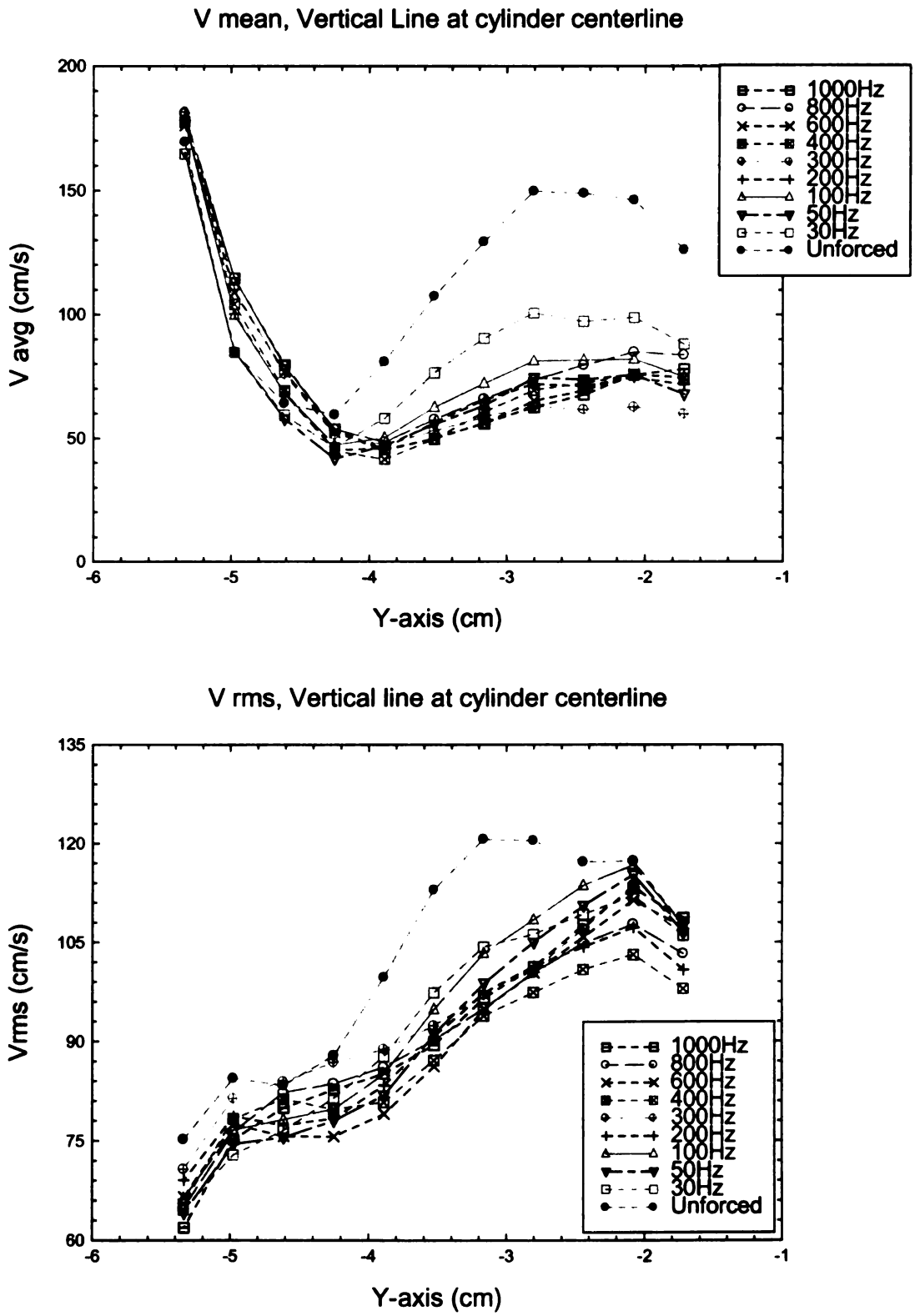

Figure 30. Effect of perturbations on the V mean and V rms at cylinder centerline, about 4.5 cm from cylinder wall

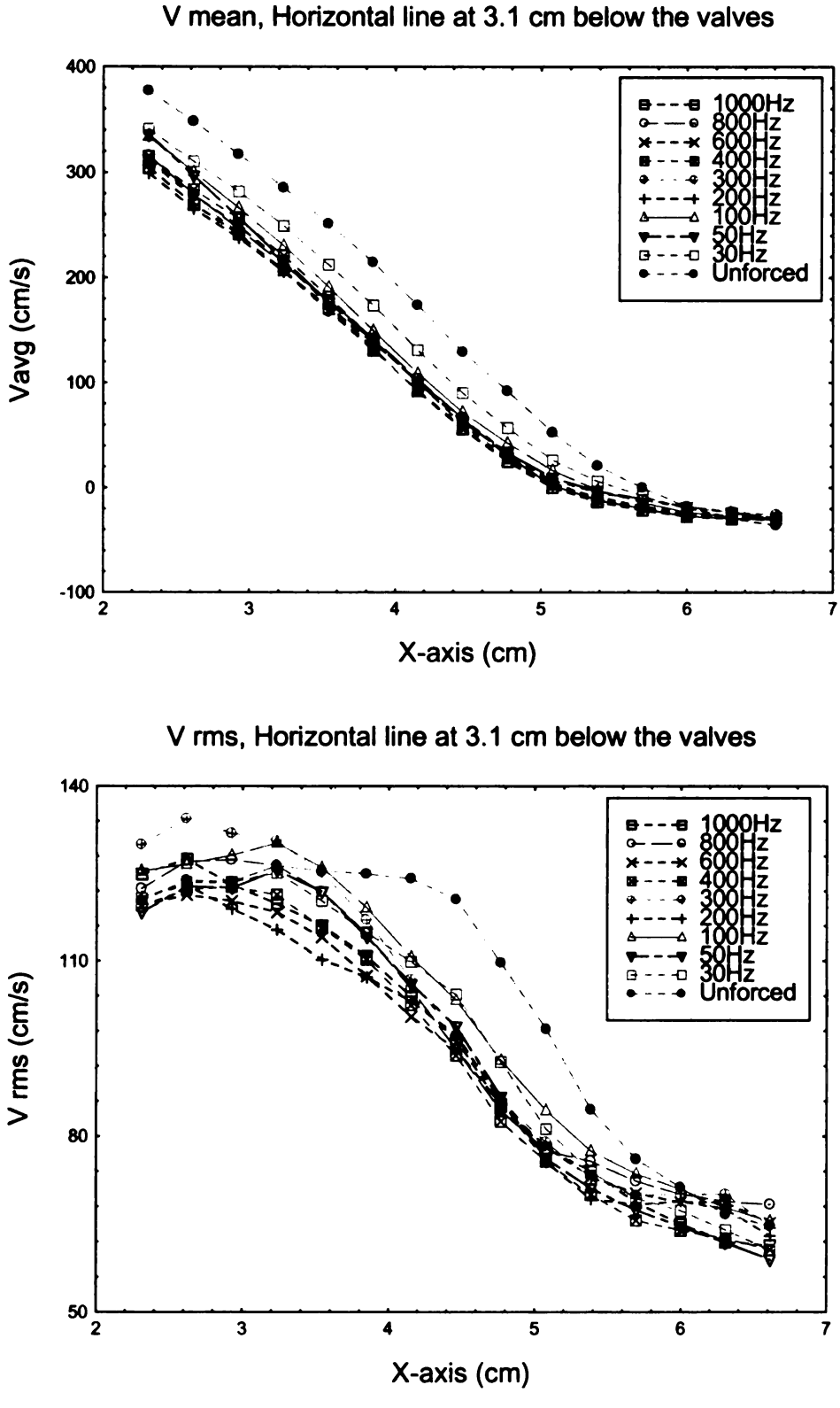

Figure 31. Effect of perturbations on the V mean and V rms at horizontal line about 3.1 cm below the intake and exhaust valves

Some observations could be made from the previous line plots. The perturbation had some effects on the V mean flow, the same effects that could be found on U mean flow. The V mean decreased as the frequency increased. In some places of the flow, the V mean decreased as much as 40% to 50% of the unperturbed flow. As for the V rms, the perturbation had some effects on the V rms too. As the frequency increased, the V rms decreased until the frequency reached between 400Hz and 600Hz. It increased beyond 600Hz. The largest reduction among all were at 400Hz and 600Hz. In 400Hz case, it showed about 20% to 30% reduction at certain region of the flow field.

3.5.2 Perturbation from 0 CAD to 180 CAD with 90^0 phase shift

Like the previous experiment, the starting and ending points of the perturbation were timed. The perturbation was turned "on" from 0 CAD to 180 CAD with an input sine wave of 28 V amplitude. Nevertheless, in this experiment, the input sine wave was shifted $+90^0$ in phase. The starting point of the input sine wave was at 90^0 instead of 0^0. The range of frequencies investigated was from 50Hz to 4000Hz.

The main observation of the experiment was that the perturbation did not reduce the U rms and V rms. The main effect of the perturbation was that it increased the U rms and V rms instead to about 10% to 20% increment.

The color contour plots of the results with frequency range from 50Hz to 500Hz are shown in Figure 32, 33, 34 and 35.

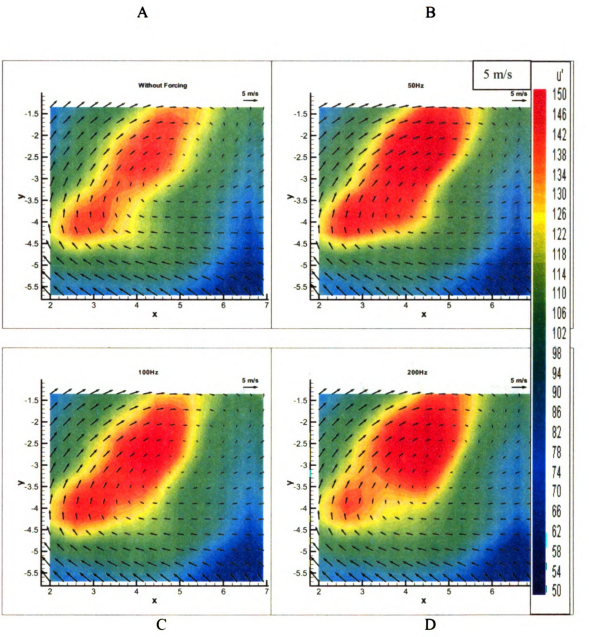

Figure 32. Ensemble averaged results showing rms velocity (cm/s),U mean (cm/s), (A): without perturbation and with perturbation (B):50Hz, (C):100Hz, (D):200Hz at 270 CAD

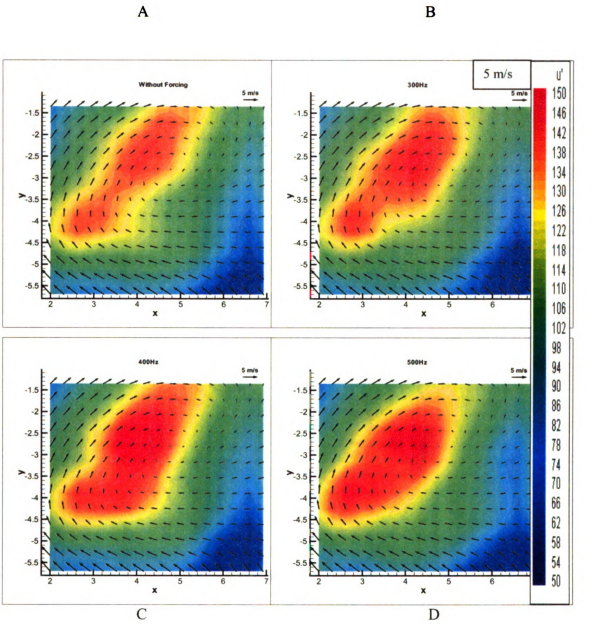

Figure 33. Ensemble averaged results showing rms velocity (cm/s),U mean (cm/s), (A): without perturbation and with perturbation (B):300Hz, (C):400Hz, (D):500Hz at 270 CAD

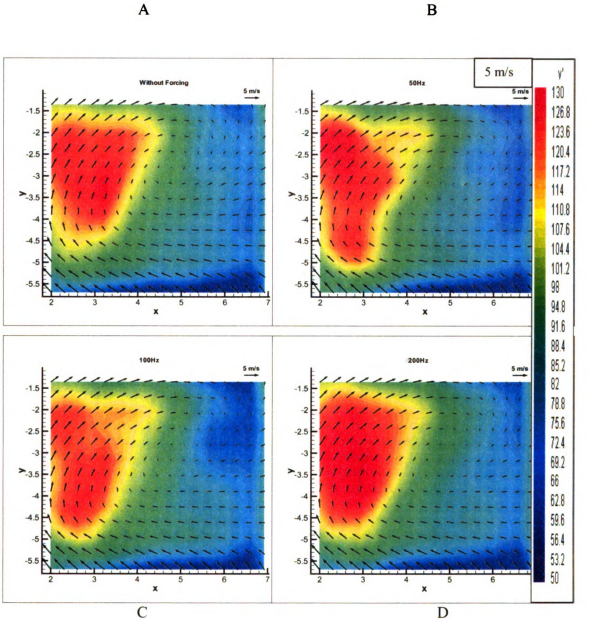

Figure 34. Ensemble averaged results showing rms velocity (cm/s),V mean (cm/s), (A): without perturbation and with perturbation (B):50Hz, (C):100Hz, (D):200Hz at 270 CAD

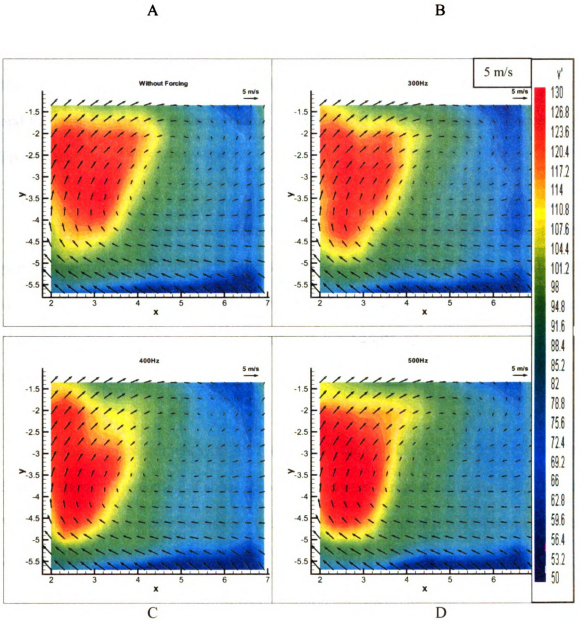

Figure 35. Ensemble averaged results showing rms velocity (cm/s),V mean (cm/s), (A): without perturbation and with perturbation (B):300Hz, (C):400Hz, (D):500Hz at 270 CAD

3.5.3 Perturbation from 0 CAD to 180 CAD with -90^0 phase shift

In this experiment, the start of the perturbation sine wave was shifted -90^0. Like the previous experiment, the starting and ending points of the perturbation were timed and the perturbation was performed from 0 CAD to 180 CAD. The range of frequencies investigated was from 50Hz to 4000Hz.

The results did not show a clear trend as in the cases of free-run and timed perturbation without phase shift. In the previous cases, free-run and timed perturbation without phase shift cases, both cases showed that the perturbation reduced the U rms and V rms as the frequency increased until 400Hz. Beyond 400Hz, the perturbation increased the U rms and V rms.

As for this experiment with -90^0 phase shift, the best U rms reduction case was at 50Hz. It showed a reduction of about 10% to 20% at certain region of the flow. As for the V rms, the best reduction case was at 500Hz. It also showed a reduction of about 10% to 20% at certain region of the flow.

The color contour plots of the results with frequency range from 50Hz to 500Hz are shown in Figure 36-39.

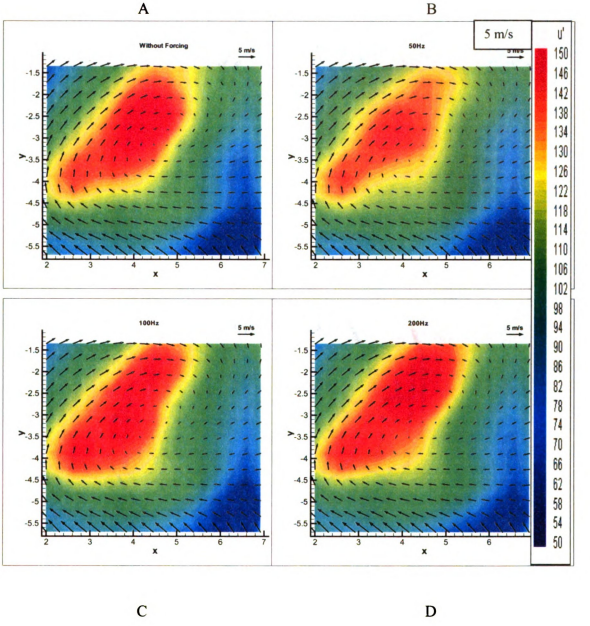

Figure 36. Ensemble averaged results showing rms velocity (cm/s),U mean (cm/s), (A): without perturbation and with perturbation (B):50Hz, (C):100Hz, (D):200Hz at 270 CAD

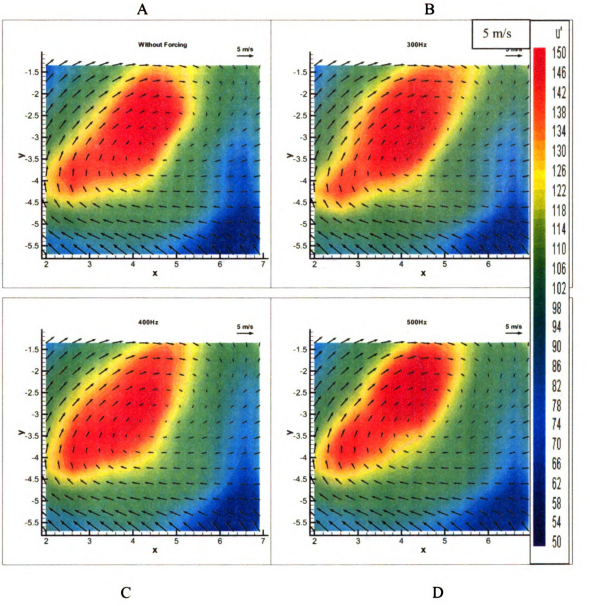

Figure 37. Ensemble averaged results showing rms velocity (cm/s),U mean (cm/s), (A): without perturbation and with perturbation (B):300Hz, (C):400Hz, (D):500Hz at 270 CAD

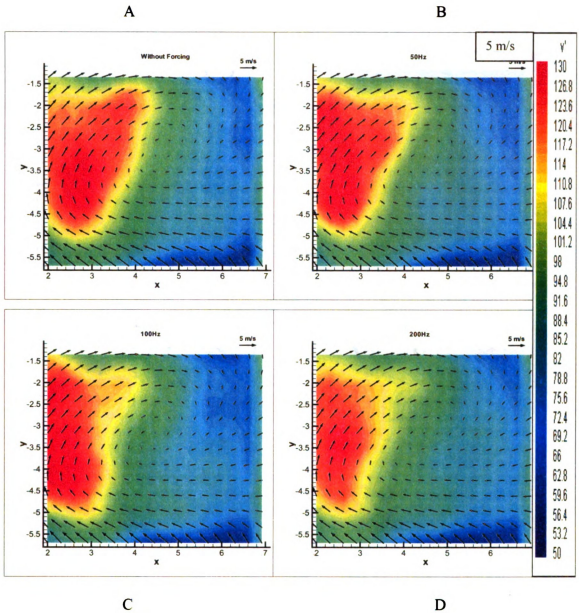

Figure 38. Ensemble averaged results showing rms velocity (cm/s),V mean (cm/s), (A): without perturbation and with perturbation (B):50Hz, (C):100Hz, (D):200Hz at 270 CAD

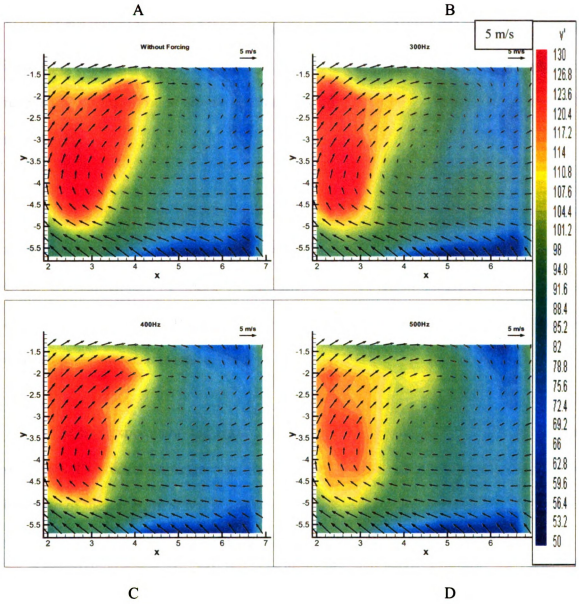

Figure 39. Ensemble averaged results showing rms velocity (cm/s),V mean (cm/s), (A): without perturbation and with perturbation (B):300Hz, (C):400Hz, (D):500Hz at 270 CAD

3.6 Fixed-time perturbations : Perturbation from 0 CAD to 90 CAD

After doing the fixed-time perturbation (0 CAD to 180 CAD) experiment, it was interesting to see what effect the flow would have if the duration of the perturbation were reduced. With this in mind, the flow in this experiment was only perturbed from 0 CAD to 90 CAD.

In this experiment, the starting and ending points of the perturbation were fixed. It started to perturb when the piston reached TDC and stopped when the piston reached 90 CAD. The experiment was done on 600 rpm and 270 CAD. The range of frequencies investigated was from 50 Hz to 4000 Hz. Each frequency case had an average from 500 continuous, instantaneous realizations.

For this experiment, the results did not have a clear trend of U rms and V rms reduction. The reduction range was from 10% to 20% for both U rms and V rms. The best case of the experiment was the 600Hz case for maximum U rms reduction. As for V rms, the best reduction case occurred at 1000Hz.

The color contour plots of the results with frequency range from 600Hz to 1000Hz are shown in Figure 40 and 41.

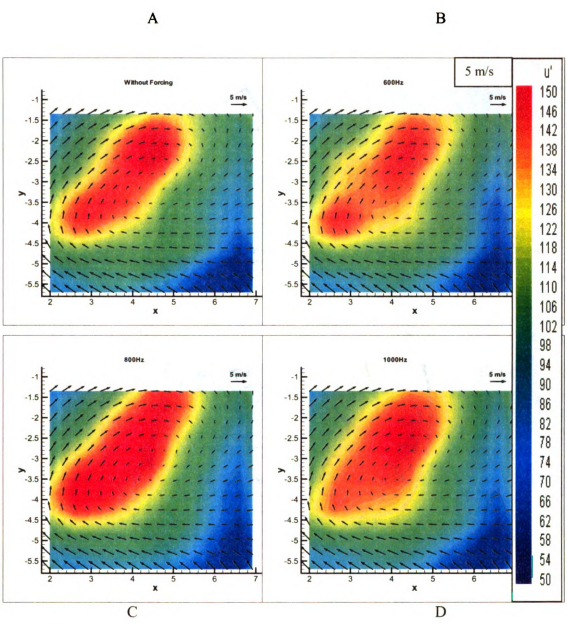

Figure 40. Ensemble averaged results showing rms velocity (cm/s),U mean (cm/s), (A): without perturbation and with perturbation (B):600Hz, (C):800Hz, (D):1000Hz at 270 CAD

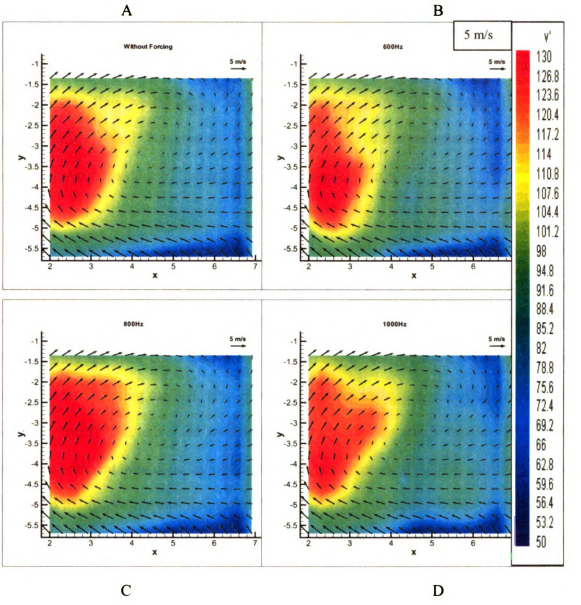

Figure 41. Ensemble averaged results showing rms velocity (cm/s),V mean (cm/s), (A): without perturbation and with perturbation (B):600Hz, (C):800Hz, (D):1000Hz at 270 CAD

3.7 Sweeping perturbations : sweep frequencies starting from 100Hz

The main reason that motivated this experiment was that the intake valves opened in a linear manner during the intake stroke. If the perturbation were fixed at certain frequency, the flow would not be perturbed at that frequency in the beginning of the valves opening period. To improve the maximum effect of the perturbation to the flow, the perturbation was done by sweeping the frequencies linearly.

This part of the experiment was done by utilizing the sweeping mode of the function generator. As in the previous few experiments, all the perturbation frequencies were fixed. For example, when the flow was said to be perturbed at 400Hz, it was done by perturbing the flow constantly at 400Hz throughout the experiment using free-run method or fixed timing method. However, in this experiment, the perturbed frequencies increased linearly but at a fixed starting point of perturbation which was at TDC. Each case of experiment was done by perturbing the flow starting at 100Hz and then swept linearly to the respective end frequency. Nevertheless, the duration of the sweeping was still only from 0 CAD to 180 CAD. In the case of engine running at 600 rpm, the duration of sweeping was 0.05 seconds.

The range of frequencies investigated in the experiment was from 200Hz to 2000Hz. The first case of sweeping frequencies was sweeping from 100Hz to 200Hz and the last case was sweeping from 100Hz to 2000Hz. The cases investigated were sweeping from 100Hz to 200Hz, sweeping from 100Hz to 300Hz, sweeping from 100Hz to 400Hz, sweeping from 100Hz to 600hz, sweeping from 100Hz to 800Hz, sweeping from 100Hz

to 1000Hz, sweeping from 100Hz to 1200Hz, sweeping from 100Hz to1400Hz, sweeping from 100Hz to 1600Hz, sweeping from 100Hz to 1800Hz and sweeping from 100Hz to 2000Hz (refer to Table 2).

Table 2. Cases investigated in the sweeping perturbation experiment.

100Hz to 200Hz	100Hz to 300Hz	100Hz to 400Hz	100Hz to 600Hz
100Hz to 800Hz	100Hz to 1000Hz	100Hz to 1200Hz	100Hz to 1400Hz
100Hz to 1600Hz	100Hz to 1800Hz	100Hz to 2000Hz	

The range of U rms and V rms reductions was from 20% to 25% in the experiment. The best reduction case for U rms was sweeping from 100Hz to 1200Hz case and the best reduction case for V rms was sweeping from 100Hz to 800Hz case. The color contour plots and line plots are shown in Figure 42-50. From the line plots in Figure 50, the U mean and V mean did not change much if compared with the fixed-time perturbation experiment.

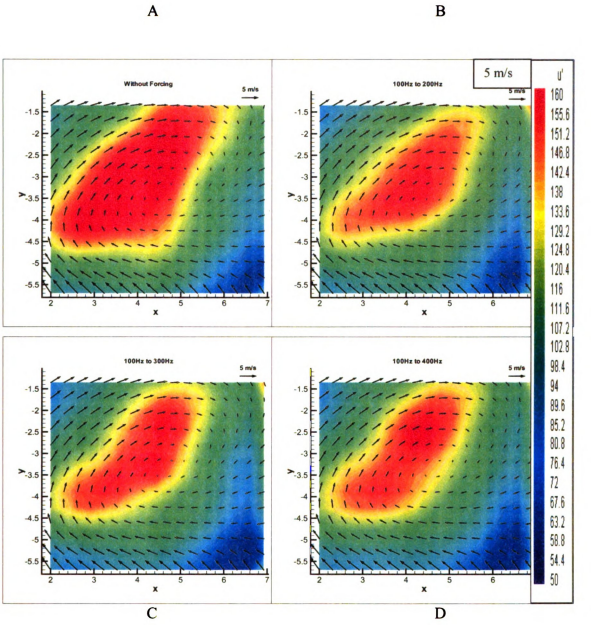

Figure 42. Ensemble averaged results showing rms velocity (cm/s),U mean (cm/s), (A): without perturbation and with perturbation (B):100Hz-200Hz, (C):100Hz-300Hz, (D):100Hz-400Hz at 270 CAD

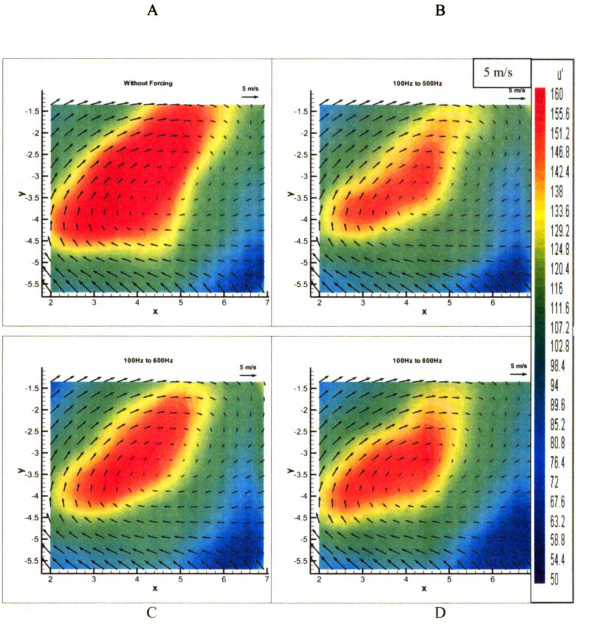

Figure 43. Ensemble averaged results showing rms velocity (cm/s),U mean (cm/s), (A): without perturbation and with perturbation (B):100Hz-500Hz, (C):100Hz-600Hz, (D):100Hz-800Hz at 270 CAD

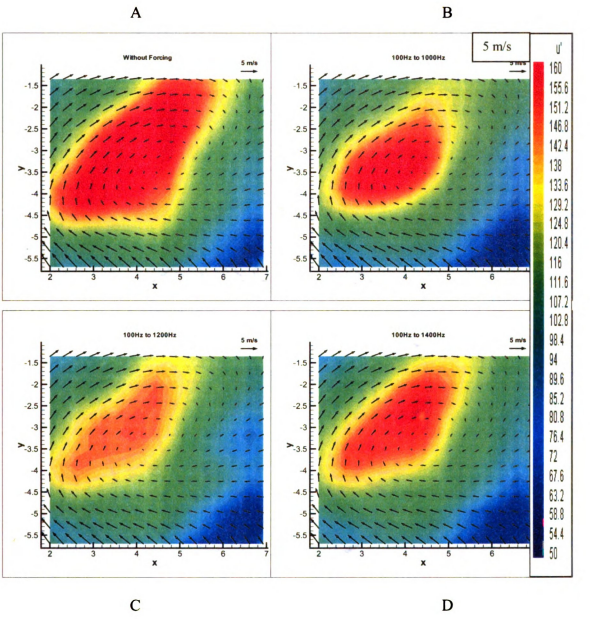

Figure 44. Ensemble averaged results showing rms velocity (cm/s),U mean (cm/s), (A): without perturbation and with perturbation (B):100Hz-1000Hz, (C):100Hz-1200Hz, (D):100Hz-1400Hz at 270 CAD

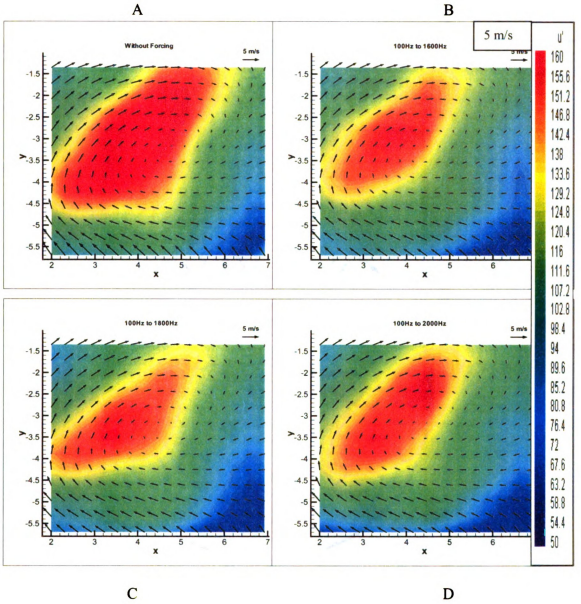

Figure 45. Ensemble averaged results showing rms velocity (cm/s),U mean (cm/s), (A): without perturbation and with perturbation (B):100Hz-1600Hz, (C):100Hz-1800Hz, (D):100Hz-2000Hz at 270 CAD

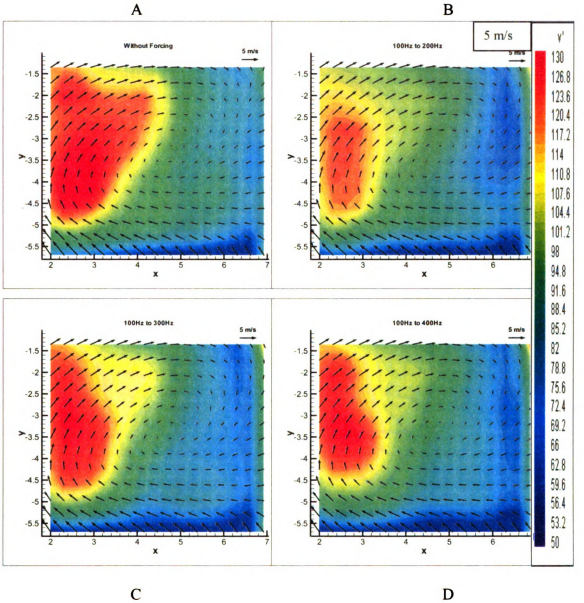

Figure 46. Ensemble averaged results showing rms velocity (cm/s),V mean (cm/s), (A): without perturbation and with perturbation (B):100Hz-200Hz, (C):100Hz-300Hz, (D):100Hz-400Hz at 270 CAD

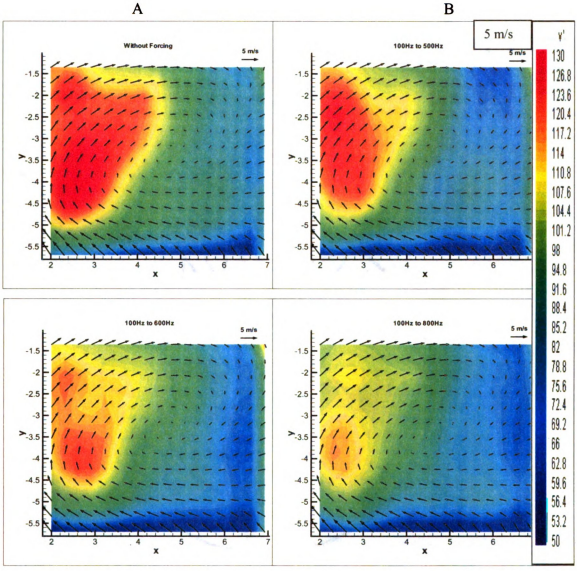

Figure 47. Ensemble averaged results showing rms velocity (cm/s),V mean (cm/s), (A): without perturbation and with perturbation (B):100Hz-500Hz, (C):100Hz-600Hz, (D):100Hz-800Hz at 270 CAD

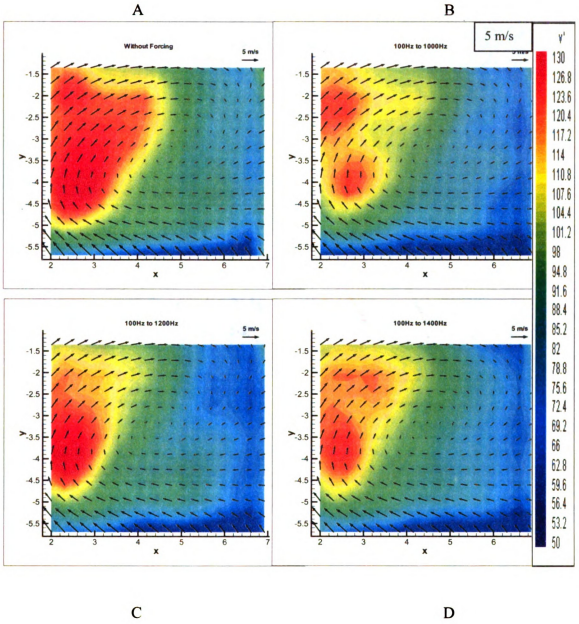

Figure 48. Ensemble averaged results showing rms velocity (cm/s),V mean (cm/s), (A): without perturbation and with perturbation (B):100Hz-1000Hz, (C):100Hz-1200Hz, (D):100Hz-1400Hz at 270 CAD

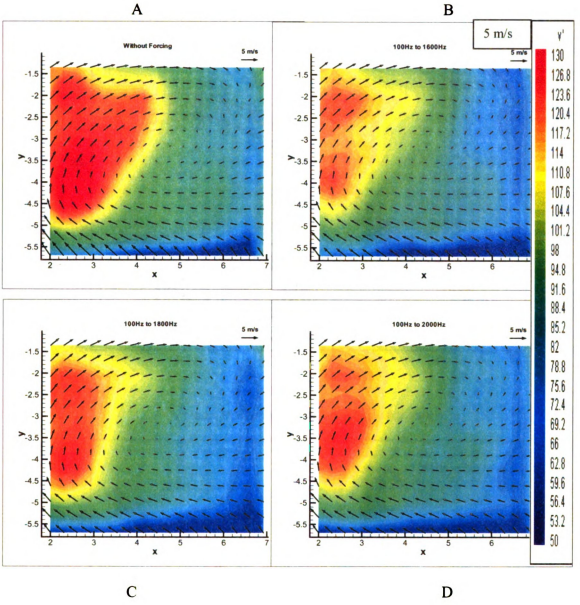

Figure 49. Ensemble averaged results showing rms velocity (cm/s),V mean (cm/s), (A): without perturbation and with perturbation (B):100Hz-1600Hz, (C):100Hz-1800Hz, (D):100Hz-2000Hz at 270 CAD

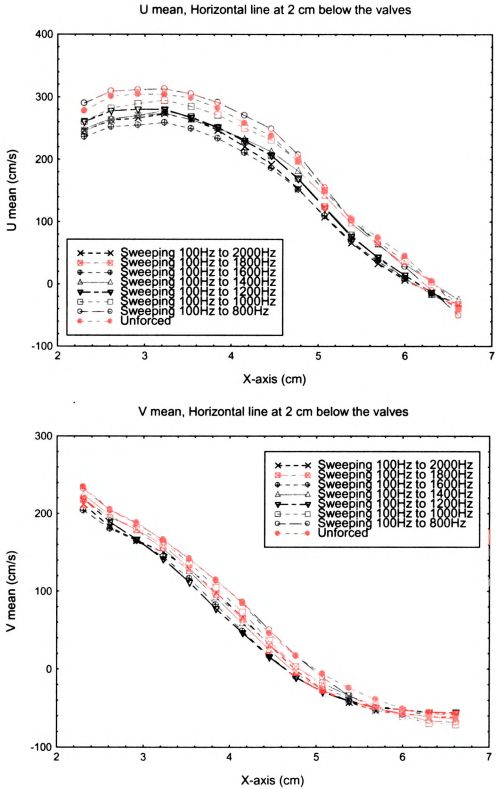

Figure 50. Effect of perturbations on the U mean and V mean at horizontal line about 2 cm below the intake and exhaust valves

3.8 Sweeping perturbations : sweep frequencies starting from 30Hz

The last part of 270 CAD experiment was to lower the starting value of the sweeping frequency to 30Hz. From previous sweeping experiment, it was found that the sweeping effects were about 20% to 25% reduction. With this in mind, it was desired to further the investigation of the sweeping effects by lowering the sweeping frequency to 30Hz instead of 100Hz. In each case of the experiment it was done by perturbing the flow starting at 30Hz and then swept linearly to the respective end frequency. The duration of sweeping was still 0.05 seconds. The range of the experiment was from 200Hz to 2000Hz. The other words, the first case of the experiment was sweeping from 30Hz to 200Hz and the last case was sweeping from 30Hz to 2000Hz.

The main observation of the experiment was that the reduction effects were not as strong as the previous 100Hz sweeping cases. The reduction was about 5% to 10% for both U rms and V rms. The best reduction case for U rms and V rms was sweeping from 100Hz to 400Hz case. The color contour plots are shown in Figure 51-58. U mean and U rms plots are shown first then followed by V mean and V rms.

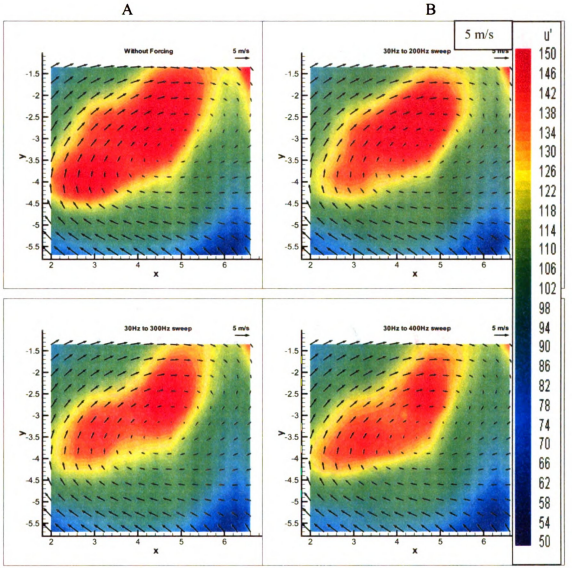

Figure 51. Ensemble averaged results showing rms velocity (cm/s),U mean (cm/s), (A): without perturbation and with perturbation (B):30Hz-200Hz, (C):30Hz-300Hz, (D):30Hz-400Hz at 270 CAD

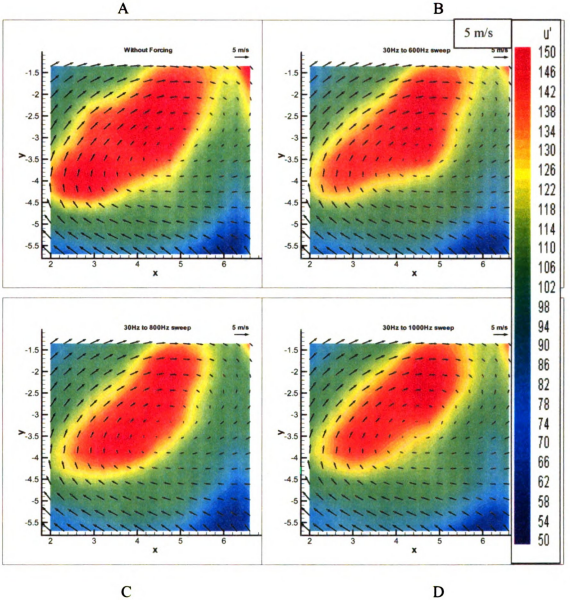

Figure 52. Ensemble averaged results showing rms velocity (cm/s),U mean (cm/s), (A): without perturbation and with perturbation (B):30Hz-600Hz, (C):30Hz-800Hz, (D):30Hz-1000Hz at 270 CAD

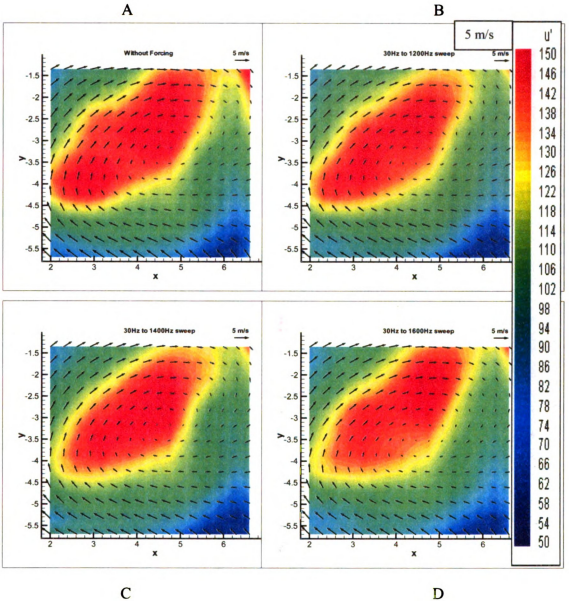

Figure 53. Ensemble averaged results showing rms velocity (cm/s),U mean (cm/s), (A): without perturbation and with perturbation (B):30Hz-1200Hz, (C):30Hz-1400Hz, (D):30Hz-1600Hz at 270 CAD

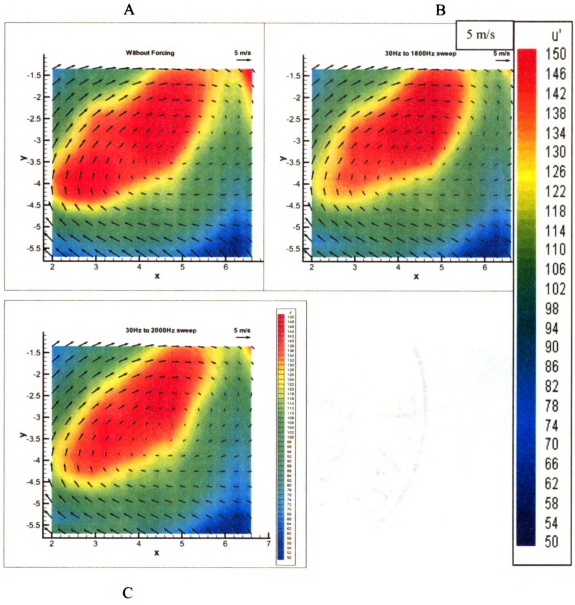

Figure 54. Ensemble averaged results showing rms velocity (cm/s),U mean (cm/s), (A): without perturbation and with perturbation (B):30Hz-1800Hz, (C):30Hz-2000Hz at 270 CAD

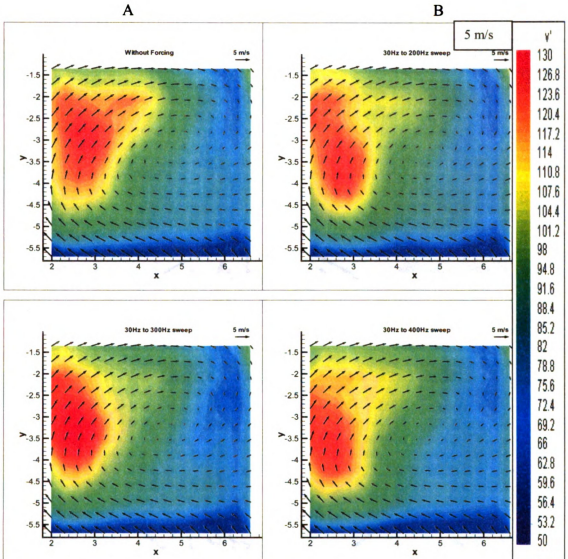

Figure 55. Ensemble averaged results showing rms velocity (cm/s),V mean (cm/s), (A): without perturbation and with perturbation (B):30Hz-200Hz, (C):30Hz-300Hz, (D):30Hz-400Hz at 270 CAD

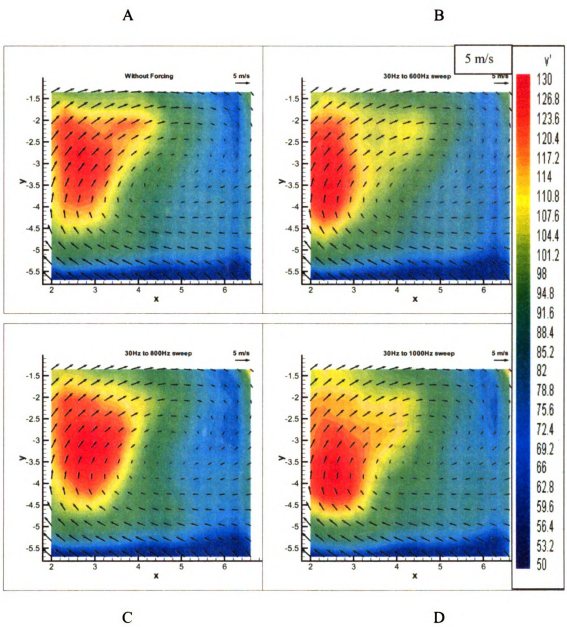

Figure 56. Ensemble averaged results showing rms velocity (cm/s),V mean (cm/s), (A): without perturbation and with perturbation (B):30Hz-600Hz, (C):30Hz-800Hz, (D):30Hz-1000Hz at 270 CAD

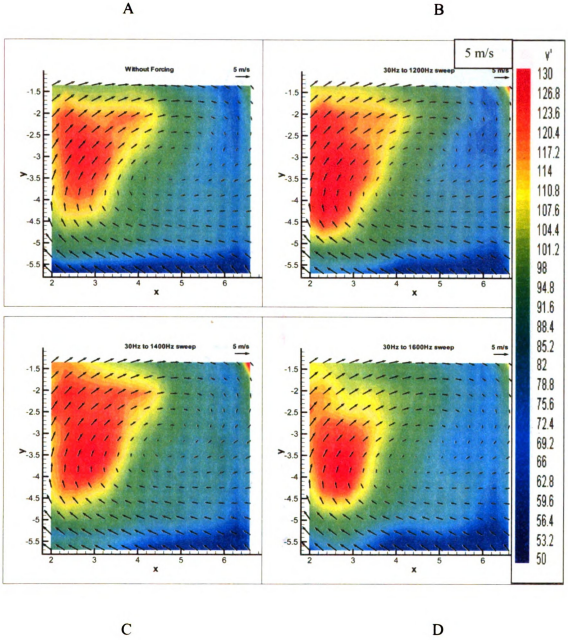

Figure 57. Ensemble averaged results showing rms velocity (cm/s),V mean (cm/s), (A): without perturbation and with perturbation (B):30Hz-1200Hz, (C):30Hz-1400Hz, (D):30Hz-1600Hz at 270 CAD

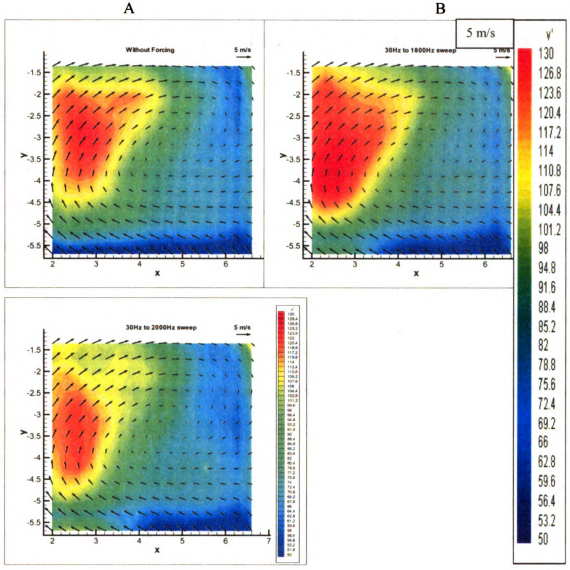

Figure 58. Ensemble averaged results showing rms velocity (cm/s),V mean (cm/s), (A): without perturbation and with perturbation (B):30Hz-1800Hz, (C):30Hz-2000Hz at 270 CAD

Chapter 4

RESULTS AND DISCUSSIONS FOR 90 CAD AND 180 CAD

4.1 Introduction

The purpose of this research was to investigate the cycle-to-cycle variation and the effect of perturbation during the early intake stroke and the late intake stroke. The crank angles chosen for this part of experiment were 90 CAD and 180 CAD. The reason was that 90 CAD is in the middle of intake stroke process and 180 CAD is at the end of intake stroke process. The velocity vectors at 90 CAD are very high. They are in the range of 10 m/s to 13 m/s. The U rms has a range of 100 cm/s to 250 cm/s and the V rms has a range of 120 cm/s to 350 cm/s. If compared with the 270 CAD, U rms and V rms for 270 CAD have only a range of 50 cm/s to 150 cm/s. As for 180 CAD, the velocity has a range of 1 m/s to 2 m/s. The U rms and V rms have a range of 70 cm/s to 170 cm/s.

Several of the instantaneous realizations are shown in Figure 59. All of them were taken at 600 rpm and 90 CAD. Each of them corresponded to successive cycles at 90 CAD. From the images, it is obvious that cycle-to-cycle variation exists in the early intake stroke.

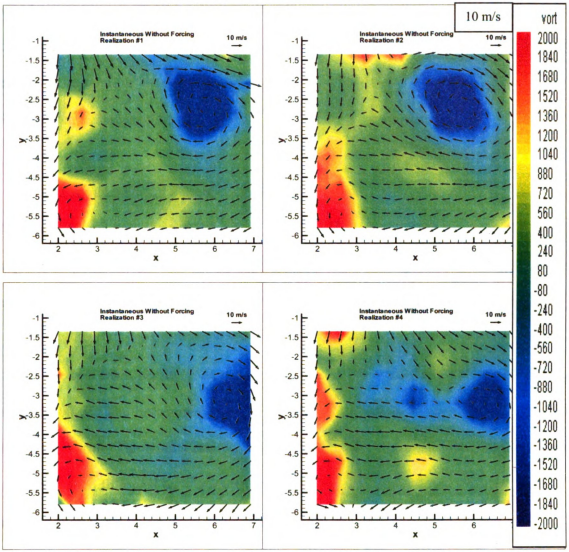

Figure 59. Cycle-to-cycle variation at 90 CAD

4.2 Fixed-time perturbation for 90 CAD: forcing from 0 CAD to 90 CAD

This experiment was done by running the engine at 600 rpm and 90 CAD. The perturbation process started when the piston reached Top Dead Center (TDC) and continued to perturb until it reached 90 CAD. The duration of perturbation was 0.025 seconds. The range of frequencies investigated was from 50Hz to 4000Hz. Each of the frequency cases had an average of 500 instantaneous realizations.

The results showed that the perturbation had some effects on the intake flow. The U rms and V rms had a reduction of about 20%-25% in certain region of the flow. The range of frequencies that had an effect on the flow was from 50Hz to 600Hz. It was found that beyond 1000Hz, the effect was less. The same observation was found in 270 CAD.

The best cases results of the experiment, namely from 50Hz to 1000Hz are shown in Figure 60-65. The best reduction case for this experiment was 400Hz for U rms and 600Hz for V rms. The results are organized in following manner; starting with U mean and U rms, then followed by V mean and V rms. In Figure 66, the line plots for U and V mean are shown. From the plots, both U and V mean did not change much.

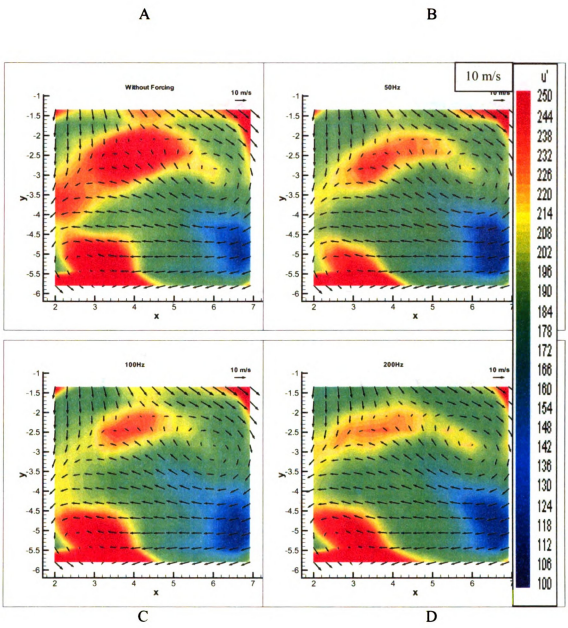

Figure 60. Ensemble averaged results showing U rms velocity (cm/s),U mean (cm/s), (A): without perturbation and with perturbation (B):50Hz, (C):100Hz, (D):200Hz at 90 CAD

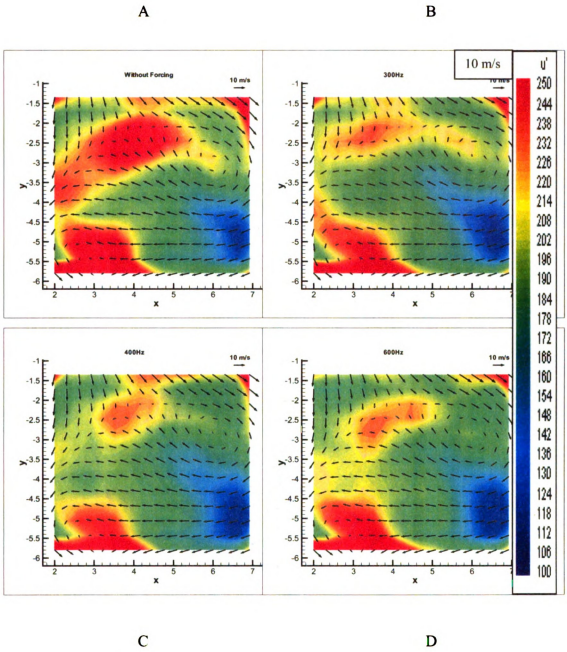

Figure 61. Ensemble averaged results showing U rms velocity (cm/s),U mean (cm/s), (A): without perturbation and with perturbation (B):300Hz, (C):400Hz, (D):600Hz at 90 CAD

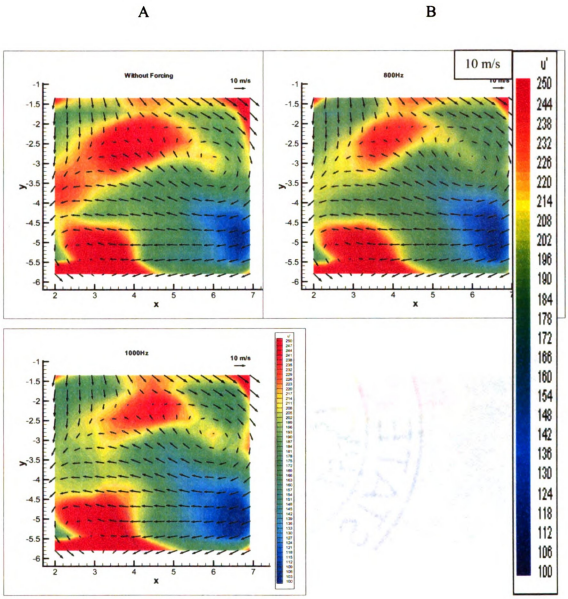

Figure 62. Ensemble averaged results showing U rms velocity (cm/s),U mean (cm/s), (A): without perturbation and with perturbation (B):800Hz, (C):1000Hz at 90 CAD

A B

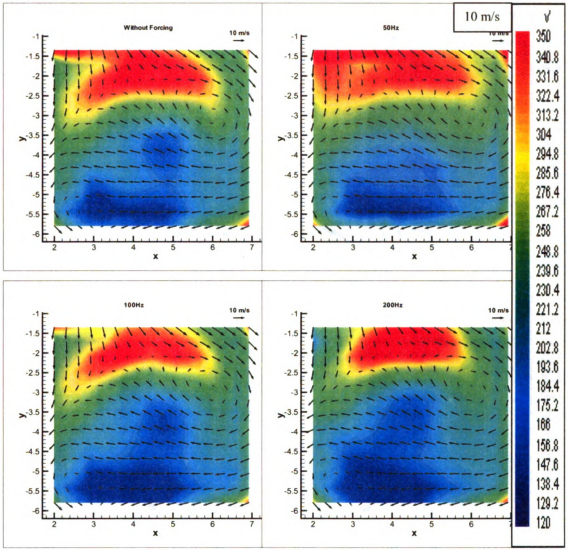

C D

Figure 63. Ensemble averaged results showing V rms velocity (cm/s),V mean (cm/s), (A): without perturbation and with perturbation (B):50Hz, (C):100Hz, (D):200Hz at 90 CAD

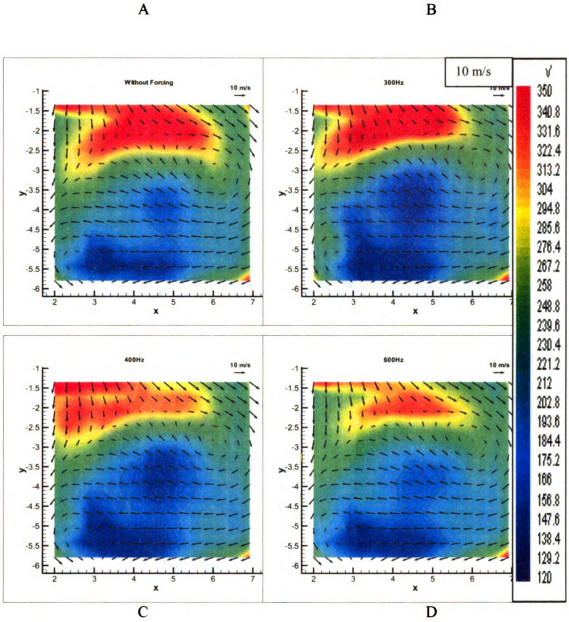

Figure 64. Ensemble averaged results showing V rms velocity (cm/s),V mean (cm/s), (A): without perturbation and with perturbation (B):300Hz, (C):400Hz, (D):600Hz at 90 CAD

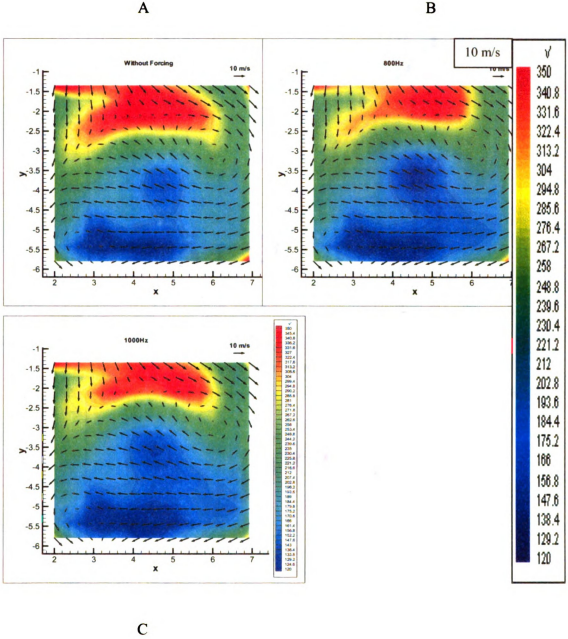

Figure 65. Ensemble averaged results showing V rms velocity (cm/s),V mean (cm/s), (A): without perturbation and with perturbation (B):800Hz, (C):1000Hz at 90 CAD

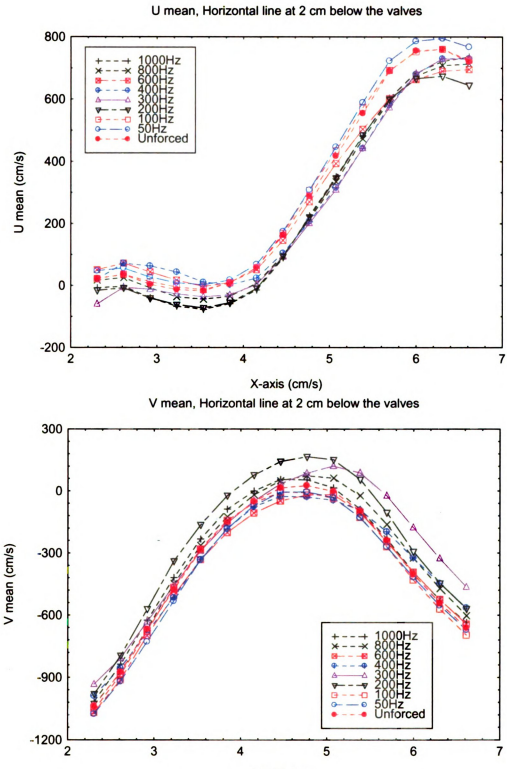

Figure 66. Effect of perturbations on the U mean and V mean at horizontal line about 2 cm below the intake and exhaust valves

4.3 Fixed-time perturbation for 180 CAD: forcing from 0 CAD to 180 CAD

This experiment was performed in the same condition as 90 CAD except that the crank angle of interest was 180 CAD. The perturbation process started when the piston reached Top Dead Center (TDC) and continued to perturb until it reached 180 CAD. The duration of perturbation was 0.05 seconds. The range of frequencies investigated was from 50Hz to 2000Hz. Each of the frequency case had an average of 500 instantaneous cases.

The results did not show any obvious reduction in either U rms or V rms. All the frequency cases in U rms showed similar U rms values. There was no obvious best reduction in U rms. As for V rms, the best case would be 300 Hz. However, the reduction was about 5%-10% in certain regions.

The results of the experiment, namely from 50Hz to 1000Hz are in Figure 67-72. The results are organized in following manner; starting with U mean and U rms, then followed by V mean and V rms. From the line plots in Figure 73, the U mean and V mean did not change much except for 200Hz which increased the mean velocity.

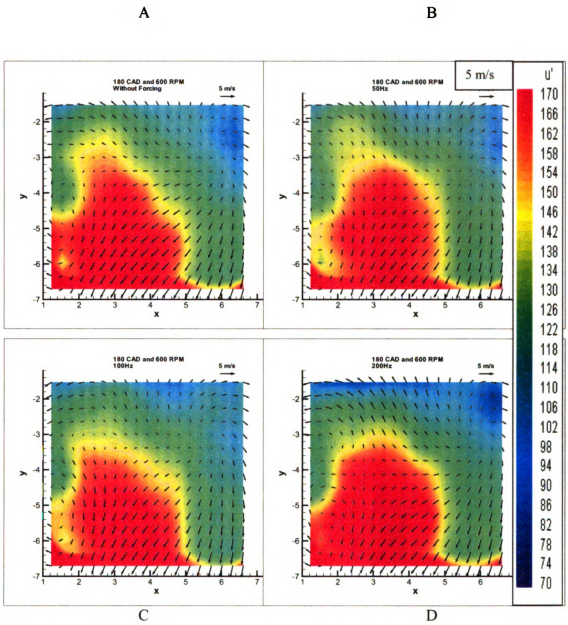

Figure 67. Ensemble averaged results showing U rms velocity (cm/s),U mean (cm/s), (A): without perturbation and with perturbation (B):50Hz, (C):100Hz, (D):200Hz at 180 CAD

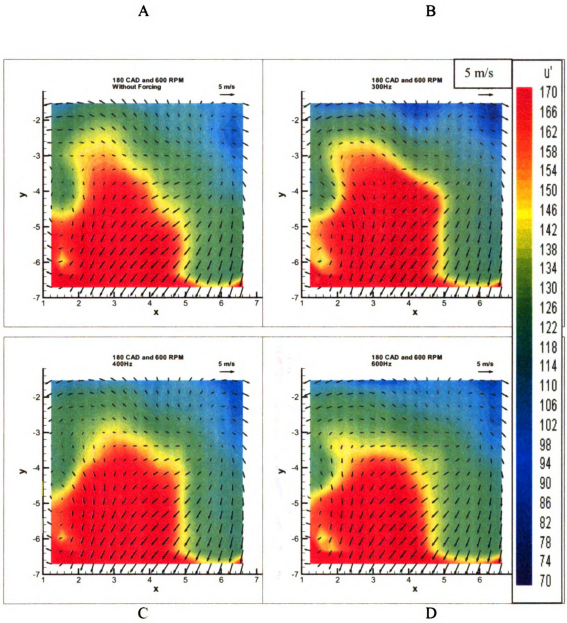

Figure 68. Ensemble averaged results showing U rms velocity (cm/s),U mean (cm/s), (A): without perturbation and with perturbation (B):300Hz, (C):400Hz, (D):600Hz at 180 CAD

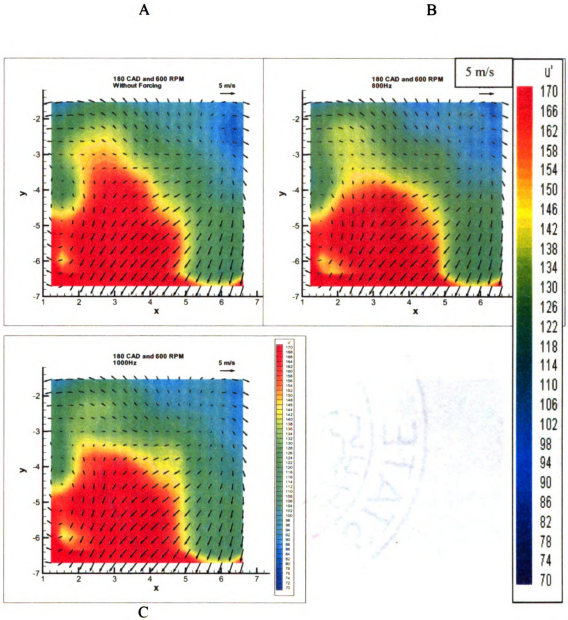

Figure 69. Ensemble averaged results showing U rms velocity (cm/s),U mean (cm/s), (A): without perturbation and with perturbation (B):800Hz, (C):1000Hz at 180 CAD

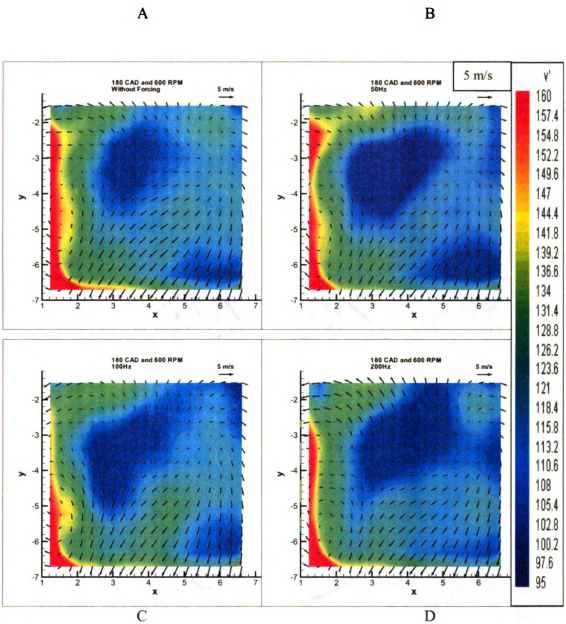

Figure 70. Ensemble averaged results showing V rms velocity (cm/s),V mean (cm/s), (A): without perturbation and with perturbation (B):50Hz, (C):100Hz, (D):200Hz at 180 CAD

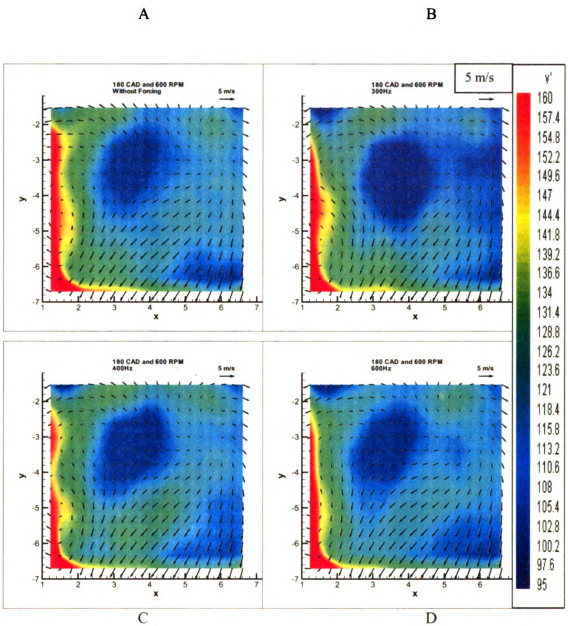

Figure 71. Ensemble averaged results showing V rms velocity (cm/s),V mean (cm/s), (A): without perturbation and with perturbation (B):300Hz, (C):400Hz, (D):600Hz at 180 CAD

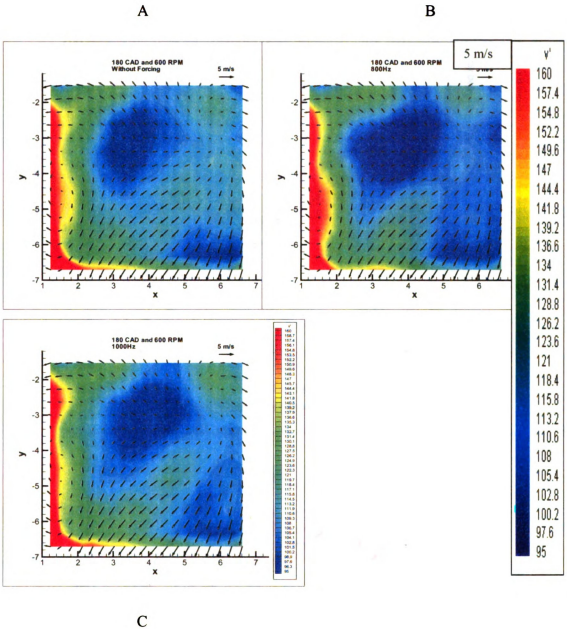

Figure 72. Ensemble averaged results showing V rms velocity (cm/s),V mean (cm/s), (A): without perturbation and with perturbation (B):800Hz, (C):1000Hz at 180 CAD

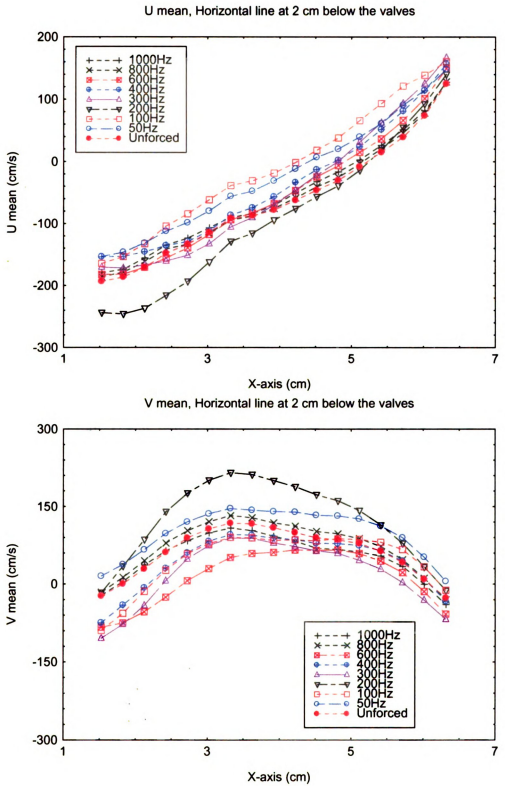

Figure 73. Effect of perturbations on the U mean and V mean at horizontal line about 2 cm below the intake and exhaust valves

Chapter 5

RESULTS AND DISCUSSIONS FOR 270 CAD RUNNING AT 1200 RPM

5.1 Introduction

The purpose of this experiment was to investigate the cycle-to-cycle variation and the effect of perturbation at 270 CAD with the engine running at 1200 rpm. In an earlier chapter, the 270 CAD and 600 rpm experiments indicated that when perturbed with 300 Hz or 400 Hz, the U rms and V rms were reduced to about 25%-30%. With this promising result, it gave a motivation to further investigate the effect of perturbation at higher engine speed. Thus, the experiment was repeated at 1200 rpm.

At 1200 rpm, U rms ranges from 100 cm/s to 250 cm/s and V rms ranges from 120 cm/s to 230 cm/s. If compared with the 600 rpm, U rms and V rms for 270 CAD have only a range of 50 cm/s to 150 cm/s. In other words, the U rms and V rms values are doubled at 1200 rpm.

At 1200 rpm and 270 CAD, there is a significant cycle-to-cycle variation. A few of the instantaneous, continuous realizations are shown in Figure 74.

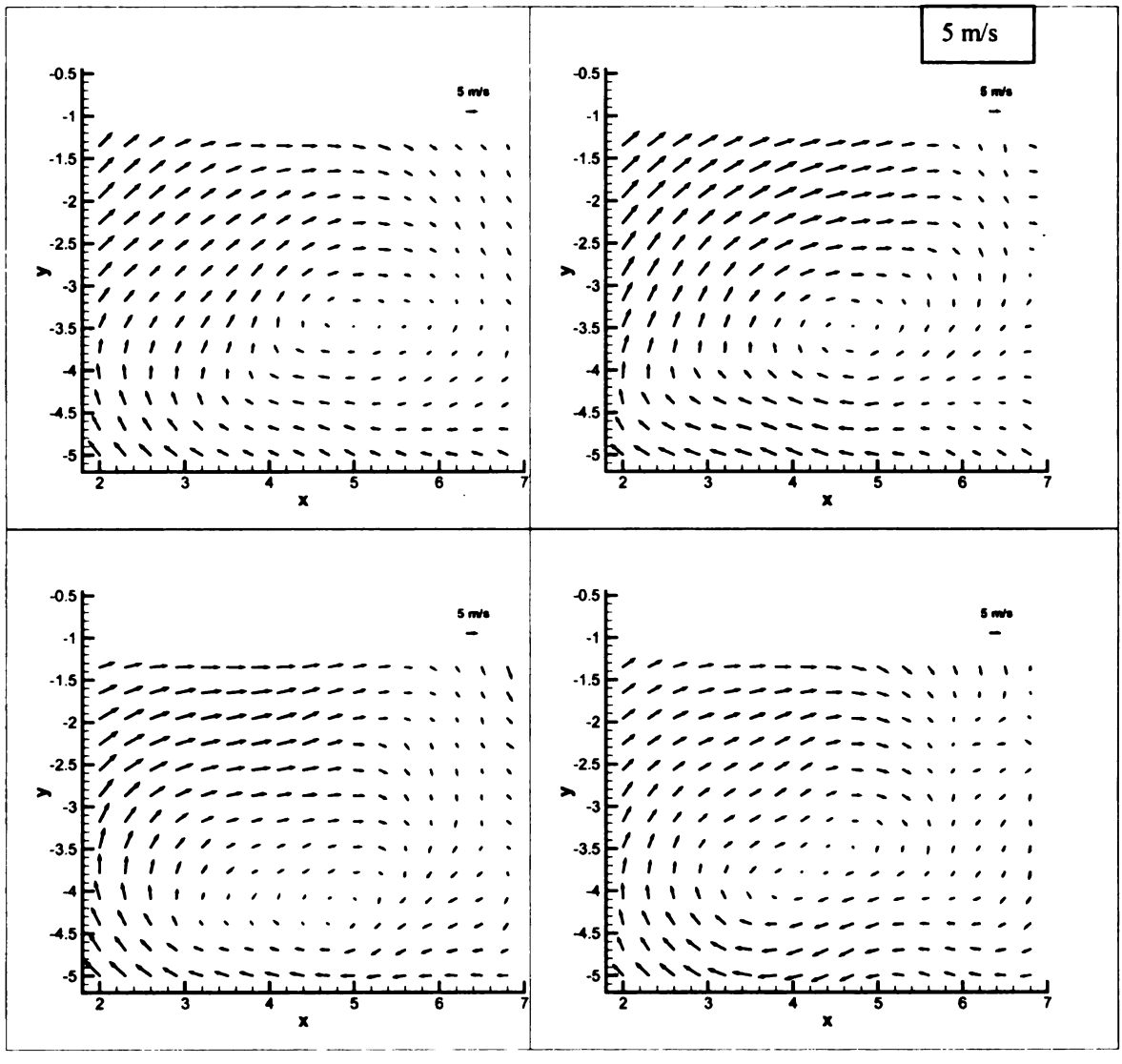

Figure 74. Cycle-to-cycle variation at 270 CAD and 1200 rpm

5.2 Fixed-time perturbation for 270 CAD: forcing from 0 CAD to 180 CAD

This experiment was done by running the engine at 1200 rpm and 270 CAD. The perturbation process started when the piston reached Top Dead Center (TDC) and continued to perturb until it reached 180 CAD. The duration of perturbation was 0.025 seconds. The range of frequencies investigated was from 50Hz to 2000Hz. Each of the frequency cases had an average of 500 instantaneous realizations.

The results showed that the perturbation had some effects on the flow. The U rms and V rms had a reduction of about 20%-25% in certain region of the flow. The range of frequencies that had an effect on the flow was from 600Hz to 2000Hz. It was found that below 600 Hz and beyond 2000Hz, the effect was less.

The best cases results of the experiment, namely from 600Hz to 2000Hz are shown in Figure 75-80. The best reduction cases for this experiment were 1400Hz for U rms and 1800Hz for V rms. At 600 rpm, the best reduction cases were 300 Hz and 400 Hz. The results are organized in following manner; starting with U mean and U rms, then followed by V mean and V rms. From the line plots in Figure 81, the U mean decreased about 30% - 40% as the frequencies of the perturbations increased. V mean did not changed much with frequencies.

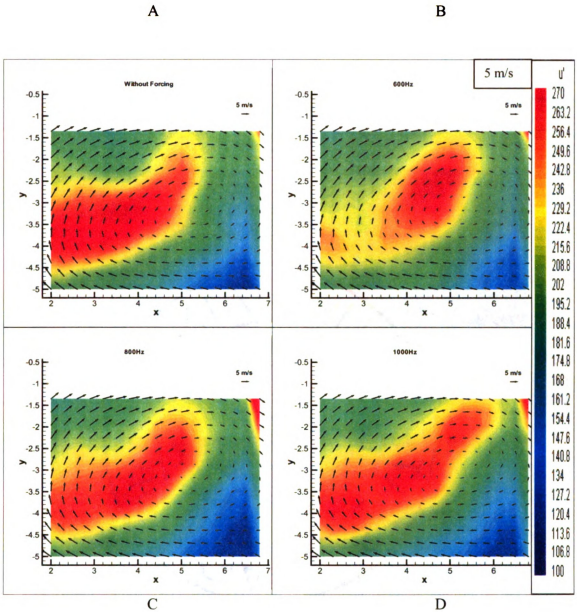

Figure 75. Ensemble averaged results showing U rms velocity (cm/s),U mean (cm/s), (A): without perturbation and with perturbation (B):600Hz, (C):800Hz, (D):1000Hz at 270 CAD and 1200 rpm

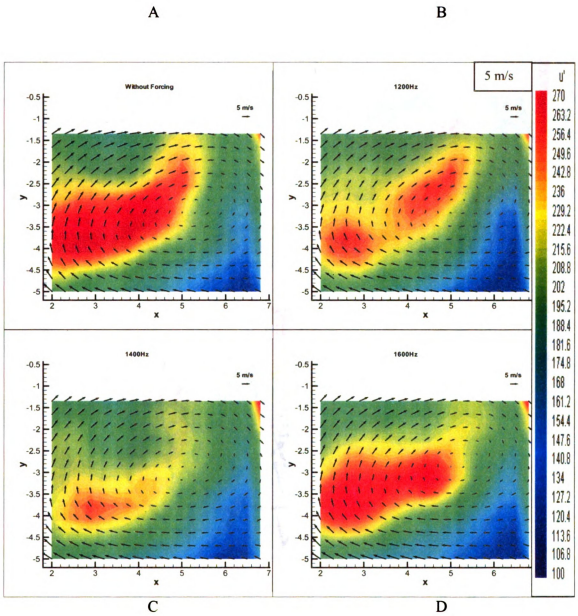

Figure 76. Ensemble averaged results showing U rms velocity (cm/s),U mean (cm/s), (A): without perturbation and with perturbation (B):1200Hz, (C):1400Hz, (D):1600Hz at 270 CAD and 1200 rpm

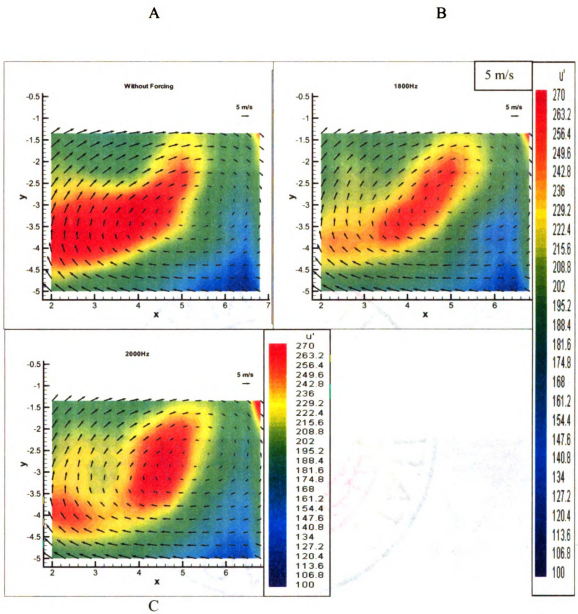

Figure 77. Ensemble averaged results showing U rms velocity (cm/s),U mean (cm/s), (A): without perturbation and with perturbation (B):1800Hz, (C):2000Hz at 270 CAD and 1200 rpm

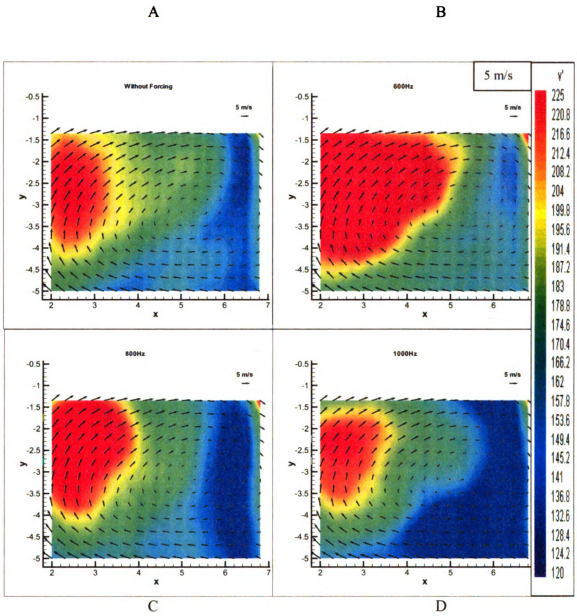

Figure 78. Ensemble averaged results showing V rms velocity (cm/s),V mean (cm/s), (A): without perturbation and with perturbation (B):600Hz, (C):800Hz, (D):1000Hz at 270 CAD and 1200 rpm

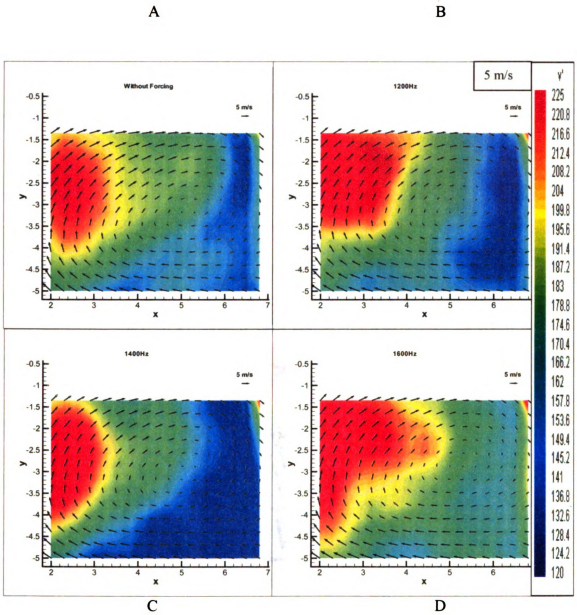

Figure 79. Ensemble averaged results showing V rms velocity (cm/s),V mean (cm/s), (A): without perturbation and with perturbation (B):1200Hz, (C):1400Hz, (D):1600Hz at 270 CAD and 1200 rpm

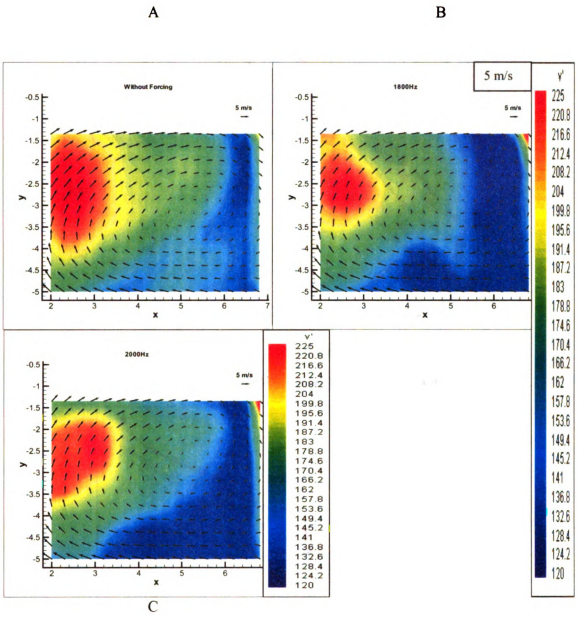

Figure 80. Ensemble averaged results showing V rms velocity (cm/s),V mean (cm/s), (A): without perturbation and with perturbation (B):1800Hz, (C):2000Hz at 270 CAD and 1200 rpm

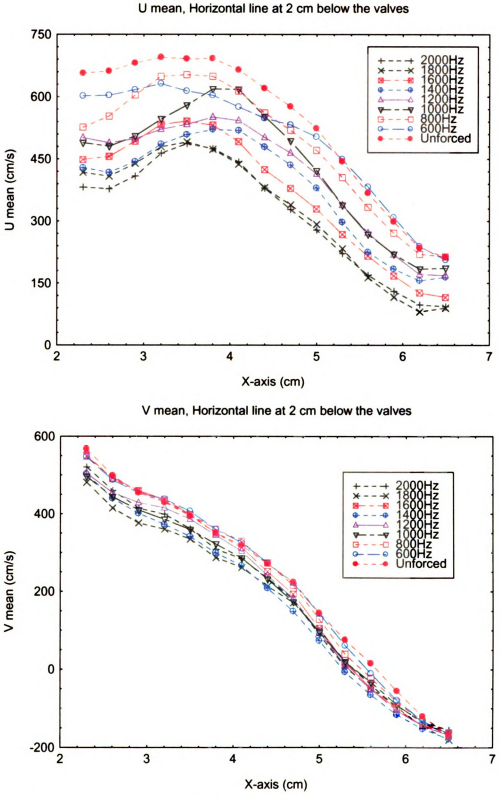

Figure 81. Effect of perturbations on the U mean and V mean at horizontal line about 2 cm below the intake and exhaust valves

Chapter 6

CONCLUSIONS

The objective of this study was to investigate the effects of perturbing the flow in the engine cylinder using a 4-ohms speaker. This study was conducted on a 1999 model year Ford cylinder head with 4 valves and double overhead cams. The engine cylinder head was part of the left bank of a V8 prototype engine with 90.2 mm bore and 90^0 degrees bank angle. Molecular Tagging Velocimetry (MTV) was used to measure the velocity field at a tumble plane which is located at the center of the cylinder, about 2 cm from each side of the cylinder wall. The main conclusions from this study are listed.

1. The amplitude effect experiment showed that the largest amplitude (28 V) of the perturbation gave the maximum U rms and V rms reduction.

2. Free-run perturbation at 270 CAD and 600 rpm showed that the effective perturbation frequency range is from 50Hz to 400Hz. For U rms, the best reduction case was 400Hz. It showed about 25%-30% reduction at certain region of the flow field. As for V rms, the best reduction case was 200Hz. It showed about 25%-30% reduction at certain region of the flow field too.

3. Fixed-time perturbation from 0 CAD to 180 CAD, at 270 CAD and 600 rpm showed that U rms was reduced about 20%-30% when perturbed at 300Hz and 400Hz. As for V rms, the best reduction cases were at 400Hz and 600Hz.

4. The sweeping perturbation experiment (sweeping frequency started at 100Hz) showed that the U rms and V rms were reduced to about 20%-25%. The best reduction case for U rms was sweeping from 100Hz to 1200Hz. The best reduction case for V rms was sweeping from 100Hz to 800Hz.

5. The rest of experiments for 270 CAD and 600 rpm did not show any clear trend nor huge U rms and V rms reduction compared with free-run and fixed-time perturbation experiments.

6. For 600 rpm experiment, with f=300Hz, D=37mm and U=10m/s, the St=1.11. With f=400Hz, the St=1.48. Thus, 1.11<St<1.48. This is consistent with Ambrose's finding of Strouhal number, St = 1.19 (St=fD/U) as a preferred frequency.

7. At the early crank angles such as 90 CAD, fixed-time perturbation showed about 20%-25% reduction for both U rms and V rms.

8. When the engine speed was increased to 1200 rpm, the fixed-time perturbation showed about 20%-25% reduction for both U rms and V rms at certain locations in the engine cylinder.

Chapter 7

RECOMMENDATIONS

1. In future, the speaker could be placed closer to the intake valves. In this study, the speaker was mounted about 10 inches from the intake valves. If the speaker could be moved closed to the intake valves, it would increase the strength of the perturbation.

2. Next step would be to take the best perturbation cases and try them on a firing engine.

APPENDICES

Appendix A

Supplementary Plots and Graphs for Chapter 3

A.1 Supplementary graphs for free-run perturbation

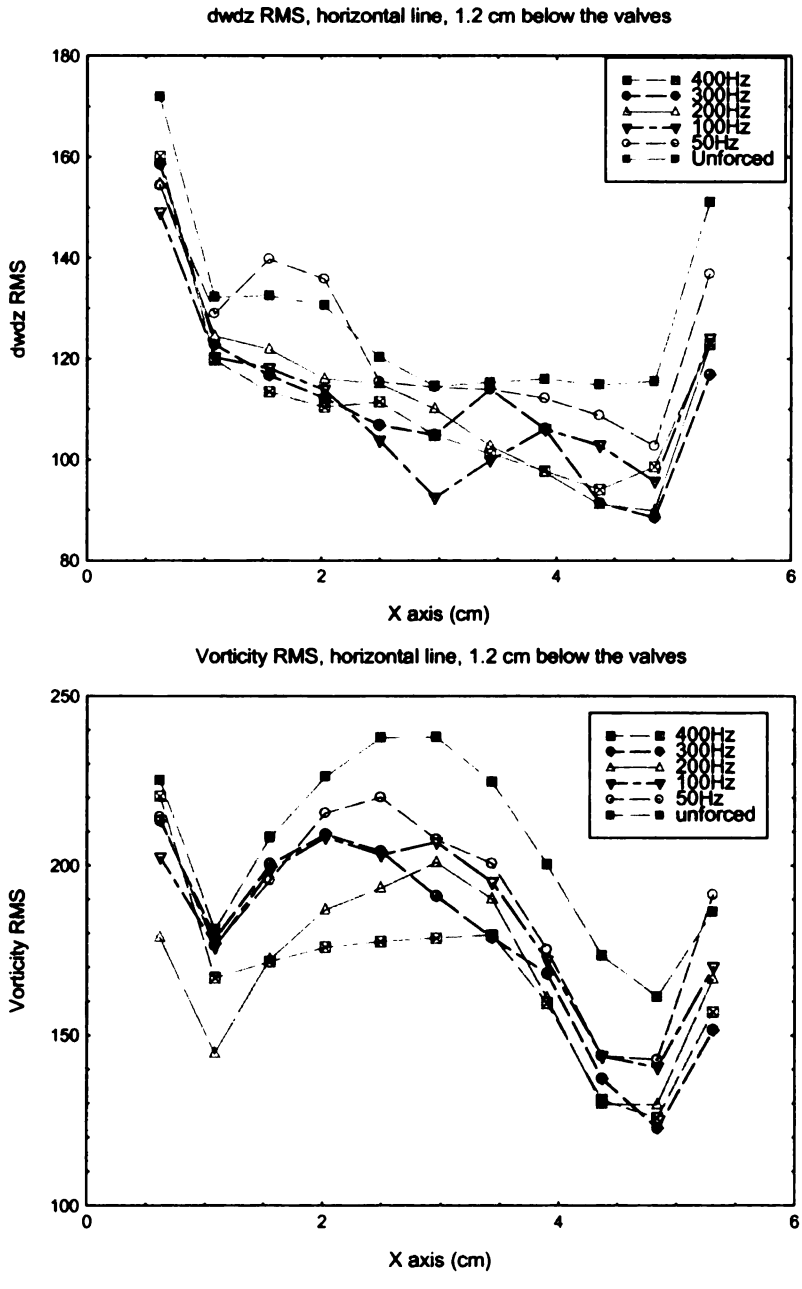

Figure A1. Dwdz RMS and Vorticity RMS for horizontal line, about 1.2 cm below the valves

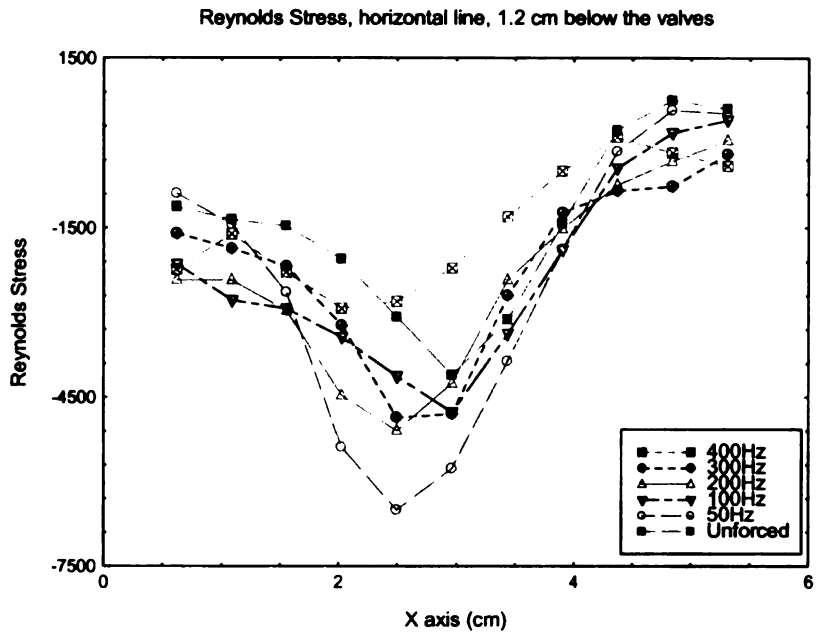

Figure A2. Reynolds stress for horizontal line, about 1.2 cm below the valves

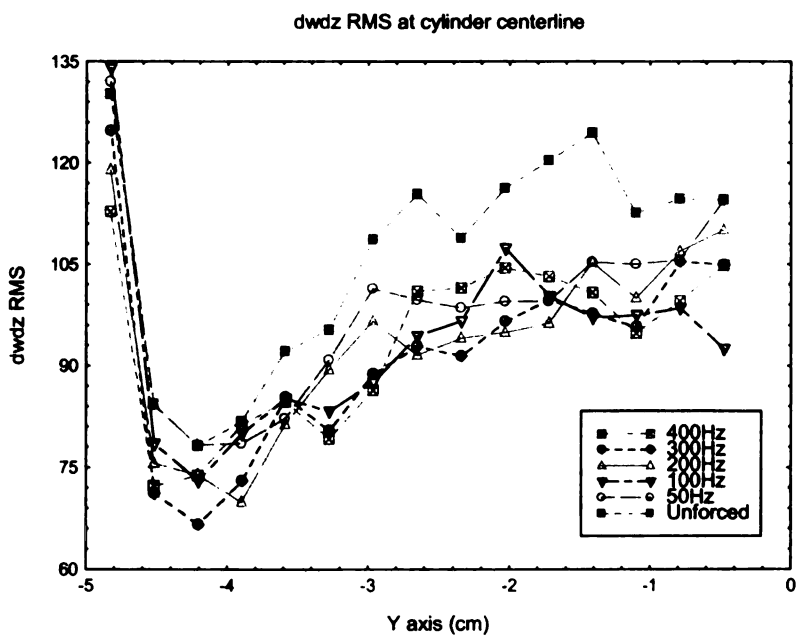

Figure A3. Dwdz rms at cylinder centerline, about 4.5 cm from cylinder wall

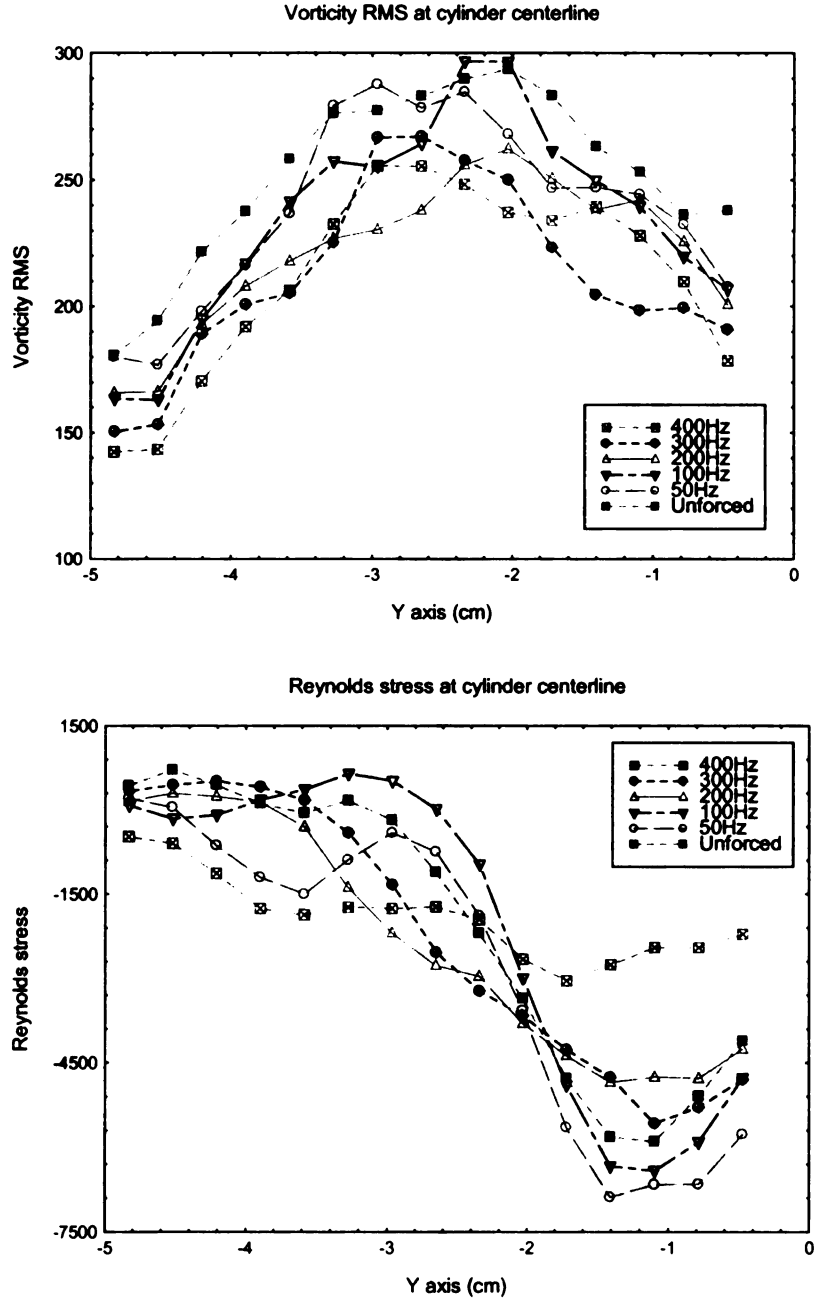

Figure A4. Vorticity rms and Reynolds stress at cylinder centerline, about 4.5 cm from cylinder wall

A.2 Fixed-time perturbations : Perturbation from 0 CAD to 180 CAD with no phase shift

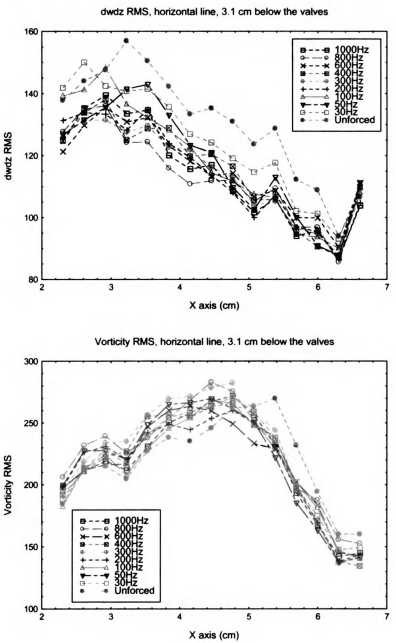

Figure A5. Dwdz RMS and Vorticity RMS for horizontal line, about 3.1 cm below the valves

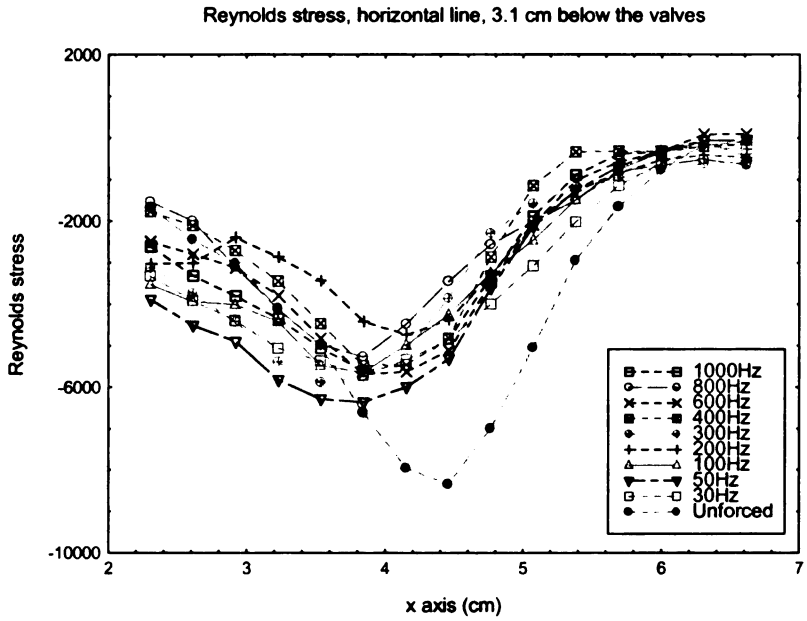

Figure A6. Reynolds stress for horizontal line, about 3.1 cm below the valves

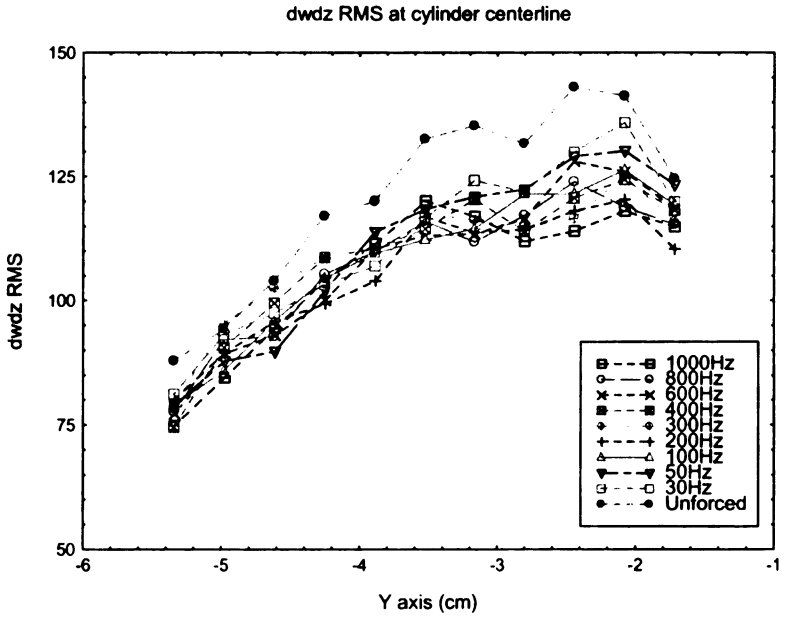

Figure A7. Dwdz rms at cylinder centerline, about 4.5 cm from cylinder wall

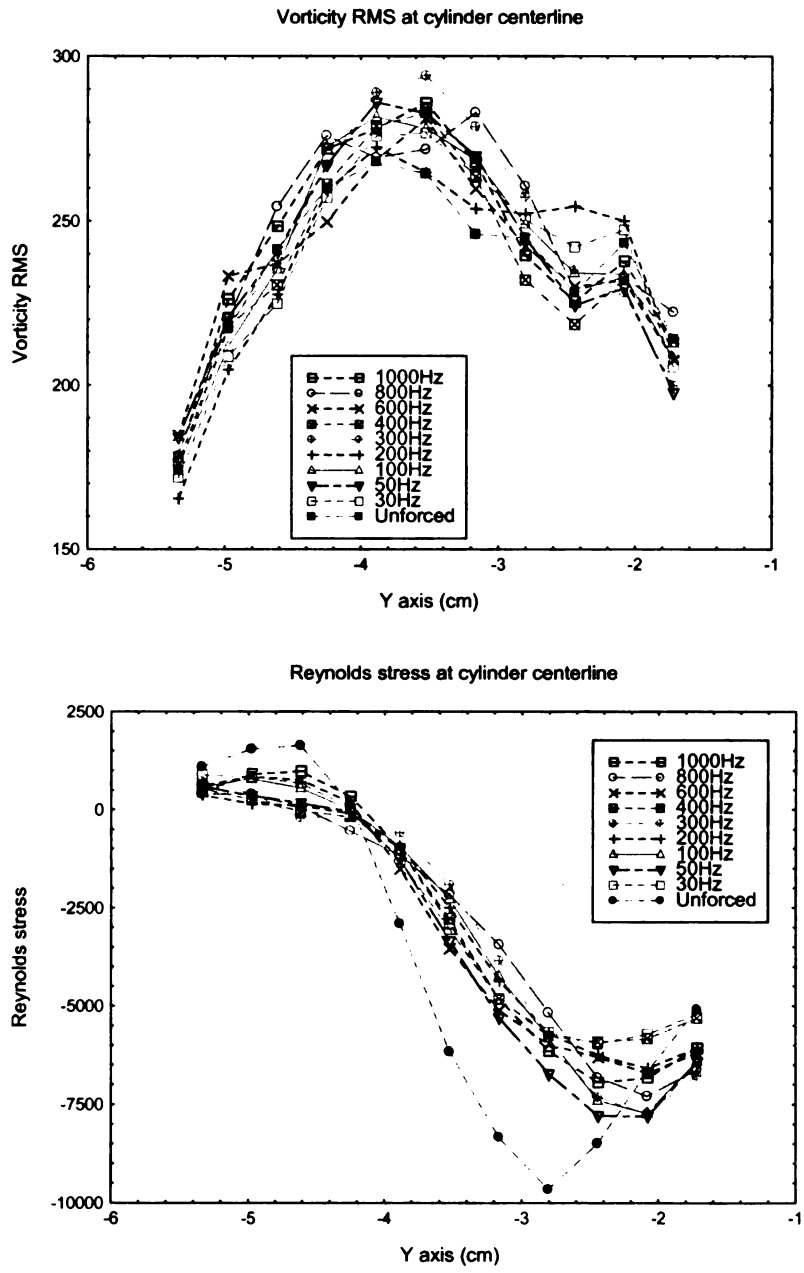

Figure A8. Vorticity rms and Reynolds stress at cylinder centerline, about 4.5 cm from cylinder wall

A.3 Sweeping perturbations : sweep frequencies from 100Hz to 2000Hz

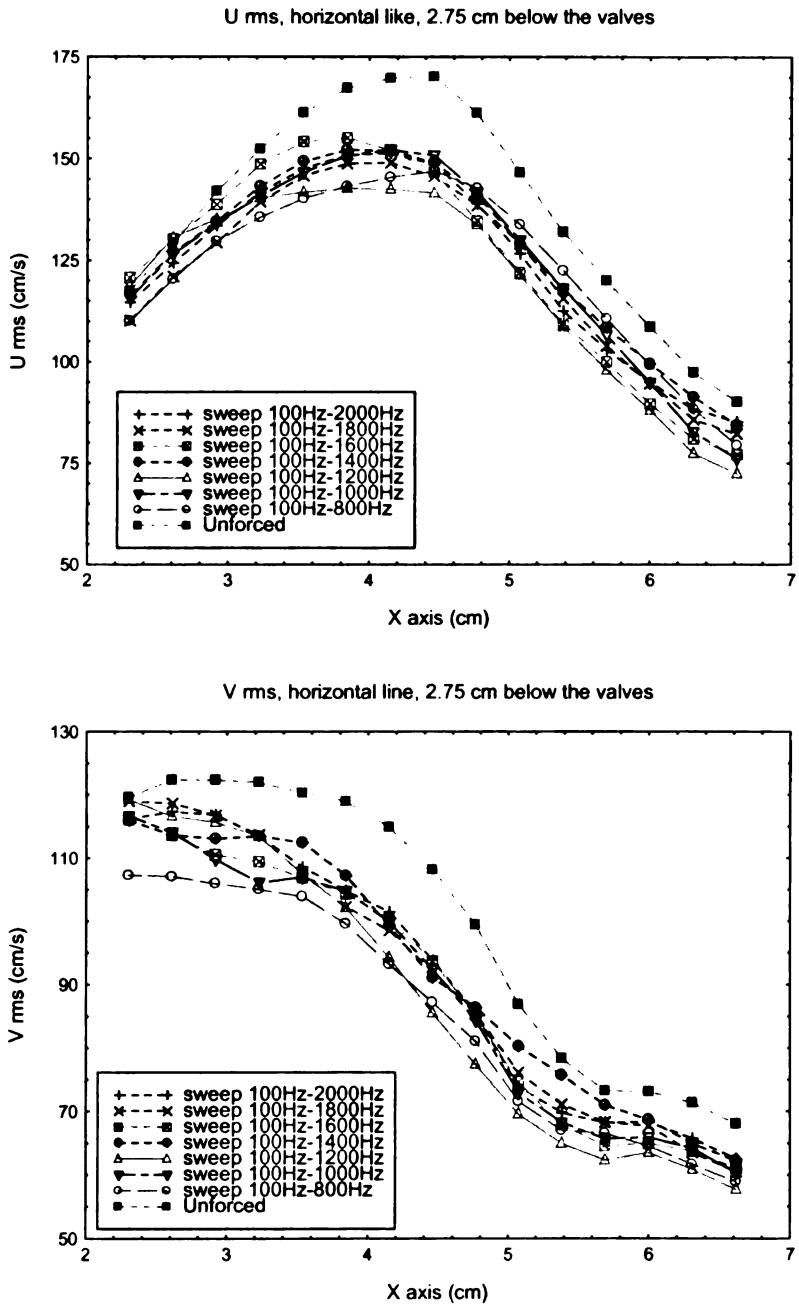

Figure A9. U RMS and V RMS for horizontal line, about 2.75 cm below the valves

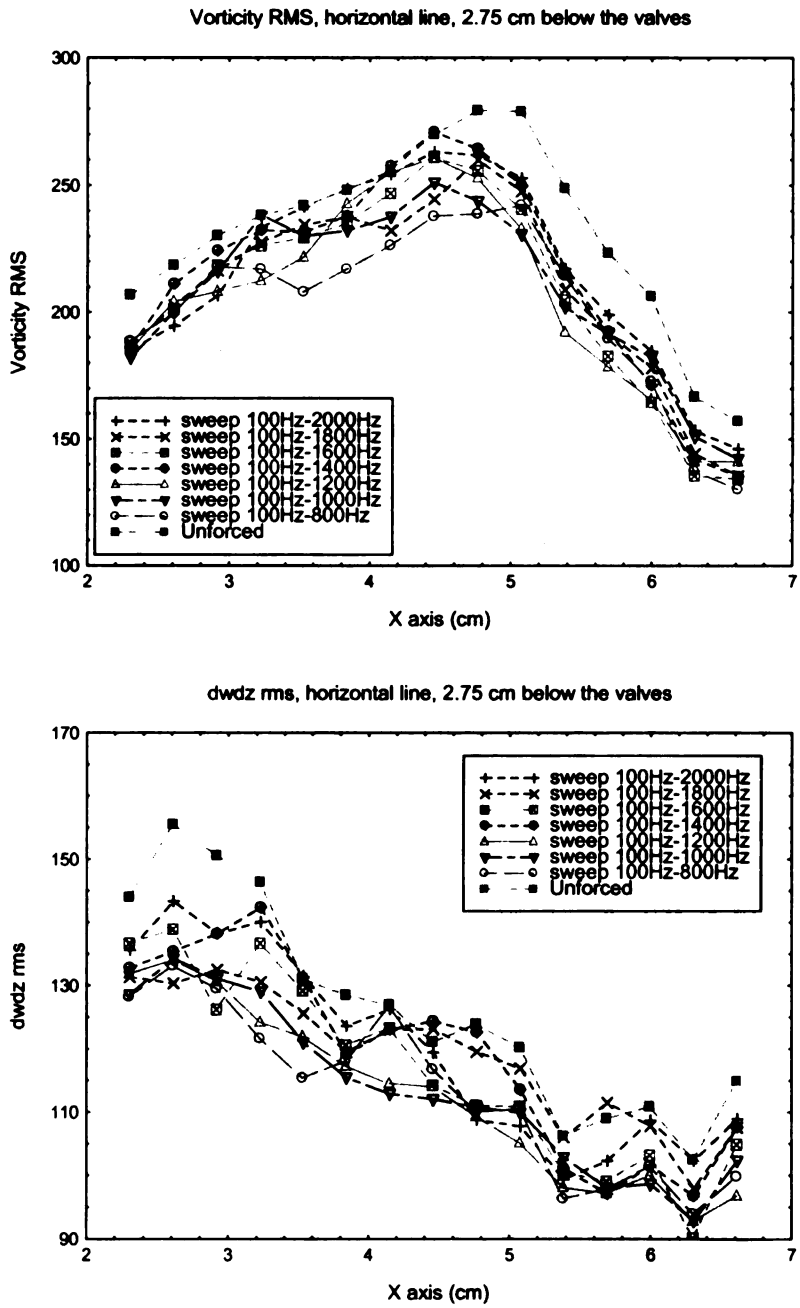

Figure A10. Vorticity RMS and dwdz RMS for horizontal line, about 2.75 cm below the valves

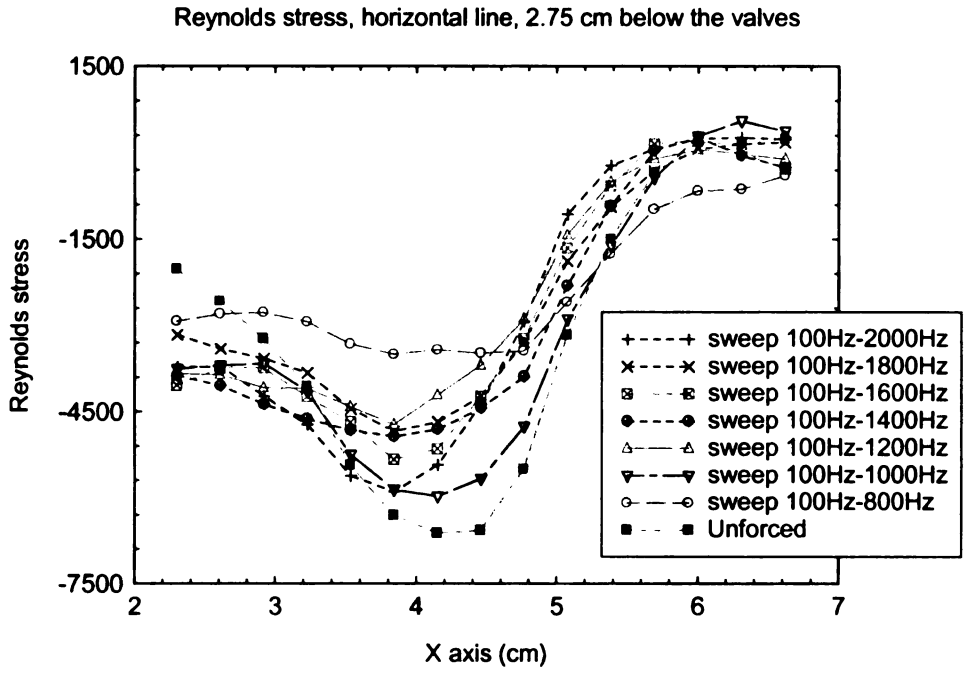

Figure A11. Reynolds stress for horizontal line, about 2.75 cm below the valves

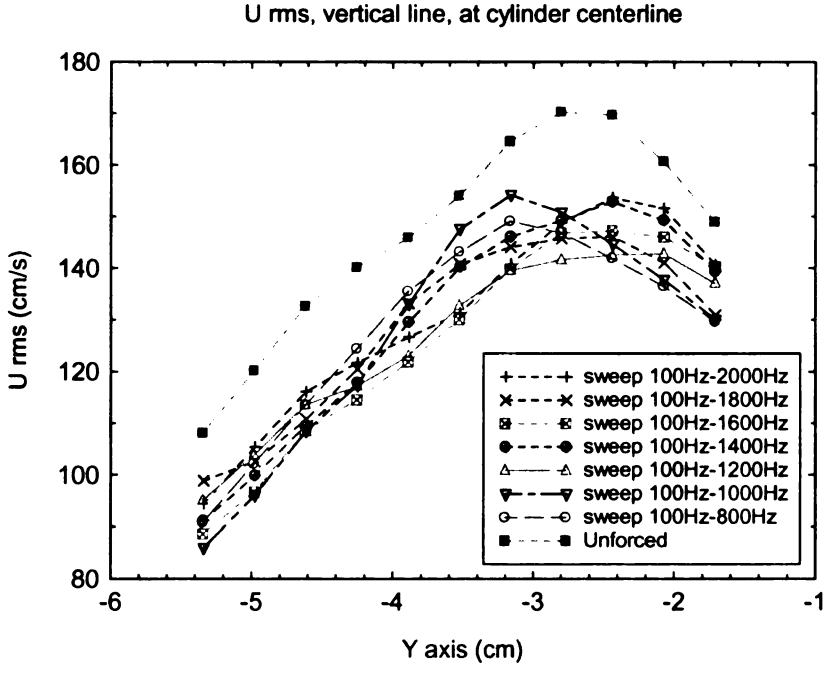

Figure A12. U rms at cylinder centerline, about 4.5 cm from cylinder wall

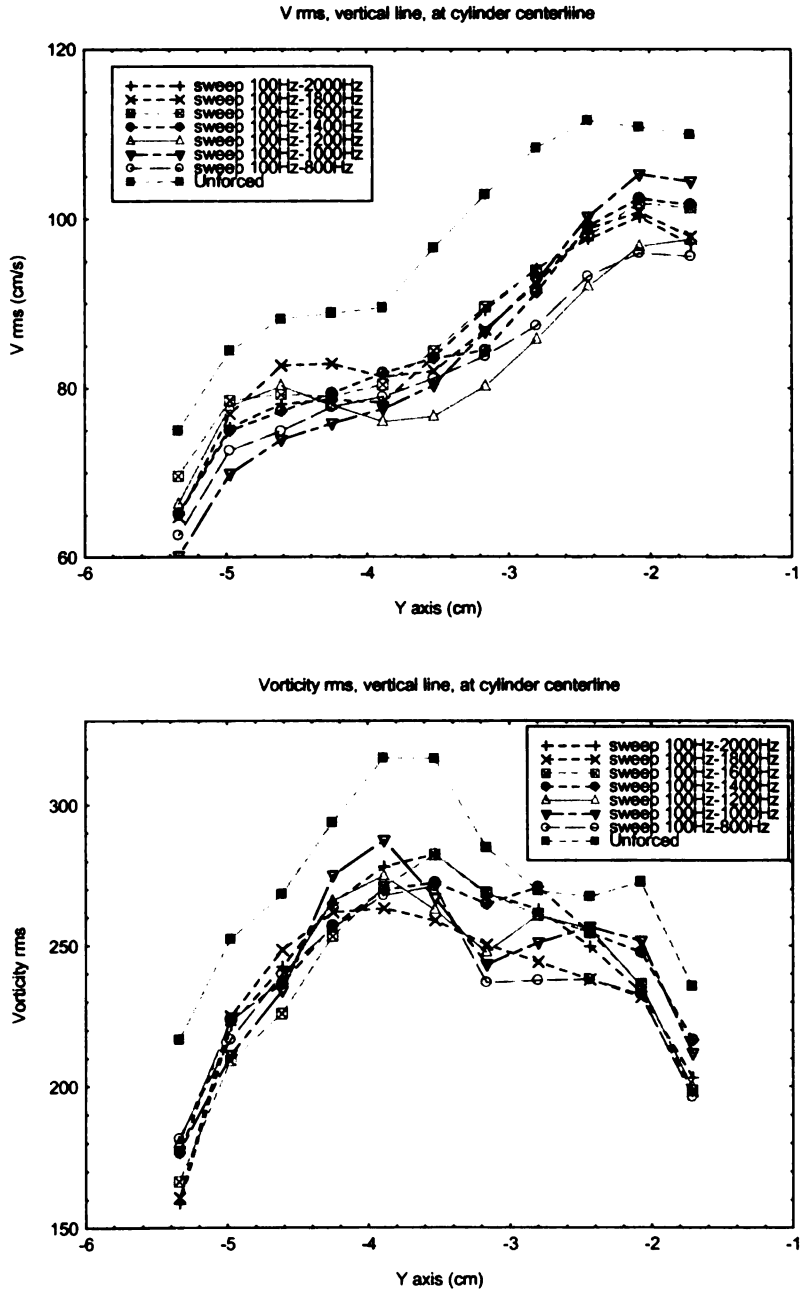

Figure A13. V rms and vorticity rms at cylinder centerline, about 4.5 cm from cylinder wall

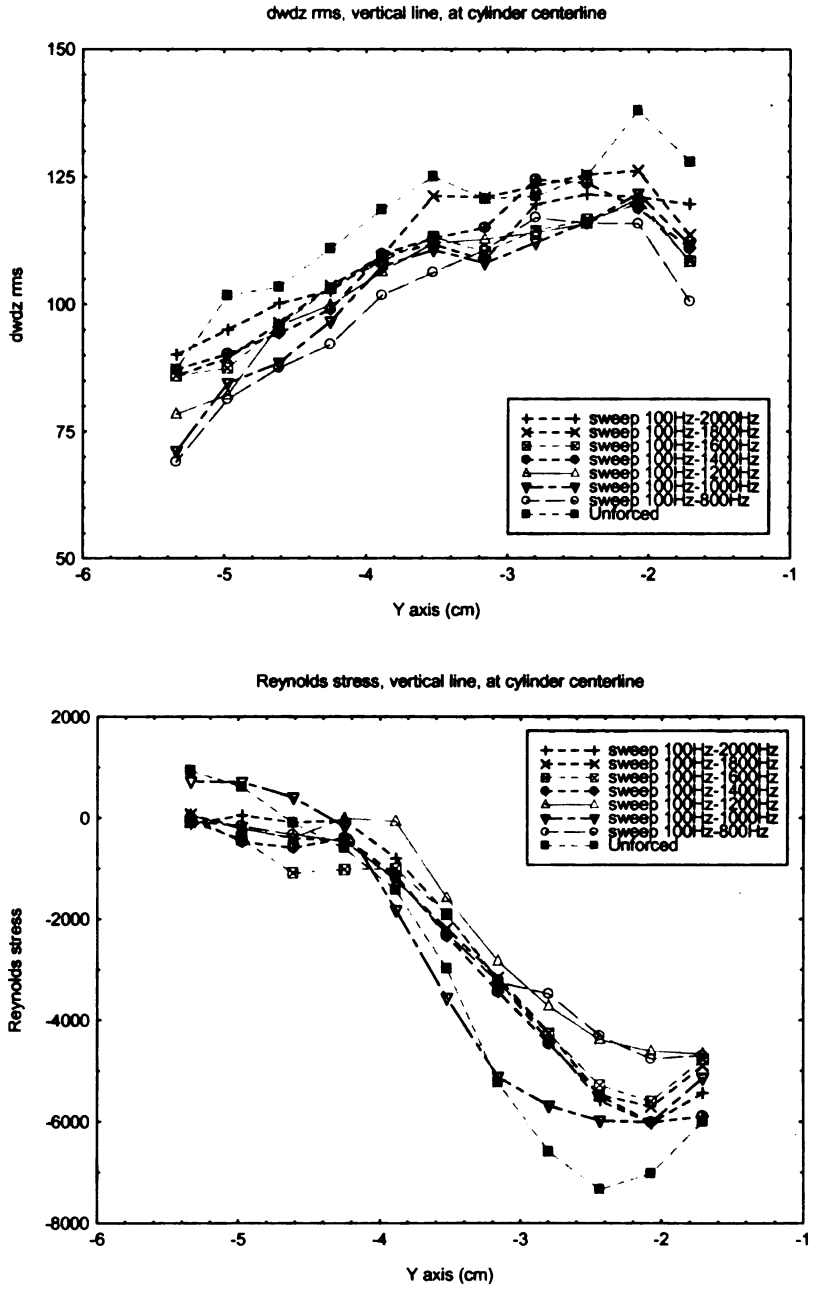

Figure A14. Dwdz rms and Reynolds stress at cylinder centerline, about 4.5 cm from cylinder wall

Appendix B

Experimental Equipment and Devices

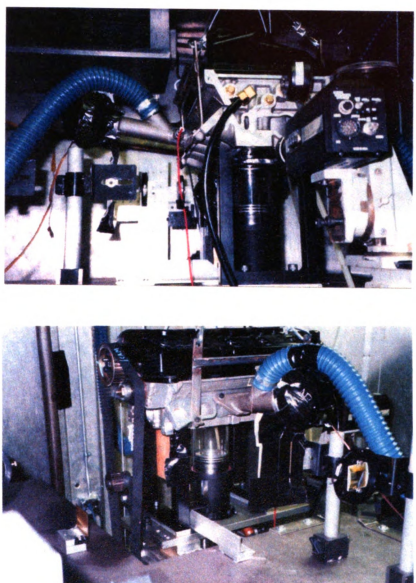

Figure B1. Engine from different point of view

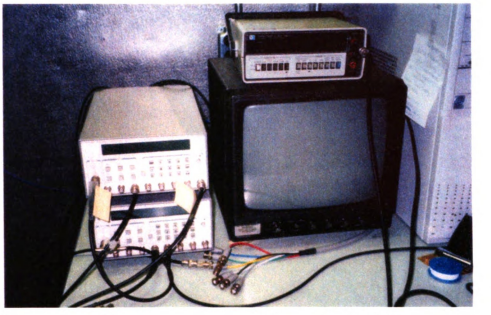

Figure B2. Delay generators, digital multimeter and monitor

Figure B3. Gateway E-5200 Pentium III computer

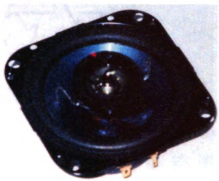

Figure B4. Kenwood KFC-1077 4-ohm speaker

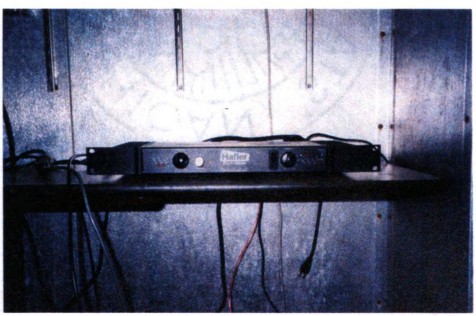

Figure B5. Hafler P-1000 amplifier

Figure B6. HP function generator

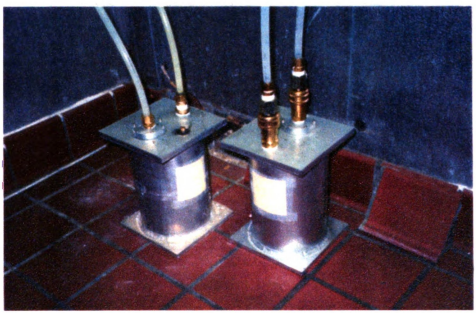

Figure B7. Biacetyl seeding chamber and acetone seeding chamber

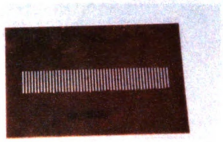

Figure B8. Beam blocker

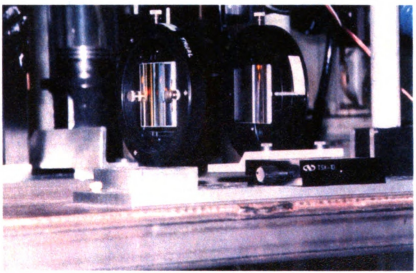

Figure B9. Variable-focal-length lens (VFL)

Figure B10. Engine encoder

Figure B11. Nitrogen bank

Appendix C

Zero-delayed or reference realizations investigation

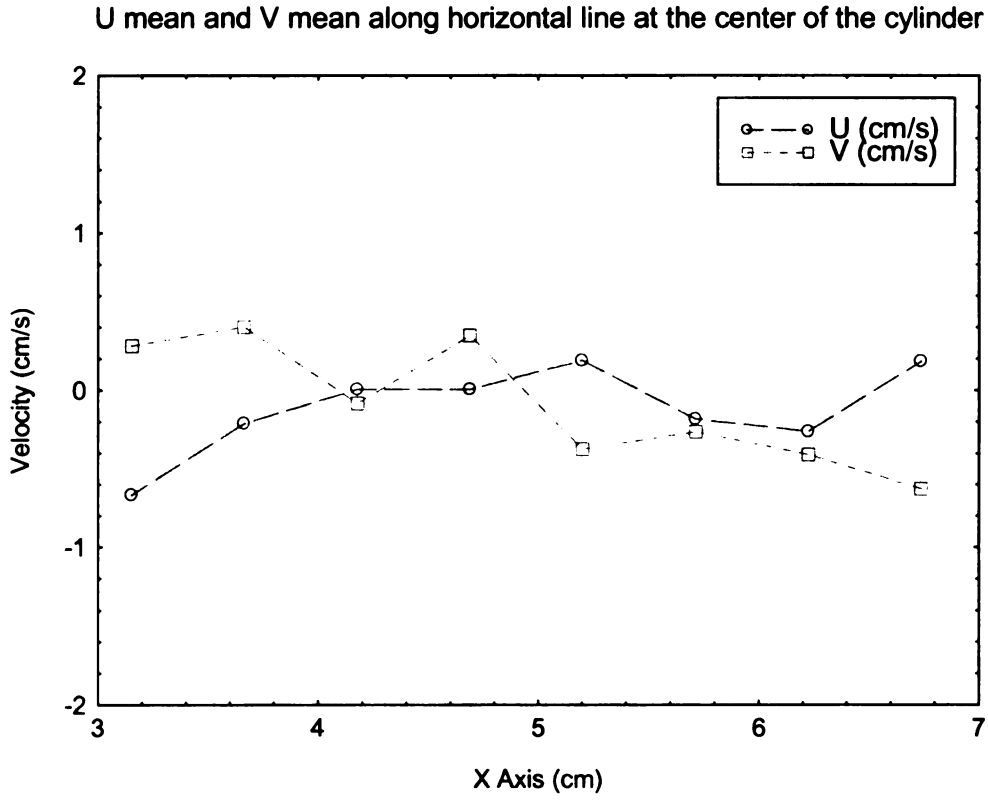

Figure C1. Zero-delay: U mean and V mean along horizontal line at the center of the cylinder

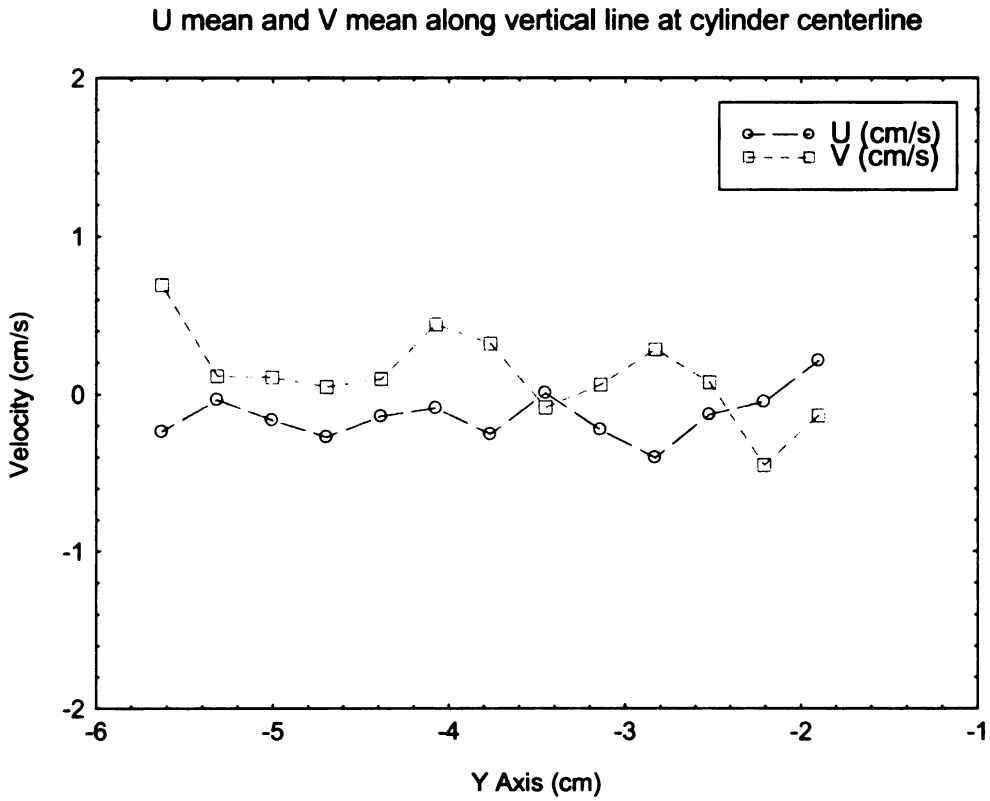

Figure C2. Zero-delay: U mean and V mean along vertical line at the center of the cylinder

The purpose of this experiment is to investigate the stability of the zero-delayed average and instantaneous realizations. The results indicated that both U and V mean were very close to zero velocity.

BIBLIOGRAPHY

Bibliography

1. Hascher, H. G., Jaffri, K., Noval, M., Lee, K., Schock, H., Bonne, M., Keller P., "An Evaluation of Turbulent Kinetic Energy for the In-cylinder Flow of a Four-Valve 3.5L SI Engine using 3-D LDV Measurements." SAE 970793, 1997

2. Zhang, L., Ueda, T., Takatsuki, T., Yokota, K., "Cycle-to-cycle Variations of In-cylinder Flow in a Motored Engine." JSME International Journal, Series B. Vol.38. No.3. 1995

3. Ambrose, G., "A Study of the Effects of Exciting the Intake Flow in an Internal Combustion Engine Model." Master's thesis, Michigan State University, 1997

4. Tang, S. K. and Ko, N. W. M., "Experimental Investigation of the Structure Interaction in an Excited Coaxial Jet." Experimental Thermal and Fluid Sciences, Vol 8, pp. 214-229, 1994

5. Dai, W., Trigui, N., Lu, Y., "Modeling of Cyclic Variations in Spark-ignition Engines." SAE International, 2000

6. Koochesfahani, M. M. and Stier, B., "Molecular Tagging Velocimetry in Gas Phase and its Application to Jet Flows." ASME Fluids Engineering Division Summer Meeting, FEDSM'97, 1997

7. Zaman, K. M. B. Q. and Hussain, A. K. M. F., "Vortex Pairing in a circular jet under Controlled Excitation. Part 1. General Jet Response." Journal of Fluid Mechanics, Vol. 101, part 3, pp. 449-441, 1980

8. Zaman, K. M. B. Q. and Hussain, A. K. M. F., "The 'Preferred Mode' of the Axisymmetric jet." Journal of Fluid Mechanics, Vol. 110, pp. 39-71, 1981

9. Koochesfahani, M. M. and MacKinnon, C. G., "Influence of Forcing on the Composition of Mixed Fluid in a two-stream Shear Layer." Physics of Fluids A, Vol. 3, pp. 1135-1142, 1991

10. Cohn, R. K., Gendrich, C. P., Mackinnon, C. G., and Koochesfahani, M. M., "Crossflow Velocimetry Measurements in a Wake Flow." Bulletin of the American Physical Society, p. 1962, 1995

11. Cohn, R. K. and Koochesfahani, M. M., "Structure of the Velocity and Vorticity Field in a Confined Wake." Bulletin of the American Physical Society, p. 2197, 1997

12. Gendrich, C. P., Bohl, D. G. and Koochesfahani, M. M., "Whole-Field Measurements of Unsteady Separation in a Vortex Ring/Wall Interaction." AIAA Paper #97-1780, 1997

13. Gendrich, C. P. and Koochesfahani, M. M., "A Spatial Correlation Technique for Estimating Velocity Fields Using Molecular Tagging Velocimetry." Experiments in Fluids, Vol. 22, pp. 67-77, 1996

14. Gendrich, C. P., Koochesfahani, M. M., and Nocera, D. G., "Molecular Tagging Velocimetry and Other Novel Applications of a New Phosphorescent Supramolecule." Experiments in Fluids, Vol. 23, pp. 361-372, 1997

15. Hill, R. B. and Klewicki, J. C., "Data Reduction Methods for Flow Tagging Velocity Measurements." Experiments in Fluids, Vol. 20, pp. 142-152, 1991

16. Cohn, R. K., "Effect of Forcing on the Vorticity Field in a Confined Wake." PhD. Thesis, Michigan State University, 1999

17. Heywood, J. B., "Internal Combustion Engine Fundamentals." McGraw-Hill, New York, 1998

18. Hascher, H., "The Influence of Speed, Stroke and Load Variations on the Major In-Cylinder Flow Patterns of a Four-Valve Spark-Ignition Engine." PhD. Thesis, Michigan State University, 1999

19. Stier, B. and Koochesfahani, M. M., "Whole Field MTV Measurement in a Steady Flow Rig Model of an IC Engine." Presented at the 1998 SAE International Congress & Exposition, Detroit, MI, February 23-26, 1998, SAE Paper 98-0481, 1998

20. Koochesfahani, M. M., "Molecular Tagging Velocimetry (MTV): Progress and Application." AIAA Paper no. AIAA-99-3786 (Invited), 1999

21. Stier, B. and Koochesfahani, M. M., "Molecular Tagging Velocimetry (MTV) measurements in Gas Phase Flows." Experiments in Fluids, 26(4), pp. 297-304, 1999